Reviews of Modern Plasma Physics (2024) 8:24
https://doi.org/10.1007/s41614-024-00158-3

REVIEW PAPER

Bright X/γ-ray emission and lepton pair production by strong laser fields: a review

Tong-Pu Yu[1] · Ke Liu[1] · Jie Zhao[1] · Xing-Long Zhu[2,3] · Yu Lu[1] · Yue Cao[1] · Hao Zhang[1] · Fu-Qiu Shao[1] · Zheng-Ming Sheng[2,3]

Received: 3 September 2023 / Accepted: 24 March 2024

Abstract

The advent of high-power ultra-short laser pulses opens up new frontiers of relativistic non-linear optics, high energy density physics and laboratory astrophysics. As the laser electric field in the particle rest frame approaches the Schwinger field $E_{cr} = 1.3 \times 10^{18}$ Vm^{-1}, the laser interaction with matter enters into the quantum electrodynamics (QED) dominated regime, where extremely rich non-linear phenomena take place, such as a violent acceleration of charged particles, copious lepton pair production, and ultra-brilliant X/γ-ray emission. Among them, X/γ-ray emission based on the laser-plasma is generally characterized by large photon flux, high brilliance, small source size, and high photon energy, which can even annihilate into lepton pairs by colliding with photons. Though various schemes have been proposed for bright high-energy photon emission and lepton generation and acceleration, many predictions remain to be confirmed and thoroughly tested in experiments. In this review, we introduce recent advances in bright X/γ-ray radiation and lepton pair generation in the QED regime by the interaction of relativistic intense lasers with various plasma targets. The characteristics of the radiation and secondary particles generated via these schemes are summarized, and the experimental progresses are elaborated.

Keywords Strong-field QED · Laser-plasma interaction · Inverse Compton scattering · Betatron radiation · X/γ-rays · Electron-positron pair

Tong-Pu Yu and Ke Liu have contributed equally to this work.

✉ Tong-Pu Yu
tongpu@nudt.edu.cn

[1] Department of Physics, National University of Defense Technology, Changsha 410073, China

[2] Key Laboratory for Laser Plasmas Ministry of Education, School of Physics and Astronomy, Shanghai Jiao Tong University, Shanghai 200240, China

[3] Tsung-Dao Lee Institute, Shanghai Jiao Tong University, Shanghai 200240, China

Published online: 01 June 2024

1 Introduction

The combination of special relativity and quantum mechanics leads to the formulation of quantum field theory (QFT). The DFT describes the behaviour of the most elementary particles observed in nature, including the electromagnetic phenomena. When electrodynamics was extended into the quantum domain, it was quantum electrodynamics (QED) (Feynman 1949). Thus the QED is the relativistic QFT of electrodynamics, describing mathematically all phenomena involving the light interacting with matter (Feynman 1985). Essentially, QED is the model for "elementary" processes in electromagnetic interactions, which has been considered as the most precise and stringently tested theory in physics (Venkataraman 1994) since it has been demonstrated extraordinary levels of agreement between the experiments and the QED predictions, e.g., for the measurement of the electron anomalous magnetic moment (Aoyama et al. 2012). Due to its success, QED has been the prototype for other quantum field theories. However, such precision test of QED has been performed in the perturbative regime and this agreement becomes an open question in the non-perturbative regime of QED. For example, as the electromagnetic fields become sufficiently intense, e.g., in the strong laser fields, the interaction may become highly-nonlinear. Since the strong lasers possess the most powerful macroscopic electromagnetic fields on Earth, it thus provides us with a unique opportunity to probe the non-perturbative particle physics and even shed some light on the existence of dark matter and beyond-the-standard-model physics.

The high-power laser plays a key role in strong-field QED research. Since the theory of stimulated radiation was proposed by Einstein in 1916 (Einstein 1916) and the worldwide first ruby laser was invented in 1960, the laser has become an indispensable tool in all areas like scientific researches, manufacturing, medicine, metrology, communications, and defense technologies, etc. In 1985, the chirped pulse amplification (CPA) (Strickland and Mourou 1985) technique was invented, allowing for the construction of compact TW (1 TW $= 10^{12}$ W) laser systems in the mid-1980s. The advent of CPA enables for the first time the research on the physics of laser-plasma interaction at relativistic laser intensity, i.e., $I > 10^{18}$ W/cm^2, and pulse duration from 10 fs (1 fs $= 10^{-15}$ s) to 1 ps (1 ps $= 10^{-12}$ s). After decades of development, the laser power has been enormously improved to the petawatt (PW, 1 PW=10^{15} W) level. Nowadays, there have been many 1–10 PW high power laser facilities around the world, e.g., Vulcan (Danson et al. 2004), the ELI-pillars (Lureau et al. 2020; Jójárt et al. 2023; Nejdl et al. 2022), SULF (Li et al. 2018), SILEX-II (Hong et al. 2021), GIST (Sung et al. 2017), CORELS (Sung et al. 2016), just to cite a few. Moreover, several for 10–100 PW lasers are either under construction or planned, such as ELI-200 PW, EP-OPAL-75 PW, SEL-100 PW, GEKKO-EXA-50 PW, and XCELS-200 PW (Danson et al. 2019; Turner et al. 2022). The interaction of such high-power laser pulses with matter becomes highly-nonlinear so that particle creation/annihilation gets possible, which has been well formulated mathematically by QED. This can create extreme physical conditions possessing ultra-strong electromagnetic (EM) fields,

ultra-high energy densities and ultra-fast time scales, which can only be found previously in nuclear explosions and astronomical environments. The strong laser has provided unprecedented opportunities for studies on high energy density physics (Garanin et al. 2021), laboratory astrophysics (Zhang et al. 2016), and nuclear physics (Fu et al. 2022), and spawned many new interdisciplinary fields, such as attosecond and zettasecond science, next-generation accelerators (Tajima and Dawson 1979) and novel radiation sources including THz waves, mid-infrared pulses, high harmonics, X/γ-rays (Corde et al. 2013), etc.

In this topical review, we first make a short introduction to the classical electrodynamics. Then we introduce the QED by dividing it into two major categories: one is the linear QED and the other non-linear QED. In the subsequent chapters, we discuss the non-perturbative effects of the non-linear QED. Then we focus on the recent advances in bright X/γ-ray radiation and lepton pair generation by strong laser fields. The characteristics of the radiation and secondary particles such as positrons, muons and pions generated via these schemes are finally summarized, and the experimental progresses are elaborated.

1.1 Classical electrodynamics

Classical electrodynamics is the classical field theory of electromagnetic phenomena, describing the interactions between electric charges, currents and fields. It treats the light as an electromagnetic wave. The most fundamental equations of classical electrodynamics are Maxwell's equations and Lorentz force equation (Jackson 1998). The Maxwell's equations

$$\begin{cases} \nabla \cdot \mathbf{E} = \dfrac{\rho}{\varepsilon_0} \\ \nabla \times \mathbf{E} = -\dfrac{\partial \mathbf{B}}{\partial t} \\ \nabla \cdot \mathbf{B} = 0 \\ \nabla \times \mathbf{B} = \mu_0 \left(\mathbf{j} + \varepsilon_0 \dfrac{\partial \mathbf{E}}{\partial t} \right) \end{cases} \tag{1}$$

describe the dynamics of electric and magnetic fields with charges and currents, where $\mathbf{E}$ is the electric field, $\mathbf{B}$ is the magnetic field, ρ is the electric charge density, $\mathbf{j}$ is the electric current density, ε_0 is the vacuum permittivity, μ_0 is the vacuum magnetic permeability. The Lorentz force equation

$$\mathbf{F} = q\mathbf{E} + q\mathbf{v} \times \mathbf{B} \tag{2}$$

describes the electromagnetic force on the charged particles, where q is the electric charge of the particle and $\mathbf{v}$ is the velocity of the particle.

According to classical electrodynamics, the accelerated charged particles can emit electromagnetic radiation, which is described by Liénard-Wiechert potentials (Liénard 1898; Wiechert 1901; Landau and Lifshitz 1980; Jackson 1998)

$$\varphi = \frac{1}{4\pi\varepsilon_0}\frac{e}{\left(R - \frac{\mathbf{v}\cdot\mathbf{R}}{c}\right)}, \quad \mathbf{A} = \frac{\mu_0}{4\pi}\frac{e\mathbf{v}}{\left(R - \frac{\mathbf{v}\cdot\mathbf{R}}{c}\right)}, \tag{3}$$

or the 4-vector form

$$A^i = e\frac{u^i}{R_k u^k}, \tag{4}$$

where $\mathbf{R}$ is the radius vector from the point where the charged particle is located at the point of observation, e is the electric charge of an electron, c is the speed of light in a vacuum, and u^k is the 4-velocity of the charged particle. Thus the expressions of the electromagnetic field can be written as

$$\begin{aligned}\mathbf{E} =& -\nabla\varphi - \frac{\partial\mathbf{A}}{\partial t}\\ =& \frac{1}{4\pi\varepsilon_0}\left\{e\left[\frac{\mathbf{n}-\boldsymbol{\beta}}{\gamma^2(1-\boldsymbol{\beta}\cdot\mathbf{n})^3R^2}\right] + \frac{e}{c}\left[\frac{\mathbf{n}\times[(\mathbf{n}-\boldsymbol{\beta})\times\dot{\boldsymbol{\beta}}]}{(1-\boldsymbol{\beta}\cdot\mathbf{n})^3R}\right]\right\},\end{aligned} \tag{5}$$

$$\mathbf{B} = \nabla\times\mathbf{A} = \frac{1}{c}\mathbf{n}\times\mathbf{E}, \tag{6}$$

where $\mathbf{n}$ is the direction of $\mathbf{R}$, $\boldsymbol{\beta} = \mathbf{v}/c$. Here, the first term of the electromagnetic field which is independent of acceleration is static fields, while the second term depending on $\dot{\boldsymbol{\beta}}$ is radiation field.

Since ones concern is more about the total radiation emitted by the charged particles, the angular distribution of radiation and its frequency spectrum can be derived further. The energy flux is given by the Poynting vector $\mathbf{S} = \frac{1}{\mu_0}\mathbf{E}\times\mathbf{B} = \frac{1}{\mu_0 c}|\mathbf{E}_a|^2\mathbf{n}$, where $\mathbf{E}_a$ is the radiation term of electric field. The power radiated per unit solid angle is

$$\frac{\mathrm{d}P(t)}{\mathrm{d}\Omega} = |\mathbf{A}(t)|^2, \tag{7}$$

where$\mathbf{A}(t) = \sqrt{\frac{1}{\mu_0 c}}R\mathbf{E}_a$. The energy radiated per unit solid angle is

$$\frac{\mathrm{d}W}{\mathrm{d}\Omega} = \int_{-\infty}^{\infty}|\mathbf{A}(t)|^2\mathrm{d}t = \int_{-\infty}^{\infty}|\mathbf{A}(\omega)|^2\mathrm{d}\omega = \int_0^{\infty}\frac{\mathrm{d}^2I}{\mathrm{d}\omega\mathrm{d}\Omega}\mathrm{d}\omega, \tag{8}$$

with $\mathbf{A}(\omega) = \frac{1}{\sqrt{2\pi}}\int_{-\infty}^{\infty}\mathbf{A}(t)e^{i\omega t}\mathrm{d}t$ the Fourier transform of $\mathbf{A}(t)$. Since $t = t' + R(t')/c$ is the retarded time, the distance from the particle to the observation point $R(t') \simeq x - \mathbf{n}\cdot\mathbf{r}(t')$, where x is the distance from the origin of coordinates to the observation point, $\mathbf{r}(t')$ is the position of the particle relative to the origin. Omit the primes on the time for brevity, the energy radiated per unite solid angle per unit frequency interval is given as (Landau and Lifshitz 1980; Jackson 1998)

$$\frac{\mathrm{d}^2 I}{\mathrm{d}\omega \mathrm{d}\Omega} = 2|\mathbf{A}(t)|^2 = \frac{1}{4\pi\varepsilon_0}\frac{e^2}{4\pi^2 c}\left|\int_{-\infty}^{\infty}\frac{\mathbf{n}\times[(\mathbf{n}-\boldsymbol{\beta})\times\dot{\boldsymbol{\beta}}]}{(1-\boldsymbol{\beta}\cdot\mathbf{n})^2}e^{i\omega(t-\mathbf{n}\cdot\mathbf{r}(t))}\mathrm{d}t\right|^2. \quad (9)$$

For a charged particle in relativistic circular motion, the radiation spectrum is (Schwinger 1949; Jackson 1998)

$$\frac{\mathrm{d}^2 I}{\mathrm{d}\omega \mathrm{d}\Omega} = \frac{1}{4\pi\varepsilon_0}\frac{e^2}{3\pi^2 c}\left(\frac{\omega\rho}{c}\right)^2\left(\frac{1}{\gamma^2}+\theta^2\right)^2\left[K_{2/3}^2(\xi)+\frac{\theta^2}{(\frac{1}{\gamma^2})+\theta^2}K_{1/3}^2\right], \quad (10)$$

where $K_{1/3}(\xi)$ and $K_{1/3}(\xi)$ are the modified Bessel functions, $\xi = (\omega\rho)/(3c)\left(1/\gamma^2+\theta^2\right)^{3/2}$. Since it was first observed in electron synchrotron (Elder et al. 1947), this kind of radiation is called synchrotron radiation. As a typical example in laser-plasma community, the betatron radiation which has been extensively investigated both in theory and experiments is actually a kind of synchrotron radiation and will be detailed in Sect. 2.1.

1.2 Linear QED

The existence of anti-particles relates to the QED vacuum. In quantum mechanics and QFT (Weinberg 1995), the vacuum is defined as the state with the lowest possible energy, i.e., the ground state of the Hilbert space, which is finite and non-zero. QED vacuum is a state with no matter particles and photons. In QED vacuum, the electric and magnetic fields have zero average values but their variances are not zero, so the QED vacuum contains fluctuation (Milonni and Smith 1975), which are an essential and ubiquitous part of QFT. Even a single pair created by a super-strong laser field in vacuum would cause the fast development of an avalanche-like QED cascade (Fedotov et al. 2010; Elkina et al. 2011). The cascade rapidly depletes the incoming laser pulse and limits the attainable intensities of the laser. Conventional perturbative QED calculation is usually expressed as a series expansion with respect to the coupling constant (fine-structure constant) $\alpha = e^2/4\pi\epsilon_0\hbar c \approx 1/137$, with $\hbar$ the reduced Planck constant. Feynman developed a series of rules to draw diagrams and then to write down the mathematical expressions of QED processes. The Feynman diagrams of some lowest-order QED processes are shown in Fig. 1.

Taking Compton scattering process as an example, as shown in Fig. 1a, b, it is the scattering of a high-energy photon after an interaction with a charged particle, usually a high-energy electron. The invariant matrix element can be written as following (Peskin and Schroeder 1995)

$$i\mathcal{M} = -ie^2\epsilon_\mu^*(k')\epsilon_\nu(k)\bar{u}(p')\left[\frac{\gamma^\mu \not{k}\gamma^\nu + 2\gamma^\mu p^\nu}{2p\cdot k}+\frac{-\gamma^\nu \not{k}'\gamma^\mu + 2\gamma^\nu p^\mu}{-2p\cdot k'}\right]u(p), \quad (11)$$

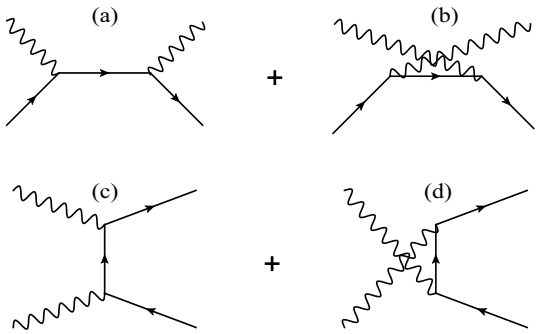

Fig. 1 Feynman diagrams of the lowest-order **a**, **b** Compton scattering and **c**, **d** Breit-Wheeler pair production. The wave line represents photon, the solid line with the arrow following (against) the time evolution direction represents electron (positron). The time evolves from left to right

where $\epsilon(k)$ and $\epsilon^*(k')$ are the polarization vectors of the initial and final state photon, k and k' are the momenta of the initial and final state photon, $u(p)$ and $\bar{u}(p')$ represent the initial and final state electron, p and p' are the momenta of the initial and final state photon, the Feynman slash notation $\not{k} = \gamma^\mu k_\mu$, and γ^μ is the Dirac matrix. The differential cross-section of Compton scattering with respect to the scattering angle can be expressed as

$$\begin{aligned}\frac{\mathrm{d}\sigma}{\mathrm{d}\cos\theta} =& \frac{1}{2\omega}\frac{1}{2m_e}\cdot\frac{1}{8\pi}\frac{(\omega')^2}{\omega m_e}\left(\frac{1}{4}\sum_{\text{spins}}|\mathcal{M}|^2\right)\\ =& \frac{\pi\alpha^2}{m_e^2}\left(\frac{\omega'}{\omega}\right)^2\left[\frac{\omega'}{\omega}+\frac{\omega}{\omega'}-\sin^2\theta\right],\end{aligned} \tag{12}$$

where ω and ω' are circular frequencies of the initial and final state photon, θ is the angle between the initial and final state photon, and m_e is the rest mass of the electron. This is the so-called (spin-averaged) Klein-Nishina formula (Klein and Nishina 1929). One can calculate the cross-section of Breit-Wheeler process in the same way.

1.3 Non-linear QED

The success of QED largely rests on its perturbation theory, expressed in Feynman diagrams, which, however, also leads to predictions beyond the perturbation theory. For example, in the presence of strong EM fields, it predicts that electrons and positrons will be spontaneously produced, thus causing the decay of the fields. This cannot be understood in terms of any finite number of Feynman diagrams and hence is described as non-perturbative. The linear QED is perturbative but the non-linear QED includes both the perturbative and non-perturbative regime. Essentially, the QED processes in a strong EM field are very different from the perturbative ways. In perturbative QED, the rate of the n-photon process is multiplied by the factor α^n, and the cross-section of the n-photon process should also be multiplied by I^n with I the intensity of laser field or by Z^n with Z the proton number of atomic nucleus (Greiner et al. 1985; Di Piazza et al. 2012; Hu 2020). Thus the perturbative calculation is inapplicable to the strong-field

case. With the upcoming PW-class laser facilities, one may measure non-perturbative QED in experiments and its transition from the perturbative regime to the non-perturbative regime. To describe this quantum non-linearity (Ritus 1985; Di Piazza et al. 2012; Gonoskov et al. 2022), the two gauge- and Lorentz-invariant parameters are introduced as follows,

$$\begin{aligned}\chi_e &= \frac{\sqrt{-\left(F_{\mu\nu}p^{\nu}\right)^2}}{m_e c E_{cr}} \\ &= \frac{\gamma}{E_{cr}}\sqrt{(\mathbf{E}+\mathbf{v}\times\mathbf{B})^2-(\mathbf{E}\cdot\mathbf{v}/c)^2},\end{aligned} \tag{13}$$

$$\begin{aligned}\chi_\gamma &= \frac{\hbar\sqrt{-\left(F_{\mu\nu}k^{\nu}\right)^2}}{m_e c E_{cr}} \\ &= \frac{\hbar\omega}{m_e c^2 E_{cr}}\sqrt{\left[\mathbf{E}+\left(c^2\mathbf{k}/\omega\right)\times\mathbf{B}\right]^2-\left[\mathbf{E}\cdot(c\mathbf{k}/\omega)\right]^2},\end{aligned} \tag{14}$$

where $F_{\mu\nu}$ is the EM field tensor, γ is the Lorentz factor, $E_{cr}=m_e^2c^3/e\hbar$ is the Schwinger field (Schwinger 1951) by which an electron gains energy m_ec^2 across a reduced Compton wavelength $\bar{\lambda}=\hbar/m_ec$. When $\chi_e>1$ or $\chi_\gamma>1$, the QED processes should not be treated perturbatively. For an electron in strong EM fields, χ_e represents the ratio of the field strength observed in the electron's rest frame to the Schwinger field E_{cr}. Since a photon travels at the speed of light, it does not have a rest frame. For a photon with angular frequency ω in strong laser fields to create an electron-positron pair, it must gain energy of $\Delta E=2\sqrt{p^2c^2+m_e^2c^4}-\hbar\omega\approx m_e^2c^4/\hbar\omega$ from the fields during the pair formation time $\Delta t\approx m_ec/eE_{eff}$, where $E_{eff}=\gamma|\mathbf{E}+\left(c^2\mathbf{k}/\omega\right)\times\mathbf{B}|$ is the field effective magnitude with which the electron or positron acquires a transverse momentum of m_ec over the formation time. This process should be smaller than the vacuum fluctuation according to the uncertainty principle, which means $\Delta E\Delta t<\hbar$, or $\chi_\gamma>1$ (Bassompierre et al. 1995; Gonoskov et al. 2022).

The dynamics of a single electron or positron in the presence of an EM field is governed by the Dirac equation,

$$[\gamma^{\mu}(p_{\mu}-eA_{\mu})-m_ec]\psi=0, \tag{15}$$

where A_{μ} is the potential of the field, ψ is spinor wave function of electron or positron. If the field is a plane EM wave, the solution to Eq. (15) is called the Volkov state (Wolkow 1935):

$$\begin{aligned}\psi_{p,s}(x) &= \left[1+\frac{e\not{k}\not{A}}{2kp}\right]\frac{u_{p,s}}{2\sqrt{E_p}}e^{iS_p(x)}, \\ S_p(x) &= -p\cdot x+f(\phi),\end{aligned} \tag{16}$$

where $u_{p,s}$ is the free spinor with momentum p and spin s, $\not{A} = \gamma^\mu A_\mu$, x is the four space-time coordinate and $\phi = k \cdot x$ is the phase of the plane EM wave, $f = f_1 + f_2$, $f_1 = \int_{\phi_0}^{k\cdot x} \mathrm{d}\phi \frac{eA\cdot p}{k\cdot p}$, $f_2 = \int_{\phi_0}^{k\cdot x} \mathrm{d}\phi \frac{e^2 p^2}{2k\cdot p}$. Described by Volkov states in the strong laser field QED, the electrons or positrons in the external fields are indicated by double solid lines in Feynman diagrams, called "dressed electrons" under Furry picture (Furry 1951), as shown in Fig. 2.

For example, the non-linear Compton scattering process $e(p) + l\gamma_L(k) \to e'(p') + \gamma(k')$ becomes $e_V(p) \to e'_V(p') + \gamma(k')$ in a strong field. Consider a laser pulse described by the potential of a transverse plane wave modified by an envelope function g, the EM vector potential is

$$A^\mu(\phi) = A_0 g(\phi) \mathrm{Re}(\epsilon_+^\mu \mathrm{e}^{-i\phi}), \tag{17}$$

where the temporal pulse shape $g(\phi) = \frac{1}{\cosh(\phi/\sigma)}$ denotes a hyperbolic secant pulse with width σ and $g(\phi) = \exp(-\phi^2/2\sigma^2)$ denotes a Gaussian pulse. The polarization of the background field is described by $\epsilon_\pm^\mu = \delta_1^\mu \cos\xi \pm i\delta_2^\mu \cos\xi$, with $\xi = 0, \pi/2$ denoting linear polarization and $\xi = \pi/4$ for circular polarization. The S matrix can be written based on the Feynman diagram (Seipt and Kämpfer 2011, 2013; Seipt et al. 2016),

$$\begin{aligned} S =& -ie\bar{\psi}(p')\gamma^\mu \epsilon'_\mu e^{ik'\cdot x}\psi(p) \\ =& -ie(2\pi)^4 \int \frac{\mathrm{d}s}{2\pi} \delta^{(4)}\big(p' + k' - p - sk\big)\mathcal{M}, \end{aligned} \tag{18}$$

$$\mathcal{M} = T_0 C_0 + T_+ C_+ + T_- C_- + T_2 C_2, \tag{19}$$

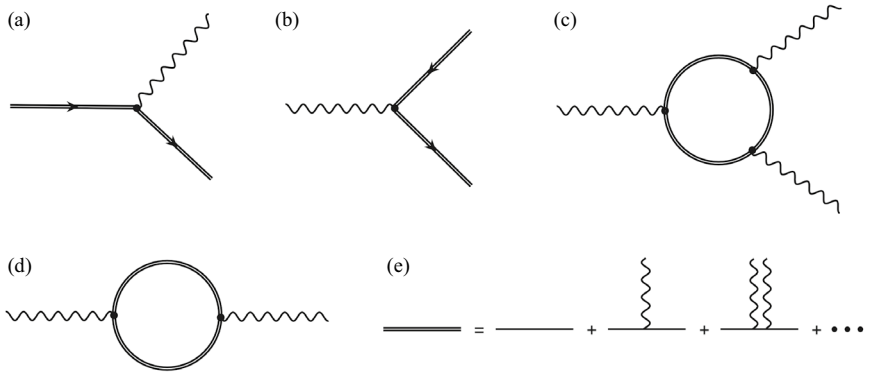

Fig. 2 Feynman diagrams of **a** non-linear Compton, **b** non-linear Breit–Wheeler, **c** photon splitting and **d** vacuum birefringence processes in strong laser fields. The double fermion lines in **e** indicate that the process occurs in an external laser field

where $\bar{\psi} = \psi^\dagger \gamma^0$, $\psi^\dagger$ is the hermitian conjugate of ψ, s parameterizes the momentum transfer by means of momentum conservation $p + sk = p' + k'$, T_j denotes the transition operators

$$T_0 = \bar{u}_{p'} \not{\epsilon}' u_p, \tag{20}$$

$$T_\pm = \bar{u}_{p'} (d_{p'} \not{\epsilon}_\pm \not{k} \not{\epsilon}' + d_p \not{\epsilon}' \not{k} \not{\epsilon}_\pm) u_p, \tag{21}$$

$$T_2 = d_p d_{p'} (\epsilon' \cdot k) \bar{u}_{p'} \not{k} u_p, \tag{22}$$

and $d_{p^{(\prime)}} = ma_0/(2k \cdot p^{(\prime)})$. The dynamic integrals over the laser phase determining the amplitude of the process are

$$C_0 = \int_{-\infty}^{\infty} \mathrm{d}\phi e^{is\phi - if(\phi)}, \tag{23}$$

$$C_\pm = \int_{-\infty}^{\infty} \mathrm{d}\phi e^{is\phi - if(\phi)} g(\phi) e^{\mp i\phi}, \tag{24}$$

$$C_2 = \int_{-\infty}^{\infty} \mathrm{d}\phi e^{is\phi - if(\phi)} g^2(\phi)[1 + \cos 2\xi \cos 2\phi], \tag{25}$$

where $f(\phi) = \int_0^\phi \mathrm{d}\phi' \{g(\phi') \mathrm{Re}(\alpha_+ \mathrm{e}^{-i\phi'} + \beta g(\phi')^2 [1 + \cos 2\xi \cos 2\phi]\}$, and $\alpha_\pm = d_p(2\epsilon_\pm \cdot p) - d_{p'}(2\epsilon'_\pm \cdot p)$, $\beta = d_p^2(k \cdot p) - d_{p'}^2(k \cdot p')$. Since $\mathrm{d}W = \frac{|S|^2}{VT} \mathrm{d}\Pi$, with $\mathrm{d}\Pi$ denoting the final state phase space, the angular- and energy-differential photon emission probability is (Seipt and Kämpfer 2011, 2013; Seipt et al. 2016)

$$\frac{\mathrm{d}W}{\mathrm{d}\omega' \mathrm{d}\Omega} = \frac{e^2 \omega' |\mathcal{M}|^2}{64\pi^3 (k \cdot p)(k \cdot p')}, \tag{26}$$

where $\mathrm{d}\Omega = \mathrm{d}\phi \mathrm{d}\theta$ is the solid angle element about the emitted photon direction. The calculation is not easy because the integrals over the plane-wave field phase is complicated. Thus, various numerical and analytical methods have been introduced to evaluate the integrals. For more details, please see the references (Mackenroth and Di Piazza 2011; Seipt et al. 2016; Fedotov et al. 2023).

1.4 Nonperturbative effects in non-linear QED

When the electric field in the electron rest frame approaches the critical field for QED, i.e., the Schwinger field $E_{cr} = 1.3 \times 10^{18}$ Vm^{-1} (Schwinger 1951), the interaction between laser and matter enters into a QED-dominated regime, a largely unexplored realm both theoretically and experimentally. In this new regime, extremely rich non-linear phenomena such as the violent acceleration of electrons and ions,

copious electron-positron pair production, ultra-brilliant X/γ-ray emission, vacuum birefringence, photon-splitting, etc, are involved. These non-linear QED processes become important and provide unique opportunities for laboratory astrophysics (Remington 2005), including the γ-ray burst, magnetospheres of pulsars creation, active galactic nuclei, and black-hole jets. As the emitted photon energy becomes comparable with the electron energy, the recoil during the photon emission significantly alters the particle's motion in the EM fields, a process known as radiation reaction (RR) (Blackburn 2020). In such ultra-intense laser fields, the emitted photons are capable of decaying into lepton pairs via Breit-Wheeler (BW) process and copious matter and antimatter can be generated in the form of electron-positron or muon pairs, forming the so-called $e^+e^-\gamma$ plasma or QED plasma (Masood 2019). Especially, the QED process and plasma physics are inseparable, which otherwise is inaccessible on earth and exists only under extreme conditions, e.g., in the interstellar.

Until now, some of the QED predictions in weak field regime have been tested in experiments with even very high accuracy (Aoyama et al. 2012; Ohayon et al. 2022). In non-linear regime, the well-known pioneering experiment, E144 at SLAC (Bula et al. 1996; Bamber et al. 1999), measured the multiphoton absorption in Compton scattering and electron-positron pair production in electron-laser colliding but never reached the Schwinger field. On the other hand, QED cascades were also predicted to limit the attainable intensity of the laser and therefore severely hindered experiments at extreme field intensities (Fedotov et al. 2010; Elkina et al. 2011). Since many predictions remain to be confirmed and thoroughly tested in strong-field experiments, a number of schemes and experiments have been proposed based on high-power lasers as mentioned above. For example, SLAC is planning the E320 experiment at FACER-II by colliding a 10 GeV electron beam with a 10 TW laser pulse, in order to observe the transition from the perturbative to the non-perturbative regime (Chen et al. 2022). The recent LUXE experiment has been also proposed at DESY in Hamburg to study the strong-field QED with a 16.5 GeV electron beam colliding with a 350 TW laser (Fleck and on behalf of the LUXE collaboration 2022). Meanwhile, the PW laser facilities at BELLA has recently commissioned its second laser pulse transport line, enabling strong-field QED experiments (Turner et al. 2022). This is undoubtedly an area of active research with a high challenge both in theory and experiments and new progresses up to and beyond the Schwinger critical field are highly anticipated (Yu et al. 2023).

2 Bright X/γ-ray emission driven by strong laser fields

Röntgen first produced and detected EM radiation in a wavelength range known as X-rays, for which he became the first Nobel Prize winner in physics. This great discovery pioneered X-ray imaging, paved the way for medical diagnosis, opened the physics revolution of the 20th century, and provided the testing tools for many major scientific discoveries. In 1900, Villard discovered γ radiation while studying radiation emitted by radium and in 1903 Rutherford named this radiation γ-rays based on their strong penetration of matter compared to α- and β-rays. Different disciplines

have different definitions to distinguish X/γ-rays, since they are overlapping in the electromagnetic spectrum. In the laser-plasma community, one generally distinguishes these two types of radiation by the wavelength (L'Annunziata 2003). With radiation shorter than some arbitrary wavelength, e.g., 10^{-11} m, we may call it γ-rays. Otherwise, it is X-rays with lower photon energy.

Bright X/γ-rays with high photon energy, high peak brilliance, short pulse duration, and small source size have become an indispensable tool in fundamental science, medicine and industry, opening new perspective for many cutting-edge applications (Gari and Hebach 1981; Corde et al. 2013; Howell et al. 2021). For example, in nuclear dynamics research, ultra-bright high-energy photon sources with pulse duration as short as attoseconds and photon energy as high as hard X-rays and even γ-rays are required. High-energy γ-ray sources enable it to image dense objects in high-resolution radiography that are not visible to low-energy X-ray sources. In addition, high-energy radiation sources with micron-scale sizes and fs-scale pulse duration allow higher resolution imaging. No matter short X-rays or γ-rays, we can produce them in ultra-intense laser-plasma interaction via electron motion in strong EM fields (Lei et al. 2018; Magnusson et al. 2019), optical frequency conversion (Tecimer 2012; Popmintchev et al. 2010; Peng et al. 2021) or inverse Compton scattering (Seipt et al. 2015; Li et al. 2020; Lv et al. 2022), which has been extensively investigated and demonstrated in experiments (Chen et al. 2013b; Ma et al. 2023; Petrillo et al. 2023). It has been shown that, as the laser intensity increases to 10^{22} W/cm^2, the charged particles under the effect of such a high-intensity laser can acquire tremendous energy from the laser field and coherently radiate high-energy γ-photons. The emitted γ-photons with momenta comparable to the electrons will also recoil on the electrons, making the motion of electrons and ions changed significantly (Nakamura et al. 2012; Ji et al. 2014b; Blackburn et al. 2014; Chen et al. 2018). On the other hand, by colliding with another radiation source like the laser or microwave, these high-energy γ-photons can annihilate into lepton pairs. Finally, the physical processes of high energy γ-photon radiation, dense electron-positron pair generation, and RR effect are coupled and interplay with each other to become a special form of matter, i.e., $e^+e^-\gamma$ plasma, exhibiting significant QED effects.

With the upgrading of next-generation synchrotrons (Bilderback et al. 2005) and the construction of X-ray free electron lasers (XFEL) (Bostedt et al. 2016), bright radiation sources in the X-ray range are now available, with peak brilliance ranges of 10^{19-24} and 10^{27-32} photons/s/mm^2/mrad^2/0.1%BW, respectively. Synchrotron radiation and XFEL sources have been widely used in fundamental research, design and production of new materials, biology and industry because of their excellent performances. However, the large size and high cost of these large-scale facilities limit ones' access to the sources. In addition, the photon energies of radiation emission by the XFEL and synchrotrons are usually limited to a few keV and a few hundred keV, respectively. Although bremsstrahlung radiation, based upon the interaction of hot electrons with solid targets, can generate γ-rays in the MeV range, the resulting pulse duration is typically as long as ps, with up to hundred-μm size and hundred-mrad divergence. It is still challenging to attain collimated γ-ray pulses with high brilliance and short duration, which becomes an outstanding problem.

Table 1 Different X/γ-ray sources based-on laser-plasma interaction

Laser intensity (W/cm^2)	Electron density (cm^{-3})	Photon energy (MeV)	Laser2photon efficiency	Divergence angle	Peak brilliance[2]
3.6×10^{18}	$\sim 1\times10^{19}$	0.3–2	-	4 mrad	3×10^{22}@0.74 MeV (Yu et al. 2016)
4.7×10^{18}	$\sim 1.1\times10^{19}$	>0.35	–	$\sim 1°$	1×10^{21}@100 keV (Phuoc et al. 2012)
4×10^{19}	3.2×10^{18}	18	–	2.5 mrad	1.8×10^{20}@15 MeV (Sarri et al. 2014)
3×10^{20}	1.1×10^{23}	0.1	1.2×10^{-4}	$\sim 5°$	3.7×10^{22}@100% (Wang et al. 2019)
2.3×10^{20}	1.1×10^{23}	0.4	1×10^{-4}	$\sim 2°$	1×10^{23} (Yi et al. 2016)
[1]4.3×10^{21}	1.65×10^{21}	34	0.51%	$\sim 11°$	1×10^{23}@1 MeV (Zhu et al. 2018)
4.3×10^{21}	7.6×10^{23}	500	10%	$\sim 1°$	1.2×10^{27}@5 MeV (Wang et al. 2018)
4.9×10^{21}	$1.2-6\times10^{19}$	3000	> 10%	$\sim 0.3°$	4×10^{26}@1 MeV (Zhu et al. 2020)
5×10^{21}	3×10^{19}	30	2%	<10 mrad	1×10^{29}@10 MeV (Thomas et al. 2012)
5.3×10^{21}	1×10^{21}	40	2%	$\sim 40°$	1.1×10^{23}@1 MeV (Huang et al. 2018)
1.4×10^{22}	2.2×10^{23}	78	1.2%	$\sim 9°$	1×10^{22}@1 MeV (Zhang et al. 2021)
[1]5×10^{22}	1.65×10^{21}	500	1.8%	$\sim 6°$	1×10^{24}@1 MeV (Hu et al. 2021)
8.6×10^{22}	$0.4-4\times10^{21}$	3000	13%	$\sim 11°$	1×10^{26}@1 MeV (Lu et al. 2021)
1×10^{23}	1.76×10^{18}	3500	–	3 mrad	5×10^{23} (Lobet et al. 2015)
3×10^{23}	4.4×10^{21}	1500	1.4%	$\sim 22°$	2×10^{24}@58 MeV (Gu et al. 2018)

[1]LG laser

[2](Photonss^{-1}mm^{-2}mrad^{-2}per0.1%BW)

As a newly emerging and rapidly developed light source, the plasma-based novel radiation sources covering a wide range of topics have received significant attention in the past ten years. Recently, several review papers have been already available for a complete review of X/γ-ray radiation. Especially, Hadjisolomou et al. (2023) compared several schemes for enhanced γ-photon emission from various targets. In this topical review, we focus on the progress of high-energy photon radiation and lepton pair generation in strong-field QED regime, especially including but not limited to the advances by the authors in recent years. Table 1 presents the beam quality of different X/γ-ray sources from several typical schemes based-on laser-plasma interaction. One sees that, depending on the laser intensity (from weak relativistic to ultra-relativistic) and plasma density (from gas to solid), the photon emission is a different case by case but betatron radiation in gas plasmas and inverse Compton scattering by solid targets have been demonstrated very efficient, which we payed more attention to in the following due to their potentials in brilliant light sources and subsequent QED processes.

2.1 Betatron radiation

Batatron radiation as a kind of solution towards high-quality short pulse radiation source originates from relativistic electrons undergoing transverse betatron oscillations in self-generated quasi-static electric field in a wakefield (Wang et al. 2002; Kiselev et al. 2004; Rousse et al. 2004). This is generally produced by a driven laser propagating in gas or near-critical density (NCD) plasma. When a relativistic laser pulse is incident into underdense plasmas, the wakefield can be excited under certain laser intensity (Lu et al. 2007) and the longitudinal field effect becomes as significant as the transverse field. The electrons in the appropriate phase of the accelerating field can be accelerated to relativistic energies on the scale of a few millimeters by the wakefield, which is well-known as the laser wakefield acceleration (LWFA) (Tajima and Dawson 1979). At the relativistic high laser intensity, the LWFA enters the so-called bubble acceleration regime, in which an ultra-strong laser pulse displaces electrons in the plasma and forms a near-spherical region behind the laser pulse, driving strongly non-linear plasma wave to form an ion cavity or bubble (Pukhov and Meyer-ter Vehn 2002). The electric field in the bubble is up to hundreds of GV/m, which accelerates and focuses the energetic electrons injected into the rear of the bubble (Lu et al. 2007). The generated electron beam is usually characterized by an energy from hundreds to thousands of MeV, normalized divergence of several to tens of mm·mrad, and duration on the order of fs (Jansen et al. 2014). In addition, the off-axis electrons oscillate transversely as they are accelerated, radiating X-rays at a forward cone angle, i.e., betatron radiation (Esarey et al. 2002). Its characteristic frequency is $\omega_\beta = \omega_\mathrm{p}/\sqrt{2\gamma_\mathrm{e}}$, where $\gamma_\mathrm{e} = (1-\beta_\mathrm{e}^2)^{-1/2}$ is the relativistic Lorentz factor related to the normalized velocity of the electron β_e. Here, $\omega_\mathrm{p} = \sqrt{4\pi n_\mathrm{p} e^2/m_\mathrm{e}}$ is the plasma frequency, and n_p is the plasma density. Betatron radiation has been considered as a unique source for high-resolution X-ray imaging in a compact laser-gas geometry. For example, a recent experiment assisted by the batatron radiation have successfully imaged, for the first time, a laser-driven shock wave in a silicon target via radiograph (Wood et al. 2018). It indicates that the compact betatron sources

have practical utilities in high energy density physics experiments for imaging and diagnosis.

At present, the energy of electrons generated from laser wakefield can reach 8 GeV (Gonsalves et al. 2019), which is very close to the grand goal of single-stage acceleration to 10 GeV and is a critical step towards multi-stage acceleration to 1 TeV in the future. Based upon the LWFA-produced electron beams, fs-scale X/γ-ray pulses in the energy range of keV to MeV can be generated via betatron radiation (Kneip et al. 2008; Cipiccia et al. 2011; Chen et al. 2013a). The resulting photon sources have a typical peak brilliance of 10^{19-23} photons/s/mm^2/mrad^2/0.1%BW, and the total photon number is limited to 10^{7-8} photons per shot with the laser-to-photon energy conversion efficiency on the order of 10^{-6}.

To enhance the betatron radiation, significant efforts have been steadily dedicated, such as via stronger transverse oscillation of electrons in the wakefields (Ta et al. 2008) and high-energy electron beam-driven plasma wakefields (Holloway et al. 2017; Ferri et al. 2018). However, it remains challenging to greatly improve the photon energy, energy conversion efficiency and brightness of γ-ray emission. Since the dephasing length of the LWFA is $L_{deph} \propto 1/n_e$, low-density plasmas are believed to be more conducive to accelerating the bubble electrons to relativistic energy and thus to attaining higher photon energies (Jansen et al. 2014). On the other hand, high-density plasmas are beneficial for betatron transverse oscillation. This contradiction limits the number of the emitted photons to 10^{7-8} and the photon energy to hundreds of keV. To overcome this dilemma, a two-stage plasma scheme has been recently proposed to combine the advantages of efficient electron acceleration in low-density LWFA and efficient photon radiation in relatively high-density LWFA (Zhu et al. 2020). This was achieved by the use of a moderate low-density plasma for high-energy electron acceleration combined with a relatively high-density plasma for efficient γ-ray emission, as shown in Fig. 3. Multi-dimensional particle-in-cell (PIC) simulations showed that the generated γ-ray beam has a peak brightness of 4×10^{26} photons/s/mm^2/mrad^2/0.1%BW at 1 MeV and cutt-off energy of up to 3 GeV. It is also shown that the energy conversion efficiency from the PW laser to electrons and photons can be as high as 50% and 10%, respectively. As a consequence, the peak brilliance and photon number of the emitted γ-rays can be improved significantly by several orders of magnitude compared with previous betatron radiation sources (Zhu et al. 2020, 2021).

Different from the normal betatron radiation, as the laser intensity and plasma density increases, the electrons can be accelerated directly by the laser pressure, which oscillates in the laser fields to emit high-energy X/γ-rays, called betatron-like radiation, a highly non-linear betatron radiation regime (Yu et al. 2013). A recent experiment demonstrated that the laser energy conversion efficiency to the X-rays emission as a PW laser pulse irradiates NCD plasma can reach 10^{-4}, which is nearly 1–3 orders of magnitude higher than the normal betatron source (Tan et al. 2021). Instead of the single-stage NCD plasma configuration, a PW laser-driven two-stage NCD plasma scenario has also been proposed to enhance the betatron-like photon emission (Lu et al. 2021). It is shown that the electrons accelerated by LWFA in the first $0.3n_c$ plasmas can be further accelerated directly by the evolved mid-infrared light after they enter into the second $3n_c$ plasmas,

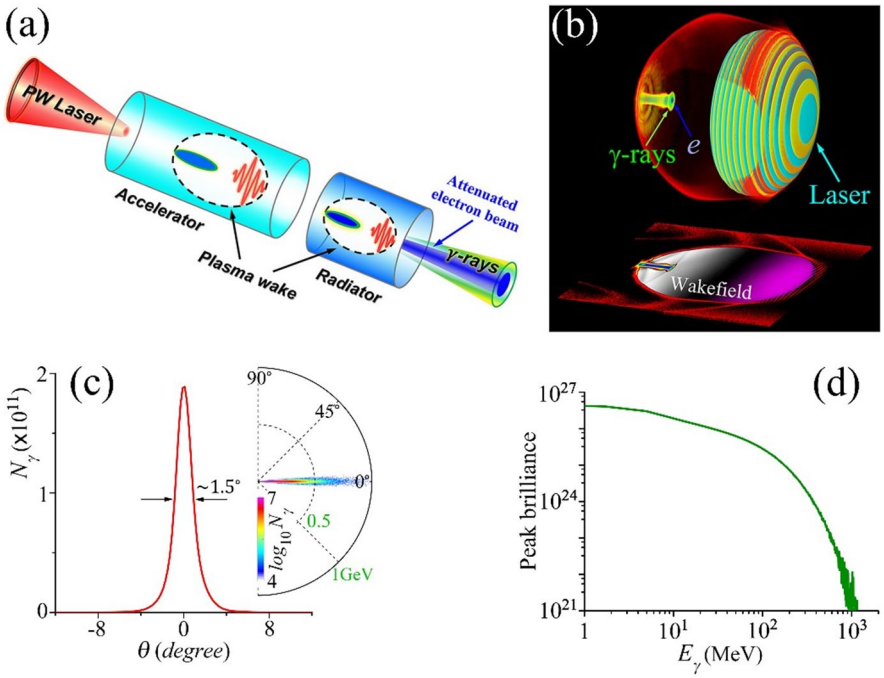

Fig. 3 **a** Concept of extremely brilliant γ-rays from a two-stage laser-plasma accelerator. **b** Three dimensional (3D) simulation results of bright γ-ray emission in this scheme. **c** The angular-spectrum and angular distribution of γ-rays emitted. **d** The peak brilliance of γ-rays as a function of the photon energy (Zhu et al. 2020)

where $n_c = m_e\omega_0^2/4\pi e^2$ is the critical density of plasma with ω_0 is the circular frequency of the driven laser. The resulting geometric brightness of the produced γ-ray is two orders of magnitude higher than that of the uniform NCD plasmas. During the process, the RR effect plays a significant role in the electron dynamics in these two-stage NCD plasmas (Guo et al. 2019). However, these electrons become "off-axis" gradually, making the photon emission highly divergent. A way to control the photon emission was proposed by Stark et al. (2016), taking advantage of a novel dense subject target ($100n_c$) with a NCD plasma channel ($10n_c$) in the middle. In this scenario, the incident PW laser pulse drives a quasi-static magnetic field of the order of Mega Tesla (MT) in the plasma. The magnetic field contributes to the continuous acceleration of electrons, thus enhancing the betatron-like emission. The application of this pre-fabricated hollow target with a relatively transparent channel can control the direction of the photon beam during the laser propagation, thus providing a possible solution for generating tens of TW-oriented MeV photon beams on the PW laser facilities.

Although the betatron-like radiation has an indubitable advantage of high flux and geometric brightness, it usually leads to a large beam divergence (Kneip et al. 2008; Huang et al. 2018). In recent years, the waveguides and nano-structured targets have

been introduced to improve the beam collimation (Wang et al. 2019; Yi et al. 2016; Wang et al. 2018; Yu et al. 2013). For example, Wang et al. (2018) used a sub-micron wire target to generate brilliant hundreds of MeV γ-rays. In their configuration, the quasi-static electric and magnetic fields generated around the wires are responsible to drive the oscillations of wire surface electrons, resulting in the generation of oriented ultra-intense γ-ray beam. The corresponding photon brightness was predicted to reach 10^{27} photons/s/mm^2/mrad^2/0.1%BW at 5 MeV, which is second only to that of the X-ray free-electron laser, while the photon energy is three orders of magnitude higher than the latter. Such bright high-energy γ-ray sources with photon energy in the MeV to GeV range are desired especially for many cutting-edge applications and scientific research (Mourou et al. 2006), such as imprinting quantum processes (ATLAS Collaboration 2017), exploring high energy particle physics (Badelek et al. 2004), photonuclear physics, and laboratory physics, etc.

2.2 Non-linear compton scattering

Non-linear Compton scattering (NCS), as a non-linear version of inverse Compton scattering (Compton 1923), is known as an emission process of X/γ-rays by the charged energetic particles scattering multiple low-energy photons provided by a very intense EM field, e.g., a relativistic laser pulse. The classic limit of the NCS is the so-called non-linear Thomson scattering or multi-photon Thomson scattering. NCS is capable of producing photons with energy comparable to the rest energy of parent particles and even higher, so that it has been widely used for triggering secondary processes such as lepton pair production, nuclear reaction and for exploring non-linear QED. In the past decades, the NCS has been extensively investigated in various areas (Nakamura et al. 2012; Ridgers et al. 2012) and it has been shown commonly existing in γ-ray bursts (MAGIC Collaboration. et al. 2019) and Sunyaev-Zel′dovich effect, underlying laboratory and astrophysical sources of high-energy X/γ-rays.

NCS has been observed and measured in the well-known E144 experiments (Bula et al. 1996; Bamber et al. 1999), where a 46.6 GeV electron beam obtained from the SLAC linear accelerator collides with a TW laser with the dimensionless laser parameter $a_0 \approx 0.4$. Recently, high-order non-linear scattering has also been observed in an experiment, where more than 500 near-infrared laser photons were scattered by a single electron into a single γ-photon with energy up to several tens MeV. In both experiments above, however, the QED effect is weak since the non-linear quantum parameter, i.e., Eq. (13), is very small, i.e, 0.17 and 0.01 in the first and second case, respectively. Here, the non-linear quantum parameter χ_e compares the field strength observed in its instantaneous rest frame with the Schwinger field E_{cr} and describes how the QED effect matters during the scattering process. Recently, SLAC is planning the E320 experiment at FACER-II by colliding a 10 GeV electron beam with a 10 TW laser pulse (Chen et al. 2022). A similar scenario has been proposed in a recent LUXE experiment, which aims at performing precise measurements of non-linear Compton scattering and BW pair production in the transition from the perturbative to non-perturbative regime (Fleck and on behalf of the

LUXE collaboration 2022). This can be achieved by means of electron-laser and photon-laser interactions with the 16.5 GeV electron beam of European XFEL and a laser beam of the power up to 350 TW. As the increase of the electron energy γ and laser intensity I_0, χ_e increases accordingly and the photon emission becomes intensified, exhibiting detectable QED effects in experiments. This can be easily realised in intense laser-plasma interaction, where the electrons can be accelerated alternatively to extremely high energies in length scales of less than several millimeters by a PW-class laser pulse. Taking a 300 TW laser and 1 GeV electron beam as an example, $\chi_e \approx 0.56$ and $\chi_\gamma \approx 0.24$, which provides a promising way for copious γ -photon emission with a much smaller scale infrastructure as compared to the large synchrotrons. This scenario has also been proposed at BELLA center, which has recently commissioned its second laser pulse transport line, enabling strong-field QED experiments by a head-on collision of laser-driven GeV electron beam with the PW laser pulse (Turner et al. 2022).

When a relativistic electron beam head-on collides with an ultra-intense laser beam, the electrons absorb multi-low-energy photons and emit high-energy γ-photons propagating in the same direction as the electrons. The probability of NCS mainly depends on the quantum parameter χ_e and the latter is determined by the vertical component of the Lorentz force. When the high-energy electrons propagate in the same direction as the laser, the vertical component of the electric field $E_\perp$ is almost canceled by $\beta \times \mathbf{B}$, which makes χ_e close to 0. In this case, the NCS gets inhibited. On the contrary, when the high-energy electrons propagate in the opposite direction of the laser, the NCS is significantly activated, leading to prominent photon radiation. In the ultra-relativistic case with $\gamma \gg 1$, χ_e reaches maximum when the electrons counter-collide with the laser field, which can be approximated as $\chi_e \approx 2\gamma(E/E_{cr})$. Therefore, it is preferable to employ two laser beams in NCS experiments with the first being the driven laser for generating high-energy electrons and the second counter-propagating from the other side as a scattering beam (Gu et al. 2016; Li et al. 2017a). However, considering the experiment difficulties in constructing a head-on collision configuration and in detecting the emitted photons, one single laser or two crossed laser beams with certain angle are usually used as an alternative.

With a single laser, a smart all-optical Compton γ-ray source was demonstrated, where the laser pulse drives a wakefield cavity first in the gas and then gets reflected by a mirror to collide with the trapped electron beam in the bubble (Phuoc et al. 2012). The experiment results show that the X-ray beams are generated in a broadband energy range extending up to a few hundred keV and with a high peak brightness of 10^{21} photons/s/mm^2/mrad^2/0.1%BW at 100 keV. Recently, Gu et al. (2018) propose a scheme for brilliant γ-ray emission with a similar configuration. In their scheme, a laser pulse of 3×10^{23} Wcm^{-2} propagates tens of microns in the NCD plasma first and then gets reflected off the solid surface, being broken into several short high harmonics. When the captured electrons collide with the reflected attosecond pulses, the peak power of the radiated γ-rays is as high as 0.74 PW, with brightness up to 2×10^{24} photons/s/mm^2/mrad^2/0.1%BW at 58 MeV. It has also been shown that high-power high-efficiency γ-ray flash can be generated in multi-petawatt laser interaction with various solid targets (Nakamura et al. 2012;

Lezhnin et al. 2018; Hadjisolomou et al. 2023). The so-called γ-flash mechanism, a kind of NCS was proposed to interpret the copious γ-photon emission, which can then been applied for short-pulse electron-positron pair production by colliding the γ -flash with a secondary laser pulse (Kolenatý et al. 2022; MacLeod et al. 2023).

By using two laser pulses with the first for accelerating electrons to relativistic energy and the other providing the field of a relativistically intense laser to scatter the electrons, many schemes have been proposed to enhance the X/γ -ray emission, as schemedically shown in Fig. 4. In theses scenarios, the generated photons can be detected and distingushed by deflecting the charged particles such as electrons, positrons, and ions, by using several magnets. For example, Thomas et al. (2012) predicted not only a high peak spectral brilliance exceeding 10^{29} photons/s/mm^2/mrad^2/0.1%BW with an approximately 2% energy conversion efficiency and a peak energy of 10 MeV, but also an angularly resolved radiation spectrum. The latter can server as a signature of QED effect. In another experiment, a similar setup has been reported but with a much lower laser intensity, where a narrow divergence γ-ray beam is generated by Thomson scattering of laser-wakefield accelerated electrons with an intense laser pulse (Sarri et al. 2014). It is demonstrated that the maximum energy of the γ-ray beam is of the order of 16–18 MeV, and its brilliance exceeds 10^{20} photons/s/mm^2/mrad^2/0.1%BW at 15 MeV.

We have also faced many theoretical problems in NCS, to name just a few, infrared behaviour (Dinu et al. 2012; Ilderton and Torgrimsson 2013), carrier envelope phase effects (Mackenroth et al. 2010; Seipt and Kämpfer 2013), spin and polarisation effects (King and Tang 2020; Tang et al. 2020), pulse shape and interference effects (Narozhnyi and Fofanov 1996; Boca and Florescu 2009), etc (Fedotov et al. 2023). For example, the emission of soft photons via NCS in a pulsed laser field is in general infrared divergent. How to remove the divergence in a low-energy part of

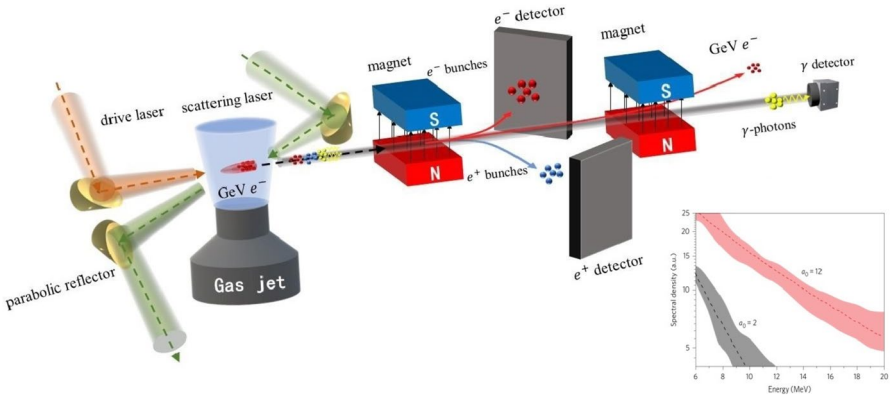

Fig. 4 Sketch of the experimental setup: a relativistic laser pulse is focussed at the edge of a gas cell to generate an ultra-relativistic electron beam. A second laser beam is incident on the electron beam with a certain angle to trigger the NCS process, so that copious high-energy photons can be produced along the electron beam propagating direction. These photons can be distinguished and detected by deflecting the charged particles using several magnets. The insect exhibits the typical energy spectra of γ-photons by colliding a 200 or 400 MeV electron beam with a scattering laser pulse at 155° in experiments (Yan et al. 2017a)

a radiation spectrum becomes a critical issue (Dinu et al. 2012; Ilderton and Torgrimsson 2013). Another key problem for ultrashort laser duration is the carrier-envelope-phase (CEP) effect, i.e., the relative phase between the pulse envelope and the carrier wave, which affects the angular emission range in the laser polarisation plane (Mackenroth et al. 2010; Seipt and Kämpfer 2013). All these have been challenges for theoreticians and hot research topics for researchers.

2.3 Photon polarization in strong laser fields

Spin is an intrinsic property about angular momentum, which is carried by all elementary particles. Spin polarization is the degree to which the spin of a beam of partiles is aligned with a specific direction. Since the cross-section of a specific reaction channel always depends on the spin orientation of the initial and final state particles, spin-polarized relativistic particle beams are ideally suited for exploring the detailed dynamics of particle physics, nuclear physics, astrophysics, etc. It is well known that each photon has a spin $\pm\hbar$, and these spins of photons are aligned in the circularly polarized (CP) laser, so that a laser pulse of finite radius has a spin angular momentum (SAM). Polarized quasi-monoenergetic γ-rays with photon energy of MeVs are ideal tools for studying the nuclear resonance fluorescence and the parities of low-lying dipole states of nucleus (Pietralla et al. 2001). Polarized GeV γ -rays can be used as tagged-photon in meson photoproduction and decay (Akbar et al. 2017). In astrophysics, the polarisation signal of X-rays or γ-rays could reveal information about the interactions of dark matter and neutrinos (Boehm et al. 2017). In high-energy physics, by employing polarized high-energy γ-rays, it is shown that the required measurement time for vacuum birefringence could be reduced by two orders of magnitude (Bragin et al. 2017).

There are two main conventional methods of producing polarized X/γ-rays. One is the linear Compton scattering between polarized laser and unpolarized electron beam (Bocquet et al. 1997; Omori et al. 2006; Howell et al. 2021). In this case, the formation length of the radiated photon is much larger than the laser wavelength, so that the polarization of the photons mainly depends on the drive laser. Though the interaction Hamiltonian $H_{int}(x) = e\bar{\psi}(x)\gamma_{\mu}\psi(x)A^{\mu}(x)$ indicates the interaction occurs at a local point x, the real QED process takes place not in one point but in some space-time domain, and the formation length is known as the longitudinal dimension of this domain (Baier and Katkov 2005). Because the scattering cross-section of the linear Compton scattering of electron and photon is small (dσ/dE~mb/MeV), the luminosity of the polarized X/γ-rays is much lower than that of the electron beams (Fukuda et al. 2003; Omori et al. 2006). Using high-intensity lasers can naturally increase the luminosity, but the NCS would dominate the interaction. The other is through the bremsstrahlung (Olsen and Maximon 1959; Abbott et al. 2016). When an electron beam passes through a thin metal foil, incoherent bremsstrahlung occurs under the action of coulomb field near the nucleus. This can produce CP γ-rays, but the scattering angle is too large to produce linearly polarized (LP) γ-rays (Uggerhøj 2005;

Giulietti et al. 2008). When an electron beam passes through a crystal, the nuclei causes periodic disturbances to the electron trajectory, resulting in coherent bremsstrahlung of the electron (Timm 1969). In the specific orientation of the crystal, the γ-ray radiation is linearly polarized. However, the damage threshold of the crystal limits the energy of the electron beams and thus the intensity of the radiated γ-rays.

As an alternative, ultra-intense laser-driven γ-ray sources can provide high-energy high-brilliance ultra-short polarized γ-ray sources. It has been reported that the laser accelerated electron beams can generate high-energy polarized γ-rays through bremsstrahlung, but the large energy spread and divergence angle limit the peak brilliance of the γ-ray sources (Giulietti et al. 2008; Schumaker et al. 2014). Using currently available laser-accelerated GeVs electron bunches scattering off laser pulses of moderately relativistic intensities, the circularly or linearly polarized γ-rays with polarization degree exceeding 78% or 91% can be generated in the weak non-linear regime (Tang et al. 2020). In this case, the probability of generating photons with different polarizations via the weak NCS process can be calculated as follows (Tang et al. 2020)

$$P_j = \frac{\alpha}{(2\pi)^2}\frac{1}{\eta_p^2}\int_0^1 \frac{s}{t}\mathrm{d}s \int \mathrm{d}^2 r^{\perp} \int \mathrm{d}\phi\, \mathrm{d}\phi' \times \left[T(\epsilon_j) e^{ic(\phi-\phi')-i\int_{\phi'}^{\phi} \frac{2p\cdot a(\phi)-a^2(\phi)}{2\kappa\cdot p}\,\mathrm{d}\phi}\right], \tag{27}$$

where $\eta_p = \kappa\cdot p/m^2$, $s = \kappa\cdot k/\kappa\cdot p$ is the light-front momentum fraction of the scattered photon, $t = 1-s$ and $c = (k^+ + q^+ - p^+)/2\kappa^0$, $\phi = \kappa\cdot x$ is the external-field phase with wave vector $\kappa = \omega_0(1,0,0,1)$ satisfying $\kappa^2 = 0$, $\kappa\cdot a = 0$. Here, the light-front coordinates are used: $x^{\pm} = x^0 \pm x^3$, $x^{\perp} = (x^1, x^2)$. It is convenient to express the photon polarization in terms of the eigenstates of the polarization operator in the background field (King and Tang 2020). For a LP background laser field with polarization either $\varepsilon_1 = (0,1,0,0)$ or $\varepsilon_2 = (0,0,1,0)$, the eigen-polarization can be introduced in terms of the orthogonal basis

$$\epsilon_1 = \varepsilon_1 - \frac{k\cdot\varepsilon_1}{k\cdot\kappa}\kappa, \quad \epsilon_2 = \varepsilon_2 - \frac{k\cdot\varepsilon_2}{k\cdot\kappa}\kappa. \tag{28}$$

For a CP background laser field with polarization $(\varepsilon_1 \pm i\varepsilon_2)/\sqrt{2}$, the eigen-bases are replaced with $\epsilon_{\pm} = (\epsilon_1 \pm \epsilon_2)/\sqrt{2}$, where the sign $+(-)$ denotes the left-hand (right-hand) rotation of the polarisation. For the details of the function $T(\epsilon_j)$ in Eq. (27), please see the references (King and Tang 2020). The polarization degree which varies from – 100 to 100%, is defined as $P = (P_1 - P_2)/(P_1 + P_2)$ ($P = (P_+ - P_-)/(P_+ + P_-)$) for a linearly (circularly) polarised background.

When $a_0 \gg 1$, the interaction between the drive laser and electron beams becomes strongly non-linear. The formation length of the radiation photon is much less than the laser length, so that the polarization properties of γ-photons are mainly dependent on the electron spin. In the quantum radiation-dominated regime, the cross sections of

NCS related to the electron spin were derived via the QED operator method in the local constant field approximation (LCFA) (Li et al. 2020)

$$\frac{\mathrm{d}^2 W_{fi}}{\mathrm{d}u\mathrm{d}\eta} = \frac{W_R}{2}\left(F_0 + \xi_1 F_1 + \xi_2 F_2 + \xi_3 F_3\right), \tag{29}$$

where $W_R = \alpha m / \left[8\sqrt{3}\pi\lambda_c (k \cdot p_i)(1+u)^3\right]$, $u = \varepsilon_\gamma / \left(\varepsilon_i - \varepsilon_\gamma\right)$, λ_c the Compton wavelength, ε_γ the emitted photon energy, ε_i the electron energy before radiation, $\eta = k \cdot r$ the laser phase, while p_i, k, and r are four-vectors of the electron momentum before radiation, laser wave-vector, and coordinate, respectively. The photon polarization is represented by the Stokes parameters (ξ_1, ξ_2, ξ_3), defined with respect to the axes $\hat{\mathbf{e}}_1 = \hat{\mathbf{a}} - \hat{\mathbf{v}}(\hat{\mathbf{v}}\hat{\mathbf{a}})$ and $\hat{\mathbf{e}}_2 = \hat{\mathbf{v}} \times \hat{\mathbf{a}}$ (McMaster 1961). The Stokes parameters and the electron spin-polarization vector in variables (F_0, F_1, F_2, F_3) include the spin properties. For the details of variables F_0, F_1, F_2, F_3 in Eq. (29), please see the reference (Li et al. 2020).

As shown in Fig. 5, multi-GeV CP (LP) γ-rays with polarization of up to about 99% (95%) can be generated by a longitudinally (transversely) spin-polarized electron beam colliding with an arbitrarily (elliptically) polarized laser pulse (Li et al. 2020). The photon brilliance is comparable to that of unpolarized multi-MeV γ -rays obtained in recent experiments (Sarri et al. 2014). Meanwhile, the laser and plasma interaction can also generate highly polarized high-energy brilliant γ-rays. For example, as the electrons in the plasma are pre-accelerated by the wakefield of the LP laser collide with the reflected laser pulse, brilliant LP γ-rays with average polarization of about 70% and energy up to hundreds of MeV can be generated via NCS (Xue et al. 2020). It has also been shown that isolated ultra-short polarized γ -ray pulse can be generated in a head-on collision configuration of two laser pulses with a nanofoil. Full 3D PIC numerical simulations together with a proof-of-principle calculations showed that the polarization degree of γ-rays of sub-fs (~800 as) is up to 92% for photons of 250 MeV (Zhang et al. 2022).

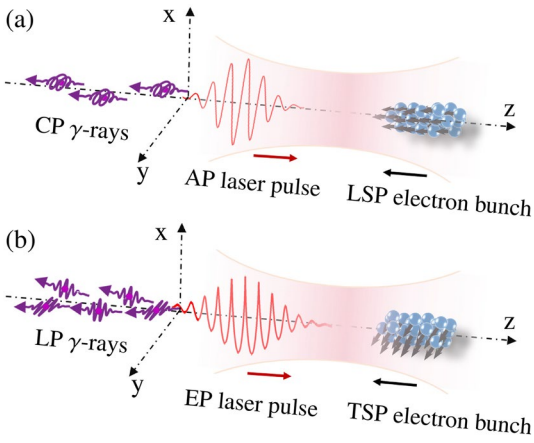

Fig. 5 Scenarios of generating CP and LP γ-rays via the NCS. **a** An arbitrarily-polarized (AP) laser pulse colliding with a longitudinally spin-polarized (LSP) electron bunch produces CP γ -rays. **b** An elliptically-polarized (EP) laser pulse colliding with a transversely spin-polarized (TSP) electron bunch produces LP γ-rays (Li et al. 2020)

2.4 X/γ-ray vortex

A photon beam carrying angular momentum may provide new degrees of freedom (He et al. 2022), such as exploring the angular momentum transfer process between light and particles, and manipulating particle dynamics. High-energy γ-rays with angular momentum play a unique role in astrophysics and particle physics. However, it is challenging to produce high energy vortex γ-rays though vortex states of photons, electrons, neutrons, and neutral atoms have been experimentally produced, albeit at low energies.

Recently, Zhang et al. (2021) have proposed an all-optical scheme to produce brilliant γ-ray beam with high angular momentum density in a laser-plasma configuration, as schematically shown in Fig. 6. In their scheme, a CP Gaussian laser with intensity of $> 10^{22}$ Wcm^{-2} is incident onto a micro-channel target and a large number of electrons are pulled out of the channel wall by the laser electric field. These electrons can be accelerated to hundreds of MeV by the longitudinal electric fields generated within the channel. At the same time, the drive laser also transfers the SAM to the orbital angular momentum (OAM) of the electrons, so that the electrons carry away an extremely high OAM. Here the OAM of electrons and γ-photons is calculated incoherently by

$$L_e = \sum_i |r_{\perp i} \times p_{\perp i}| \propto \delta\sqrt{2-\delta^2} a_0 m_e c^2 N_e/\omega_0, \tag{30}$$

where N_e is the number of electrons and δ represents the polarization state of the drive laser: $\delta = 0$ corresponding to the LP laser, $\delta = \pm 1$ corresponding to the right-handed and left-handed CP laser, respectively. For the laser EM field, its total electromagnetic angular momentum and total electromagnetic energy can be expressed respectively as

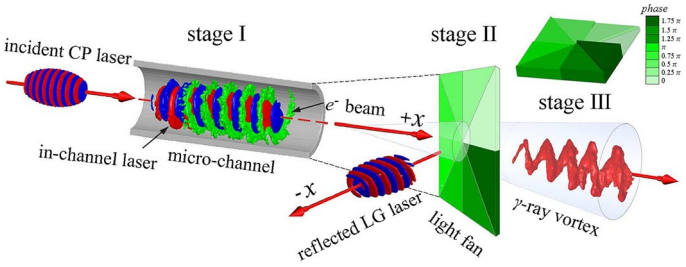

Fig. 6 Schematic of γ-ray vortex generation from a laser-illuminated light-fan-in-channel target. A CP laser pulse is incident from the left and irradiates a micro-channel target. Electrons are extracted from the channel wall, travel along the channel, and are accelerated to hundreds of MeV. Later, the laser pulse is reflected by a light fan and an LG laser pulse is thus formed which collides head-on with the dense energetic electron beam with large angular momentum, resulting in copious γ-photons emission (Zhang et al. 2021)

$$\boldsymbol{L}_{laser} = \varepsilon_0 \int \mathbf{r} \times (\mathbf{E} \times \mathbf{B}) dV = \boldsymbol{L}_x + \boldsymbol{L}_y + \boldsymbol{L}_z, \tag{31}$$

$$E_{laser} = \frac{1}{2} \int \left(\varepsilon_0 \mathbf{E}^2 + \frac{1}{\mu_0} \mathbf{B}^2 \right) \mathrm{d}V. \tag{32}$$

Thereafter, the drive laser is reflected by the light fan target and is converted to a vortex laser with a phase factor of $exp(il\varphi)$ and highly pure (1, 0) mode. Here l is the azimuthal mode index and φ is the angle of cylindrical coordinate system. When the reflected vortex laser collides with the high-energy electron beam, NCS process is triggered, resulting in a γ-ray beam with a peak brightness of 10^{22} photons $\mathrm{s}^{-1}\mathrm{mm}^{-2}\mathrm{mrad}^{-2}/0.1\%\mathrm{BW}$ at 1 MeV and a peak instantaneous radiation power of 25 TW. Full 3D PIC simulation results showed that the conversion efficiency of angular momentum from laser to photons was as high as 0.67% and the average OAM carried away by each backscattered photon was of the order of 10^4 to 10^5 units of $\hbar$. However, it is noted that the resulting γ-ray radiation is just an incoherent sum of individual non-vortex photons, so the large final beam OAM, defined with respect to the beam axis, is a collective effect of the beam as a whole, named beam angle momentum (BAM), not a manifestation of the vortex nature of each photon (Ivanov 2011, 2022).

Bright attosecond γ-ray pulses with tunable angular momentum can also be generated via Laguerre–Gaussian (LG) laser-plasma interaction (Hu et al. 2021). For a CP LG laser pulse, its SAM makes a charged particle spin with respect to its own axis, while its OAM is able to drive the particle rotate with respect to the laser axis. Under appropriate conditions, both can be transferred to particles, which is a fundamental question from a relativistic plasma optics perspective. Recently, Zhu et al. (2018) proposed a novel scheme to produce attosecond multi-MeV γ-ray pulses with tunable angular momentum by the interaction of a CP LG laser pulse with cone-foil targets. This scheme provided an all-optical, efficient three-in-one method for achieving laser focusing, electron acceleration, and γ-ray vortex radiation. In the laser-cone interaction, it was shown that a large number of background electrons can be periodically pulled out of the cone wall to form a dense attosecond electron train. In each bunch, electrons form a donut-shaped sheet with an ultra-short duration of 100 s as. Due to such specially structured laser fields, the electrons can be efficiently accelerated to hundreds of MeV and gradually form a series of annular electron bunches. Later, these high-energy electron bunches collide with the focused strong laser field reflected by the solid target and thus trigger the NCS process, generating high-brilliance multi-MeV γ-ray pulses with ultra-short duration and high beam angular momentum.

Though these proposed schemes may promise bright X/γ-ray radiation with large OAM, however, they either require precise laser-beam collisions or ingenious target designs, posing a great challenge to experiments. First, in most experiments, there is a certain angle between the incident laser and the charged particle, resulting in head-on collision difficulty. Secondly, whether the

high-energy electron beam is generated by a conventional accelerator or laser-plasma accelerator, it has a certain divergence angle dependent on the non-linear effects of laser-plasma interaction. Finally, the delay control and alignment of multiple laser beams are also important issues that must be considered in future femtosecond laser experiments. To detail these issues, Liu et al. (2020) studied the effect of incident angle on the electromagnetic characteristics and energy spectrum of radiation generated by non-linear Thomson scattering. The analytical expressions of the electric field and energy spectrum of the radiation are derived based on the Lienard–Wiechert potential from the single-particle orbit theory (Taira et al. 2017). The results showed that the energy spatial distribution of the high harmonic radiation is annular, and the symmetry of the annular radiation energy is greatly affected by the incidence angle, which may be related to the angular momentum of the vortex higher harmonic. These results will help to understand the experimental results of vortex X/γ-ray and high-energy electron-laser scattering in future.

2.5 Radiation reaction

In the classical regime, the photon emission by high-energy electrons can be modeled as incoherent synchrotron emission, also referred to as non-linear Thomson scattering (Thomson 1883). In this regime, RR is continuous, and each emitted photon carries away only a very small part of the emitting electron energy. Finally, the photon emission process can be considered as a continuous force acting on the emitting electron which turns out to be the classical RR force as described by Lorentz–Abraham–Dirac (LAD) equation (Lorentz 1904; Abraham 1905; Dirac 1938) and Landau–Lifshitz (LL) equation (Landau and Lifshitz 1980). As the energy of a single photon eventually becomes of the order of the energy of the emitting electron, the quantum nature of high-energy photon emission and its back-reaction can be only understood in a relativistic and quantum framework, that of QED, and strong-field QED (Reinhardt and Greiner 1977). In this new regime, the photon emission becomes stochastic and the spectrum is no longer continuous with the photon energy probably larger than the emitting electron energy. The energy distribution and the transverse beam structure of the charged particles can be modified significantly, resulting in the beam broadening. These unexpected phenomena also provide some important experimental signatures for identifying the QED effects in strong laser fields, which has been extensively investigated in recent experiments (Wistisen et al. 2018; Cole et al. 2018; Poder et al. 2018).

When a charged particle is accelerated or decelerated, it creates a radiation field that acts back on the particle itself (Landau and Lifshitz 1980). This is the Lorentz frictional force, which has been extensively studied and discussed with almost one century's debate on this question (Sokolov et al. 2009; Hammond 2010; Tamburini et al. 2010; Ridgers et al. 2012; Lezhnin et al. 2018). The motion equation of a single charged particle with a four-vector damping force g^i is governed by Lorentz–Abraham–Dirac equation (Lorentz 1936; Abraham 1906; Dirac 1938; Landau and Lifshitz 1980)

$$\frac{\mathrm{d}u^i}{\mathrm{d}s} = \frac{e}{mc^2}F^{ik}u_k + \frac{1}{mc}g^i, \tag{33}$$

$$g^i = \frac{2e^2}{3c}\left(\frac{\mathrm{d}^2u^i}{\mathrm{d}s^2} - u^iu^k\frac{\mathrm{d}^2u_k}{\mathrm{d}s^2}\right), \tag{34}$$

where $u_i = (\gamma, \mathbf{p}/mc)$ is the four-velocity and $F^{ik} = \partial_i A_k - \partial_k A_i$ is the electromagnetic field tensor with $A_{i(k)}$ being the electromagnetic four-vector and $i(k) = 0, 1, 2, 3$. By expressing $\mathrm{d}^2u^i/\mathrm{d}s^2$ in terms of the field tensor of the external field acting on the particle, the Landau–Lifshitz equation is obtained (Landau and Lifshitz 1980),

$$g^i = \frac{2e^3}{3mc^3}\frac{\partial F^{ik}}{\partial x^l}u_k u^l - \frac{2e^4}{3m^2c^5}F^{il}F_{kl}u^k + \frac{2e^4}{3m^2c^5}\left(F_{kl}u^l\right)\left(F^{km}u_m\right)u^i. \tag{35}$$

Calculating the space components of Eq. (35), we can get the 3D expression of the damping force in the relativistic case with respect to the laboratory frame as

$$\begin{aligned}\mathbf{f} =& \frac{2e^3}{3mc^3}\gamma\left[\left(\frac{\partial}{\partial t} + \mathbf{v}\cdot\nabla\right)\mathbf{E} + \frac{1}{c}\mathbf{v}\times\left(\frac{\partial}{\partial t} + \mathbf{v}\cdot\nabla\right)\mathbf{B}\right] \\ &+ \frac{2e^4}{3m^2c^4}\left[\mathbf{E}\times\mathbf{B} + \frac{1}{c}\mathbf{B}\times(\mathbf{B}\times\mathbf{v}) + \frac{1}{c}\mathbf{E}(\mathbf{v}\cdot\mathbf{E})\right] \\ &- \frac{2e^4}{3m^2c^5}\gamma^2\mathbf{v}\left[\left(\mathbf{E} + \frac{1}{c}\mathbf{v}\times\mathbf{B}\right)^2 - \frac{1}{c^2}(\mathbf{E}\cdot\mathbf{v})^2\right].\end{aligned} \tag{36}$$

Equation (36) is very easy to incorporate into the PIC codes. We see the third term of the radiation-damping force in Eq. (36) is proportional to γ^2, which dominates over the preceding one ($\propto \gamma$). Thus, the motion equation of the charged particle in external fields can be re-written as

$$\frac{\mathrm{d}\mathbf{p}}{\mathrm{d}t} = \mathbf{F} + \mathbf{f}, \tag{37}$$

$$\mathbf{F} = -e(\mathbf{E} + \frac{1}{c}\mathbf{v}\times\mathbf{B}), \tag{38}$$

$$\mathbf{f} = -\frac{2r_e^2}{3}\gamma^2\frac{\mathbf{v}}{c}\left[\left(\mathbf{E} + \frac{1}{c}\mathbf{v}\times\mathbf{B}\right)^2 - \frac{1}{c^2}(\mathbf{E}\cdot\mathbf{v})^2\right], \tag{39}$$

where $r_e \equiv e^2/mc^2 = 2.8\times10^{-9}$μm is the classical electron radius. We thus obtain the ratio of the damping force to the Lorenz force $f/F \sim \alpha(E/E_{cr})\gamma^2$ in the relativistic case. Taking a laser with $a_0 = 100$ and electrons with $\gamma_e = 750$ for example, the damping force is comparable to the external Lorenz force so that RR should be taken into account in modeling laser-plasma interaction.

In a classical description, the electron travels on its worldline, radiating continuously as it is accelerated in the EM fields. The typical photon energy can

be written as $0.44\chi_e\gamma_e m_e c^2$. Obviously, as χ_e approaches 1, a single photon is capable of carrying off a significant fraction of the electron energy, so that the emission recoil on the electron must be taken into account. Here, the quantum description of radiation reaction differs from classical theory in two ways. First, quantum corrections to the radiated spectrum cut off the tail of photons with energies greater than that of the electron and include spin-flip transitions. The latter markedly increases the probability of radiating photons with energies comparable to that of the electron. These modifications indicate that the total radiated power becomes smaller than the equivalent classical power by a factor of $g(\chi_e) \in (0, 1)$, with $g(\chi_e) = \chi_e^2(1 - 5.953\chi_e)$ when $\chi_e \ll 1$ and $0.5563\chi_e^2/3$ when $\chi_e \gg 1$ (Erber 1966). The quantum radiation reaction is the influence of multiple photon emissions from a charged particle on the particle's dynamics, characterized by a significant energy-momentum loss per emission (Wistisen et al. 2018). In the quantum RR, the radiation losses are inherently probabilistic. In both the classical and quantum RR, the force of radiation reaction is directed antiparallel to the electron' s instantaneous momentum, and its magnitude depends on the key parameter χ_e. More details about the classic radiation reaction and quantum regime as well as modeling them in the numerical codes can be found in the recent review by Blackburn (2020). The relation between radiation reaction in QED and the emission of multiple photons with substantial quantum recoil has been well discussed in the reference (Di Piazza et al. 2010).

The second and more significant difference is the stochastic emission of photons. Here, the electron has only a probability to emit a γ-ray photon of given energy, i.e., so-called "straggling effect", where the electron may propagate a significant distance through the strong laser fields without radiating (Blackburn et al. 2014). Since the laser pulse has a spatial intensity profile, it is possible for the electron to reach the region of highest intensity at the center with losing much less energy than a classical electron. The χ_e of an electron that has straggled in this way will be boosted above that which could be reached classically. As the tail of the photon spectrum increases non-linearly with χ_e, straggling enhances the yield of hard γ-rays (Blackburn et al. 2014; Blackburn 2020).

When the radiated photon energy reaches the same magnitude as the energy of the electron itself, the electron energy loss is constantly transformed into electromagnetic radiation, leading to significant changes in the kinetic characteristics of the electron. For example, the plasma electrons can be trapped by the laser electromagnetic fields, forming a dense electron bunch and radiating ultra-brilliant γ -rays (Ji et al. 2014a). This is the so-called radiation trapping effect. In this case, the RR force becomes comparable in magnitude to the Lorentz force, rather than being a small correction. These have been extensively investigated in many scenarios (Zhu et al. 2015; Liu et al. 2016a; Zhu et al. 2016).

In experiments, the evidences of RR have been obtained by Poder et al. (2018) and Cole et al. (2018). Here, the average energy loss of electrons and the evolution of the electron energy distribution as well as the spectral shape of the photon beams can be used to identify the RR, to measure the Gaunt factor of the RR force and the degree of the radiation stochasticity (Ridgers et al. 2017). As Fig. 7 shows,

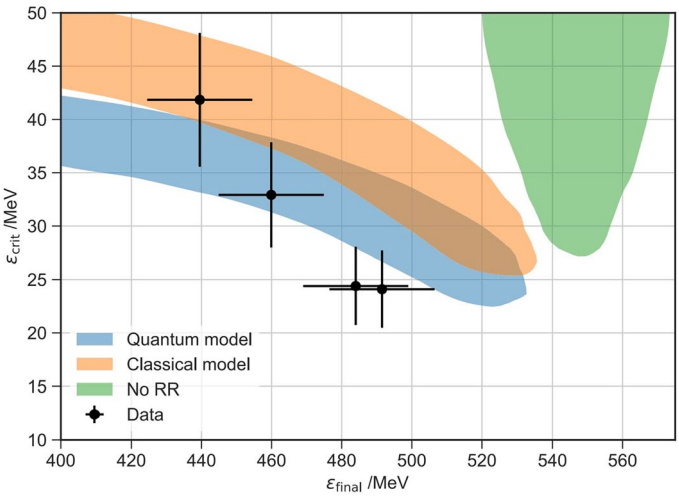

Fig. 7 Experimental evidence of RR. The correlation between the electron beam energy and the critical energy of the γ-ray measured in four successful collisions (points), which are compared with the simulations in quantum RR model (blue), classic RR model (orange), and no RR (green) (Cole et al. 2018)

the quantum RR model matches the experimental data better than the classical RR model. The best theoretical model of the experimental data is obtained by considering the RR effect and the semi-classical modification of the LL equation (Poder et al. 2018; Cole et al. 2018). With the upcoming of 10 PW-class laser facilities around the world, how to detect the signatures from the classic RR to the quantum regimes has been becoming a central issue.

3 Lepton pairs generation by ultra-intense lasers

Pair production is the creation of a sub-atomic particle and its anti-particle from a neutral boson, including creating an electron and positron, a muon and anti-muon, etc. As the antiparticle of electron, positron plays a very important role in fundamental science researches and frontier technology developments, e.g., fundamental physics, laboratory astrophysics, materials science, and medical diagnosis (Musumeci et al. 2022). In 1930, Dirac (1930) proposed the existence of "anti-electron" which possesses the same weight but opposite charge of the electron and in the next year, Anderson (1933) experimentally revealed the existence of "anti-electron" and named it positron. With the development of QFT, Schwinger demonstrated the field strength required to generate electron-positron pairs in the vacuum is $E_{cr} = 1.32 \times 10^{18}\ V/m$. Such a strong field remains unattainable in the laboratory. However, the field strength is not a Lorentz invariant, and the critical field can be reached in the particle reference system when

energetic particles collide with a strong but non-critical field. Nowadays, such strong fields can be provided by either the coulomb fields of high Z nucleus or high intensity laser fields.

Positron beams are also indispensable for the construction of lepton colliders, which would further benefit the QED study, precision quantum chromodynamics (QCD) and beyond the standard model physics. It has been indicated by recent observations that the black holes and neutron stars produce vast amounts of electron-positron pair plasmas in astrophysical jets and large clouds of lepton pair plasma have been associated with neutron stars. In the study of quasar, the relativistic particles of the jet plasma emit synchrotron radiation when gyrating in magnetic fields. However, it takes further researches on the radiation power scaling laws and the fractional linear polarization to distinguish whether the jet plasma is the normal plasma consist of electrons and protons or a pair plasma consist of electrons and positrons (Wardle et al. 1998). Thus, obtaining relativistic pair plasma in the laboratory to simulate high-energy astronomical phenomena is a natural way to study astrophysics and explore outer space. In the area of materials science, positron annihilation spectroscopy (PAS) is valued by the industry as a non-destructive and highly sensitive detection technique on an atomic scale (Audet et al. 2021). Moreover, positron is also important as a probe in medical detection, such as positron emission tomography (PET), which is safe and sensitive and has been widely used in disease diagnosis, efficacy evaluation, and new drug development (Guedj et al. 2012). In this Chapter, we focus more on how to describe the lepton pair production in strong EM fields theoretically and how to produce the lepton pairs by ultra-intense lasers.

3.1 Nonperturbative treatments for pair production from the QED vacuum

Scientists have used Einstein's famous energy–mass equivalence, $E = mc^2$, to calculate the transformation of part of the mass of nuclei into energy by nuclear fission or fusion reactions. QED predicts the reverse process can also be achieved by transforming the laser energy into mass. Over the past decades, in pursuit of experimental proof of transformation from energy to mass by QED is in full swing worldwide. Since Schwinger successfully described the process of generating electron-positron pairs in a static uniform electric field, various methods have been proposed to extend the field into space and time dependent. Here we first give a short review of the nonperturbative treatments for pair production in strong EM field. Meanwhile the pair production by ultra-intense laser interacting with matter including Trident process (Shearer et al. 1973), Bethe-Heitler (BH) process (Bethe and Heitler 1934), and Breit-Wheeler (BW) process (Breit and Wheeler 1934) are reviewed in Sect. 3.2 and Sect. 3.3. In Sect. 3.1, the natural units $\hbar = c = 1$ are used.

To explain the anomalous negative-energy quantum states predicted by the Dirac equation (Dirac 1928), Dirac (1930) proposed the concept of the Dirac sea postulated the electron vacuum as an infinite sea of electrons with negative energy, and the positron was conceived as a hole in the Dirac sea. The energy gap between

positive and negative energy level is $2m_ec^2$. The vacuum is stable without an external field. With an ultra-strong field, there is a certain probability that a negative energy electron will tunnel into the positive energy to form an electron according to the quantum tunneling effect, leaving a hole with negative energy to form a positron. The pair production rate can be estimated by the transmission coefficient of quantum tunneling $P_{e^+e_-} \sim \exp(-\pi E_{cr}/\mid \mathbf{E} \mid)$.

Due to the existence of vacuum fluctuations, vacuum can be regarded as a polarized medium. The effective action $\Gamma[A]$ of strong electromagnetic field can be formulated by using the vacuum–vacuum transition amplitude in a classical gauge field. Heisenberg and Euler (1936) first derived the one-loop effective Lagrangian describing the coupling of the static electromagnetic field with the electron vacuum loop, and corrected the Lagrangian of the electromagnetic field. Expanding the Heisenberg–Euler Lagrangian to quartic order (Dunne 2004), we obtain

$$L = \frac{1}{2}(\mathbf{E}^2 - \mathbf{B}^2) + \frac{e^4}{360\pi^2 m_e^4}\int \mathrm{d}^4x\left[(\mathbf{E}^2 - \mathbf{B}^2)^2 + 7(\mathbf{E}\cdot\mathbf{B})^2\right]. \tag{40}$$

Since the probability of a time-dependent state $|\Phi(t)\rangle = \mathrm{e}^{-iEt}|\phi\rangle$ is $P(t) = \langle\Phi(t)|\Phi(t)\rangle = \mathrm{e}^{-i(E-E^*)t}\langle\phi|\phi\rangle = \mathrm{e}^{2\mathrm{Im}(Et)}$. If we consider the vacuum state decays spontaneously in a strong field by the creation of electron–positron pairs, the pair creation rate per unit volume and time is $w = 1 - \mathrm{e}^{2\mathrm{Im}(\Gamma[A])} \cong 2\mathrm{Im}(\Gamma[A])$ (Stone 1976; Greiner and Reinhardt 2009). Schwinger (1951) used the proper time method to calculate the imaginary part of one loop effective Lagrangian, giving the probability of pair production in the vacuum under the constant electric field E_0,

$$w = \frac{e^2E_0^2}{4\pi^3}\sum_{n=1}^{\infty}\frac{1}{n^2}\exp\left(-\frac{n\pi m_e^2}{eE_0}\right). \tag{41}$$

Because of Schwinger's contribution, the process of pair production from a vacuum in a strong field through the tunneling effect is also called the Schwinger mechanism or Schwinger effect. Since Eq. (41) has an essential singularity in the limit $e \to 0$, the Schwinger particle pair generation mechanism is a non-perturbation process which cannot be calculated by a series expansion in the coupling constant.

3.1.1 Worldline instanton

Based on the Feynman path integral method, the worldline instanton technique has been used to study the perturbative and non-perturbative QED phenomena. Start from the worldline path integral expression of the Euclidean one-loop effective action for a scalar particle in an Abelian gauge background A_μ (Schubert 2001), we have

$$\Gamma[A] = \int_0^\infty \frac{\mathrm{d}T}{T}\,\mathrm{e}^{-m_e^2T}\int_{x(T)=x(0)}\mathcal{D}x\exp\left[-\int_0^T \mathrm{d}\tau\left(\frac{\dot{x}^2}{4} + ieA\cdot\dot{x}\right)\right], \tag{42}$$

where the functional integral $\int \mathcal{D}x$ is over all closed space-time paths $x^{\mu}(\tau)$ which are periodic in the proper-time parameter τ, with period T. Rescaling $\tau = Tu$, and T by m_e^2 (Affleck et al. 1982; Dunne and Schubert 2005),

$$\begin{aligned}\Gamma[A] = &\int_0^{\infty} \frac{\mathrm{d}T}{T}\, \mathrm{e}^{-T} \int_{x(1)=x(0)} \mathcal{D}x \\ &\times \exp\left[-\left(\frac{m_e^2}{4T}\int_0^1 \mathrm{d}u\dot{x}^2 + ie\int_0^1 \mathrm{d}uA\cdot\dot{x}\right)\right] \\ &\backsimeq \sqrt{\frac{2\pi}{m_e}}\int \mathcal{D}x \frac{1}{\left(\int_0^1 \mathrm{d}u\dot{x}\right)^{1/4}} \\ &\times \exp\left[-\left(m_e\sqrt{\int_0^1 \mathrm{d}u\dot{x}^2} + ie\int_0^1 \mathrm{d}uA\cdot\dot{x}\right)\right],\end{aligned} \tag{43}$$

where the approximation $m_e\sqrt{\int_0^1 \mathrm{d}u\dot{x}^2} \gg 1$ of weak-field condition is used. The functional integral may be approximated by a functional stationary phase approximation. The worldline action

$$S = m_e\sqrt{\int_0^1 \mathrm{d}u\, \dot{x}^2} + ie\int_0^1 \mathrm{d}u\, A\cdot\dot{x}. \tag{44}$$

is stationary if the path $x_{\mu}(u)$ satisfies

$$m_e\frac{\ddot{x}_{\mu}}{\sqrt{\int_0^1 \mathrm{d}u\, \dot{x}^2}} = ieF_{\mu\nu}\dot{x}_{\nu}. \tag{45}$$

A periodic solution of Eq. (45) is called a worldline instanton (Affleck et al. 1982; Dunne and Schubert 2005). The pair production rate is given by the imaginary part of the effective action

$$\mathrm{Im}\,\Gamma[A] \sim e^{-S}. \tag{46}$$

Back in 1982, Affleck et al. (1982) calculated the scalar electron-positron pair production rate in a weak constant electric field. The method was extended to compute the rate of the monopole-antimonopole pair production rate in a weak external magnetic field by using an instanton method to Feynman worldline path integral. Kim and Page (2002) proposed that the instantons of quantum tunneling may be related to the pair production of bosons. They also have calculated the pair-production rates of bosons and fermions in static uniform and inhomogeneous strong electric field. The pair production in time-dependent and space-dependent electric fields were studied by Dunne and Schubert (2005) in detail. It was shown that temporal inhomogeneities tending to enhance the local pair production, while spatial inhomogeneities tending to suppress it. Meanwhile, they also extended the worldline instanton

technique to spinor QED. Dunne and Wang (2006) extended the worldline instanton method of computing vacuum pair production rate for spatially inhomogeneous external electric fields to the multi-dimensional case.

At thermal environment, the rate of pair-production process would be enhanced by the thermal photon bath, and the worldline instanton need to be corrected. The S instanton (Gould and Rajantie 2017) and the worldline sphaleron (Gould et al. 2018) were introduced to calculate the rate of pair production at non-zero temperatures. Brown (2018) found the pair-production rate is dominated by a new instanton that involves both thermal fluctuation and quantum tunneling at non-zero temperatures. Korwar and Thalapillil (2018) computed pair production rates in the presence of homogeneous, concurrent electric, and magnetic fields at finite temperature. Worldline instanton technique also has been used for studying the non-linear BW pair production and the NCS process (Degli Esposti and Torgrimsson 2022).

The WKB approximation can be used to seek the instanton solution from $\Gamma[A]$ (Popov 1972a, b; Kim and Page 2002). WKB approximation is a semiclassical approach to investigate Schwinger pair production by solving the Dirac equation. Proposed by Jeffreys (1925), Wentzel (1926), Kramers (1926), and Brillouin (1926), WKB (or JWKB) approximation method can calculate the approximate solutions to the time-independent Schrödinger equation. The exact WKB analysis is an extension of the conventional WKB method. It was proposed and developed by Voros (1983), Dillinger et al. (1993), Aoki et al. (1995), Delabaere et al. (1997), Delabaere and Pham (1999). Its central idea is to apply the Borel resummation technique to make the series well-defined. It also provides a powerful tool to investigate Stokes phenomena of WKB solutions quantitatively.

Yi (1995) studied the one-loop contributions to the WKB exponent tunneling rate of near-extremal magnetic black holes pair production induced by background magnetic fields. Strobel and Xue (2014, 2015) studied the two-component case of a rotating electric field using the generalized WKB method and found that the pair creation rates of spinor and scalar QED are different even for one pair of turning points. Within the WKB approximation, Di Piazza (2014) constructed analytically single-particle electron states in the presence of a background electromagnetic field of general spacetime structure in the realistic assumption that the initial energy of the electron was the largest dynamical energy scale in the problem. Oertel and Schützhold (2019) studied electron-positron pair creation to spacetime-dependent fields by a WKB method based on the eikonal (or Hamilton–Jacobi) equationand applied it to the case of a spacetime-dependent mass. Taya et al. (2021) identified the generic structure of a Stokes graph for systems with the vacuum pair production and showed that the number of produced pairs was given by a product of the connection matrices for Stokes segments connecting pairs of turning points. By employing a generalized WKB approach, Kohlfürst et al. (2022) studied the electron-positron pair creation by the EM field of two colliding laser pulses and found that the pair creation rate along the symmetry plane displayed the same exponential dependence as for a purely time-dependent electric field.

3.1.2 Quantum Vlasov equation

Quantum Vlasov equation (QVE) is a kinetic method which can be derived from the Dirac equation with Bogoliubov transformation (Schmidt et al. 1998; Alkofer et al. 2001). It is suitable to deal with the generating of electron-positron pairs in the time-dependent and spatially homogeneous electric field with negligible collision effect (Schmidt et al. 1999). Start from Boltzmann equation

$$\frac{\mathrm{d}}{\mathrm{d}t}f(\mathbf{x},\mathbf{p},t)=\left(\frac{\partial}{\partial t}+\frac{\mathrm{d}\mathbf{x}}{\mathrm{d}t}\cdot\frac{\partial}{\partial\mathbf{x}}+\frac{\mathrm{d}\mathbf{p}}{\mathrm{d}t}\cdot\frac{\partial}{\partial\mathbf{p}}\right)f(\mathbf{x},\mathbf{p},t)=C(\mathbf{x},\mathbf{p},t), \tag{47}$$

where $f(\mathbf{p},t)$ is the particle distribution function, $\mathbf{x}$ and $\mathbf{p}$ are the spatial coordinate and momentum of particle, $C(\mathbf{x},\mathbf{p},t)$ is the collision term. When there is the creation or annihilation of particles, the source term $S(\mathbf{x},\mathbf{p},t)$ describing the change in the number of particles must be added to the equation. Since the laser intensity of the state-of-the art is still far from the Schwinger field E_{cr}, the number of particle pairs produced is small, the collision term can be ignored. The Boltzmann equation is also known as the quantum Vlasov equation in this situation (Kluger et al. 1998). Based on equation $\mathrm{d}f(\mathbf{p},t)/\mathrm{d}t=S(\mathbf{p},t)$ with the Schwinger source term $S(\mathbf{p},t)$, where $f(\mathbf{p},t)$ is the particle momentum distribution function, $\mathbf{p}=(\mathbf{p}_\perp,p_\parallel(t))$ is the momentum of particle with longitudinal component $p_\parallel(t)=p_\parallel-eA(t)$, the QVE can be expressed as (Schmidt et al. 1998; Xie et al. 2017)

$$\frac{\mathrm{d}f_\pm(\mathbf{p},t)}{\mathrm{d}t}=\frac{1}{2}\mathcal{W}_\pm(t)\int_{-\infty}^{t}\mathrm{d}t'\mathcal{W}_\pm(t')[1\pm 2f_\pm(\mathbf{p},t')]\cos\left[2\int_{t'}^{t}\mathrm{d}\tau\omega(\mathbf{p},\tau)\right], \tag{48}$$

where "+" ("–") corresponds to boson (fermion) pair creation, and the transition coefficients

$$\mathcal{W}_\pm(t)=\frac{eE(t)p_\parallel(t)}{\omega^2(t)}\left(\frac{\varepsilon_\perp}{p_\parallel(t)}\right)^{g_\pm-1}, \tag{49}$$

with $g_+=1$ for bosons and $g_-=2$ for fermions. Here $\omega(t)=\sqrt{\varepsilon_\perp^2+p_\parallel^2(t)}$, $\varepsilon_\perp=\sqrt{m_e^2+\mathbf{p}_\perp^2}$ is the transverse energy. In the low-density limit and a constant electric field, the pair production rate given by Schwinger's formula can be reproduced (Schmidt et al. 1998),

$$S=\lim_{t\to+\infty}(2\pi)^{-3}g\int\mathrm{d}^3\mathbf{p}S(\mathbf{p},t)=\frac{e^2E^2}{4\pi^3}\exp\left(-\frac{\pi m_e^2}{|eE|}\right). \tag{50}$$

Equation (48) is an integro-differential equation. For simplicity and convenience of numerical calculation, it is transferred into three coupled first-order linear differential equations (Bloch et al. 1999). Using QVE to solve the electron-positron pair generating problem can not only obtain the generation rate, but also obtain the momentum distribution function and the number density of pairs. It is essentially

non-perturbative and incorporates non-Markovian effects in strong field pair production.

The plasma of electron-positron quasiparticle pairs creation in a standing wave was explored using a parameter-free QVE (Blaschke et al. 2006). They found the plasma vanished almost completely when the laser field was zero, leaving a very small residual pair density. Hebenstreit et al. (2009) investigated the pair production from vacuum for short laser pulses with a subcycle structure and showed that the momentum spectrum of the created electron-positron pairs was extremely sensitive to the subcycle dynamics. Enhanced electron-positron pair creation by dynamically assisted combinational fields was investigated based on the QVE, and found that the high frequency assisted field will enhance pair production significantly (Abdukerim et al. 2012). The effects of laser pulse shape and carrier-envelope phase on pair production were investigated by solving QVE, and found that there exist the multiphoton processes and stabilization phenomenon in pair production for supercycle situation (Abdukerim et al. 2013). The effective mass problem of electrons and positrons in a strong electric field was analyzed based on accurate numerical solutions of QVE (Kohlfürst et al. 2014). The momentum spectrum and the number density of boson pair (Li et al. 2014a) and electron-positron pair (Li et al. 2014b) production from vacuum in the combined electric fields were investigated. The pair production is strongly influenced by the multiple-slit interference effect. The pair creation in a sinusoidal frequency-modulated electric field was also studied by solving the QVE numerically (Gong et al. 2020).

3.1.3 Dirac–Heisenberg–Wigner formalism

The Dirac–Heisenberg–Wigner (DHW) formalism can be regarded as an extension of the Vlasov equation. As the phase-space correlation function for the Dirac vacuum in the presence of a simple field configurations, the DHW formalism was first derived by Bialynicki-Birula et al. (1991). The start point of DHW formalism is the equal-time density operator of two Dirac field operators in the Heisenberg picture,

$$\mathcal{C}_{\alpha\beta}(\mathbf{r},\mathbf{s},t)=e^{-ie\int_{1/2}^{-1/2}\mathrm{d}\lambda\mathbf{A}(\mathbf{r}+\lambda\mathbf{s},t)\cdot\mathbf{s}}\left[\Psi_{\alpha}\left(\mathbf{r}+\frac{\mathbf{s}}{2},t\right),\Psi_{\beta}^{\dagger}\left(\mathbf{r}-\frac{\mathbf{s}}{2},t\right)\right], \tag{51}$$

where Ψ is the Dirac field operator, $\mathbf{r}$ is the center-of-mass coordinate, $\mathbf{s}$ is the relative coordinate, the factor before the commutator is a Wilson-line factor used for ensuring gauge invariance, $\mathbf{A}$ is the background field vector potential. The vacuum expectation value of the Fourier transformation of Eq. (51) with respect to the relative coordinate $\mathbf{s}$ gives the Wigner function

$$\mathcal{W}_{\alpha\beta}(\mathbf{r},\mathbf{p},t)=-\frac{1}{2}\int\mathrm{d}^3\mathbf{s}\exp(-i\mathbf{p}\cdot\mathbf{s})\langle 0|\mathcal{C}(\mathbf{r},\mathbf{s},t)|0\rangle, \tag{52}$$

Decomposing the Wigner function in terms of the Dirac gamma matrix, we have 16 Wigner components

$$\mathcal{W}_{\alpha\beta}(\mathbf{r},\mathbf{p},t)=\frac{1}{4}(\mathbb{S}+i\gamma_5\mathbb{P}+\gamma^\mu\mathbb{V}_\mu+\gamma^\mu\gamma_5\mathbb{A}_\mu+\sigma^{\mu\nu}\mathbb{T}_{\mu\nu}), \tag{53}$$

where $\mathbb{S}$, $\mathbb{P}$, $\mathbb{V}_\mu$, $\mathbb{A}_\mu$ and $\mathbb{T}_{\mu\nu}$ are scalar, pseudoscalar, vector, axial vector and tensor, respectively, $\sigma^{\mu\nu}=\frac{i}{2}[\gamma^\mu,\gamma^\nu]$. The 16 components satisfy a partial differential equation system which comes from the equation of motion. Solving the equation set, then one can get the particle momentum distribution and other observables (Bialynicki-Birula et al. 1991; Hebenstreit 2011; Kohlfürst 2015; Xie et al. 2017). Theoretically speaking, the DHW formalism method can solve the pair production problem in any kind of external field. For spatially uniform time-dependent electric fields, the DHW formalism can be reduced to the quantum Vlasov equation (Hebenstreit et al. 2010).

The pair production in the homogeneous electric field was illustrated as an simple example of DHW (Bialynicki-Birula et al. 1991). The Schwinger effect in the presence of space- and time-dependent electric field was performed with DHW (Hebenstreit et al. 2010, 2011), and the time evolution of observable quantities such as the charge density, the particle number density or the total number of created particles were also calculated. Schwinger pair production in rotating time-dependent electric fields was explored by employing real-time DHW (Blinne and Gies 2014). It was found that the electric field rotation generically enhances the pair production in comparison with LP fields. The characteristic momentum space patterns of the distribution function could serve as a decisive fingerprint of Schwinger pair production, if the QED successive cascade preserves a remnant of this pattern in the final state distributions of either electrons, positrons or photons. The effects of electric field polarizations on pair production were investigated with real-time DHW (Li et al. 2015). For a small laser frequency, the particle number density decreases with the polarization, while for a large laser frequency, the relation between them is sensitive to the field frequency non-linearly. Kohlfürst and Alkofer (2016) investigated the pair production in space- and time-dependent electromagnetic fields, especially the influence of a time-dependent, inhomogeneous magnetic field on the particle momenta and the total particle yield. Wigner function and pair production in parallel electric and magnetic fields for each Landau level was analytically calculated (Sheng et al. 2019). The effects of symmetrical frequency chirp on pair production have also been studied in detail using DWH (Wang et al. 2021a; Mohamedsedik et al. 2021; Wang et al. 2023).

3.2 Generation of electron-positron pairs with high-Z solid targets

The theoretical calculations show that the current laser intensity is not strong enough to directly produce lepton pairs from vacuum, but scientists have been able to observe the pair production in indirect ways. The laser-plasma interaction with ultra-high laser intensity is extremely complicated and highly-nonlinear, but the theoretical methods reviewed above can only deal with some simple cases, e.g., a homogeneous or rotating EM wave, posing a great challenge to time- and space-dependent EM field. Fortunately, for $a_0 \gg 1$ and $\gamma \gg 1$, the laser field can

be considered as constant since the formation length of photon emission is proportional to λ_0/a_0 and the external EM field is crossed with $\mathbf{E}\perp\mathbf{B}$, $E = B$, in the particle proper reference frame. Since the basic strong-field QED processes are formed on a length scale much smaller than the laser wavelength, the LCFA has been developed to deal with the strong-field QED processes analytically and numerically. LCFA has been implemented in almost all QED-PIC codes like EPOCH (Ridgers et al. 2014), and with some corrections and improvements allow us to compute these QED processes in arbitrary EM fields under conditions where the local quantum non-linear parameter χ_e is large, e.g., in laser-plasma interaction at extremes. Assisted by high-performance computers, numerical simulations of pair production in strong fields with LCFA have made significant progress in the past years.

Since Anderson (1933) experimentally revealed the existence of "anti-electron" and named it positron, ones have found and proposed various methods for obtaining positrons. For the applications that only require slow positron sources such as PAS and PET, the positrons can be acquired naturally from the β^+ decay of some radionuclides such as ^{22}Na and ^{40}K, together with neutrinos. Positrons can be also generated by cosmic rays and γ-ray flashes created by electrons accelerated by strong electric fields in the clouds. When high-energy positron sources are demanded, two major mechanisms are widely involved: (1) Trident process (Shearer et al. 1973), where electrons collide with the coulomb fields of high Z nucleus to generate electron-positron pairs, $e^- + Z \rightarrow Z + e^+ + 2e^-$; (2) Bethe–Heitler (BH) process (Bethe and Heitler 1934), where high-energy γ-photons are first generated via bremsstrahlung radiation when electrons hit a metal target, and γ-photons then interact with the coulomb field of the high-Z nucleus to produce positrons, $\gamma + Z \rightarrow Z + e^+ + e^-$. In both processes, the high-Z solid target plays an important role, providing a strong coulomb field for interacting with the electrons. In the past decades, plenty of works

Table 2 Positron generation with different laser intensities

Mechanism	References	Laser intensity (W/cm^2)	Positron yield
BH and Trident	Nakashima and Takabe (2002)	10^{20}	4×10^{10}
	Nakamura and Hayakawa (2016)	5×10^{22}	10^8
	Audet et al. (2021)	2.5×10^{19}	7.2×10^3
	Chen et al. (2015)	10^{20}	2×10^{12}
	Jiang et al. (2021)	4.5×10^{20}	$\sim 10^{12}$
	Liang et al. (2015)	1.9×10^{21}	$\sim 10^{10}$
	Xu et al. (2020)	4.5×10^{20}	7.6×10^7
BW	Zhu et al. (2016)	3×10^{22}(*double*)	$\sim 10^{11}$
	Yasen et al. (2021)	4×10^{23}(*double*)	10^8
	Zhao et al. (2022)	4.5×10^{22}(*double*)	$\sim 10^{11}$
	SLAC E144 Bamber et al. (1999)	0.5×10^{18}	106 ± 14
	RHIC experiments Adam et al. (2021)		6085

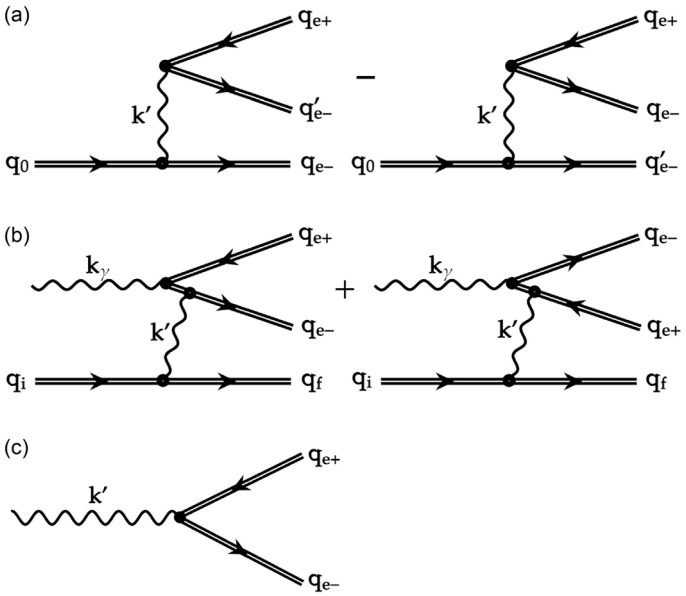

Fig. 8 Feynman diagrams for the non-linear Trident, Bethe–Heitler, and Breit–Wheeler processes. The double fermion lines indicate that the process occurs in an external laser field

have been carried out theoretically, experimentally or numerically based on the above two mechanisms, as summarised in Table 2.

It is now convenient to acquire energetic electrons on both conventional accelerators (Yakimenko et al. 2019) and laser-based accelerators (Gonsalves et al. 2019). As a result, the positron generation by seeded electrons via the Trident process or BH process are attracting increasing attention (Fig. 8). In terms of interaction manners, the designed schemes based on the Trident process or BH process can be divided into direct ones and indirect ones. In direct schemes, the Trident process and the BH process proceed simultaneously and both can produce electron-positron pairs when the ultra-intense laser interacts directly with the solid target, accompanied by some other processes such as bremsstrahlung, transition radiation and laser-ion acceleration. Since the scaling of the BH positron yield is expected to scale as Z^4 with Z the atomic number, a high-Z target, e.g., Au or Ta, is preferably employed in experiments. For example, in 1999, Cowan used an intense laser pulse with the focal intensity of 10^{20} W/cm^2 to irradiate a metal composite target (Au+Cu) and detected 103 candidate events(Cowan et al. 1999). In 2009, Chen et al. (2009) measured up to 2×10^{10} positrons per steradian ejected out the back of *mm* thick gold targets when illuminated with 1 ps 10^{20} W/cm^2 laser pulses. It was shown that the positrons are produced predominately by the BH process and have an effective temperature of 2–4 MeV. In their following experiment in 2013, quasi-monoenergetic, beamlike positron jets were observed with energy of 4 to 20 MeV and a beam temperature of 1 MeV, by irradiating a gold target with an intense picosecond laser pulse. With higher laser intensity of 10^{21} W/cm^2, Liang et al. (2015) used a 100 J laser pulse

from Texas Petawatt Laser to irradiate a metal platinum target and 10^{10} positrons are generated with the density of 10^{15} cm^{-3}. Although the positron generation cross-section of the BH process is much larger than the Trident process, the total reaction cross-section is not so different when multiplied by the cross-section of the bremsstrahlung. Nakashima and Takabe (2002) showed that the density of the target nuclei and the thickness of the target together influence which process dominates in the direct interaction process of high energy laser pulses and high-Z targets.

In the indirect schemes, the positron generation process can usually be divided into two steps, first using the laser-plasma interaction to obtain energetic electron beams, and then irradiating these electron beams onto high-Z targets to generate positrons. Compared with the direct schemes, the positron beam quality achieved in an indirect scheme can be controlled by adjusting the energy, density, and divergence angle of the relativistic electron beams. In 2000, Gahn et al. used a laser pulse with an energy of 220 mJ and pulse width of 130 fs to interact with a gas-jet target to get MeV-level electrons, which were then collided with a 2 mm-thick Pb converter to generate 10^7 positrons (Gahn et al. 2000). In 2014, Sarri et al. also reported on the generation of a high-density and neutral electron-positron pair plasma in the laboratory, with a positron density up to 10^{16} cm^{-3}. This allows for collective effects to occur (Sarri et al. 2015). Most recently, Audet et al. (2021) experimentally obtained picosecond positron beams with energies tunable from 500 keV to 2 MeV and flux of the order of 10^3 through an indirect scheme.

3.3 All-optical schemes for generating electron-positron pairs

Another important mechanism for positron generation is the Breit-Wheeler (BW) process (Breit and Wheeler 1934), where two high-energy photons collide (linear BW process): $\gamma + \gamma \rightarrow e^+ + e^-$, or a high-energy photon interacts with multiple lower-energy photons (e.g., laser photons) to produce positive and negative electron pairs (non-linear BW process): $n\gamma + \gamma \rightarrow e^+ + e^-$. The BW process can provide an all-optical method for converting light quanta into matter. Since the study of this process is of great scientific importance in QED researches, especially with the rapid development of PW laser facilitates, a large number of theoretical and numerical works has been carried out (Titov et al. 2012; Heinzl et al. 2010; Liu et al. 2016b;

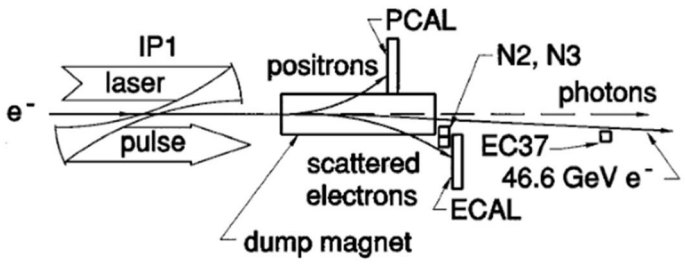

Fig. 9 Schemetic layout of the SLAC-E144 experiments (Burke et al. 1997)

Lu et al. 2018; Luo et al. 2018). For experimental demonstration, the famous SLAC-E144 experiment carried out in 1997 provided solid evidence for the non-linear BW process, where they used a 46.6 GeV electron beam obtained from the SLAC linear accelerator to collide with a laser and 106 ± 14 positrons were detected (Burke et al. 1997; Bamber et al. 1999), as presented in Fig. 9. Although the experiments were successful, the positron yield and beam qualities were not very promising for subsequent experiments or applications. One of the key factor that limits the positron yield is the laser pulse intensity employed in the experiments, which is around the relativistic threshold 10^{18} Wcm^{-2}. In 2010, Hu analysed the positron yield versus laser intensity in the SLAC experiments (Hu et al. 2010). It turns out that increasing the energy of colliding electron beams can effectively lower the threshold of the laser intensity required for positron generation in a laser-electron collision scheme, however, the positron yield would not be satisfactory. In 2020, the STAR collaboration successfully generated 6085 electron-positron pairs by using the Relativistic Heavy Ion Collider (RHIC), providing an experimental demonstration of the linear BW process (Adam et al. 2021). The observed features of the BW process present experimental confirmation of fundamental QED predictions. With the upcoming 10–100 PW scale laser facilities such as ELI-200 PW, EP-OPAL-75 PW, SEL-100 PW, GEKKO-EXA-50 PW, and XCELS-200 PW (Danson et al. 2019; Turner et al. 2022), the laser intensity will be pushed toward 10^{24} W/cm^2 which is sufficient for

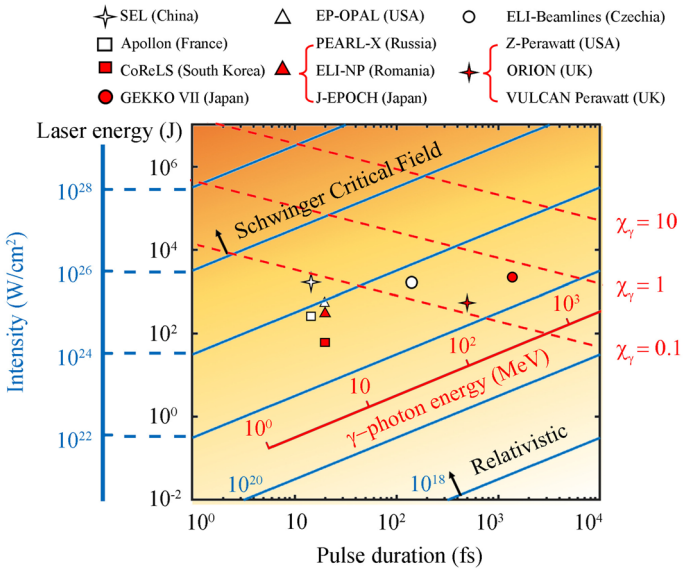

Fig. 10 Phase space distribution of laser intensity versus γ-photon energy in the non-linear BW process. The x and y axis represent the laser pulse duration and pulse energy, respectively, while the blue lines indicate the corresponding laser pulse intensity at 1 μm focal spot. For comparison, some large laser facilities are also marked in the figure. Here γ-photon energy is represented by the red axis. Assuming a headon photon-photon collision, the corresponding quantum parameter χ_γ is shown by the red dashed lines

copious positron generation via either the linear or non-linear BW process. Thus, experimental studies on the generation of electron-positron pairs via the all-optical BW process have attracted significant attentions around the world.

As mentioned in Sect. 1.3, the quantum parameter χ_γ determines the probability of electron-positron pair generation in a photon-photon collision, which can be calculated approximately by $\chi_\gamma = \hbar\omega_0|\vec{E}_\perp + \vec{k} \times c\vec{B}|/(2m_e c^2 E_{cr})$, where $\vec{E}_\perp$ is the electric field perpendicular to the velocity of γ-photon, $\vec{k}$ is the wave vector of the γ-photon, and λ_{ph} is the wavelength of the photon. Assuming a headon photon-photon collision, we draw a picture of the χ_γ distribution in the phase space of laser intensity and γ -photon energy, as shown in Fig. 10. In this figure, the laser intensity is estimated by focusing the laser pulse at 1 μm spot and the γ-photon energy is the required for copious electron-positron pair production ($\chi_\gamma \geq 0.1$) via the non-linear BW process. For comparison, some large laser facilities with the designed parameters are also marked in this figure. One sees that, with the increase of laser intensity, the required photon energy is reduced for a fixed χ_γ. For example, for the upcoming 100 PW laser SEL with $\chi_\gamma = 0.1$, MeV-class photon beams are sufficient for producing copious electron-positron pairs; for the VULCAN petawatt laser (Danson et al. 2004), we may need 100 MeV-class photons to trigger the same lever pair production.

Overall, the positron generation schemes based on the BW process can be divided into three different categories according to the medium of interaction, i.e., solid, near-critical-density (NCD) plasma and gas. To mitigate the BH and Trident process, the solid targets used in the BW-based schemes are mainly thin low-Z targets, such as Al and Sn, aiming at reflecting intense lasers instead of colliding with energetic electrons or γ-photons (Ridgers et al. 2012). For example, Liu et al. (2017) proposed that by irradiating an 5 μm-thick Aluminum foil with a laser pulse at 2×10^{23} W/cm^2, 3.8×10^7 positrons can be generated via the non-linear BW process. Although solid target usually demands only one laser pulse for copious positron generation, which largely simplifies the experimental setup, the required laser intensity are much higher than the multi-beam colliding schemes. Chang et al. (2015) proposed a scheme for enhanced production of electron-positron-pair plasmas by using two 10 PW lasers at intensities of 10^{23} W/cm^2 irradiating a thin solid foil from opposite sides. It was also shown that attosecond electron-positron pairs can be generated by a 10 PW laser irradiating a micro-wire target and colliding with a scattering laser pulse of the same intensity (Li et al. 2017b). For lowering the drive laser intensities, gas targets are often used to provide energetic electron beams via the LWFA. In a laser-gas interaction scheme, Lobet et al. numerically proved that 6×10^8 positrons can be generated via the BW process by using laser pulses of intensity of 1.6×10^{22} W/cm^2 (Lobet et al. 2017). Since the positron yield not only depends on the laser intensity, but also is connected to the seeded particle numbers, one has proposed to use NCD plasma to increase the seeded particle numbers and enhance the positron generation. Recently, Yu et al. (2019) proposed to generate two high-energy γ-photon beams by two 10 PW lasers interacting with two individual NCD plasma channels. The obtained γ-ray beams with a very low divergency then collide with each to produce copious electron-positron pairs through the linear BW process. Moreover, Duff et al. (2019) proposed a multi-stage mechanism for electron-positron pair production. In the scheme, they irradiated a $10n_c$ target

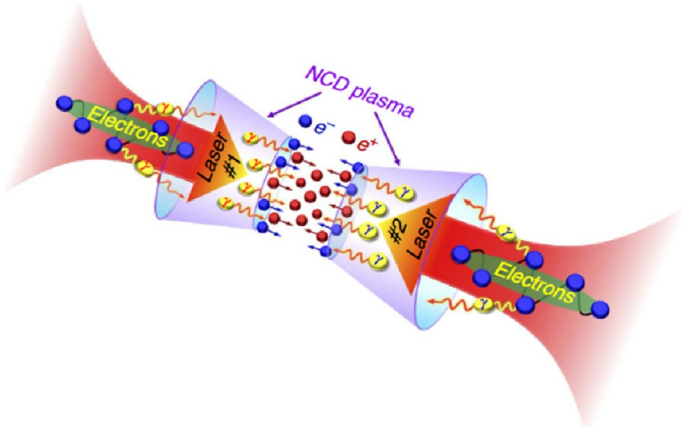

Fig. 11 Dense electron-positron pair production in a double-cone configuration. Two counter-propagating 10 PW laser pulses are focused from two directions onto the NCD-plasmas-filled double-cone targets (purple). The quivering electrons in the ultra-intense laser fields experience large RR forces by emitting γ -photons, so that they are trapped in the laser fields. These trapped electrons perform extreme oscillations in the transverse direction and emit bright γ-rays (red- and blue–yellow) around the laser axis. Finally, copious numbers of $e^{-}e^{+}$ pairs are created via the non-linear BW process (Zhu et al. 2016)

with a drive laser pulse (1×10^{23} W/cm^2) at 1 μm to obtain collimated high-energy γ -photons; then the energetic γ-photons collide with a super-intense laser pulse off-set from the central axis by a characteristic angle with the intensity of 4×10^{23} W/cm^2, so that the non-linear BW process is triggered and highly anisotropic electron-positron pairs are produced. Zhu et al. (2016, 2019) proposed that the focal spot laser intensity can be increased by one order of magnitude in a NCD-plasma-filled double cone configuration, as schematically shown in Fig. 11. Full 3D PIC simulations indicated that high-energy, high-brightness γ-rays and copious positrons can be obtained at an approachable laser intensity of 10^{22} W/cm^2.

3.4 Positron acceleration by ultra-intense lasers

While many important breakthroughs have been made in the field of laser-driven positron sources, there are some specific issues that need further investigations. The first and foremost towards the electron-positron collider applications in high-energy physics is the positron energy, which should be boosted to above GeV. Unfortunately, the energy and luminosity of the positron beams based on laser-plasma is far away from required. Since the laser wakefield acceleration works well for electrons, it is natural to think of wakefield acceleration for positrons (Lee et al. 2001). However, this path is quite challenging because the LWFA does not work properly for positrons considering the fact that the positively charged particles are easily scattered off in the wakefield cavity. To address this issue, various approaches have been proposed to improve the positron beam quality in the wakefield, such as using plasma channels (Gessner et al. 2016), vortex laser (Vieira and Mendonça 2014),

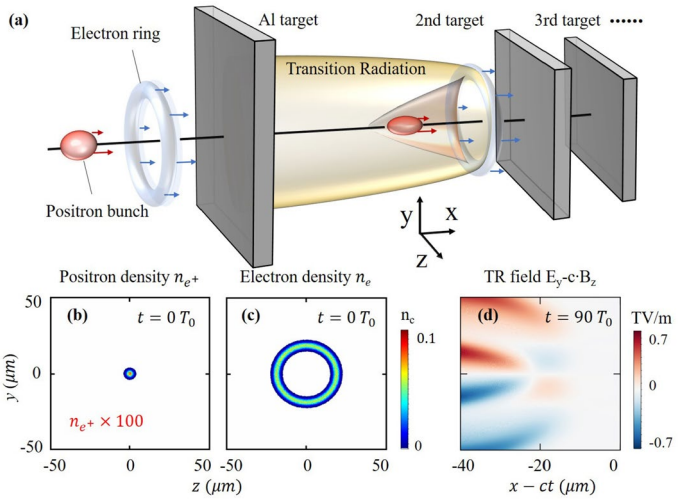

Fig. 12 **a** Schematic diagram of the multi-stage THz-driven positron acceleration. Initial injected **b** positron and **c** electron beam density distribution in the *y*–*z* plane. **d** Transverse electromagnetic field distribution in the *x*–*y* plane. (Zhao et al. 2023)

positron beam (Corde et al. 2015), asymmetric electron beam (Zhou et al. 2021), and hollow electron beam (Jain et al. 2015). In addition to the wakefield acceleration, one has also proposed to couple the positron production and acceleration together, such as using LG lasers to generate and accelerate positrons (Zhao et al. 2022), using sheath fields to accelerate positrons (Yan et al. 2017b), and using coherent transition radiation (CTR) to accelerate positrons (Xu et al. 2020), etc. For example, Xu et al. (2020) proposed to accelerate the positrons to 500 MeV by CTR together with an external 1 T magnetic field. Moreover, Kim et al. (2020) came up with a method to modulate the generated positron density, and found that the sheath field of a curved target can increase the positron density by an order of magnitude. Despite the successful acceleration and confinement of the positrons being achieved, the intense vortex laser or extra magnetic field required in these schemes poses big challenges to the present laboratory conditions.

A compromise to both the small acceleration gradient of traditional radio-frequency (RF) accelerators and the limited injection charge of laser-plasma accelerators is to use terahertz fields for particle acceleration (Xu et al. 2020). It has been shown that THz pulses can achieve approximately 100% acceleration of the injected particle beam and maintain essentially constant energy spread (Hibberd et al. 2020). Since the laser accelerators for positrons still face the challenges of limited injection charge, energy dispersion, and quick dephasing, the larger amount of injected charge and longer acceleration length that come along with THz-driven particle accelerators should benefit significantly the positron

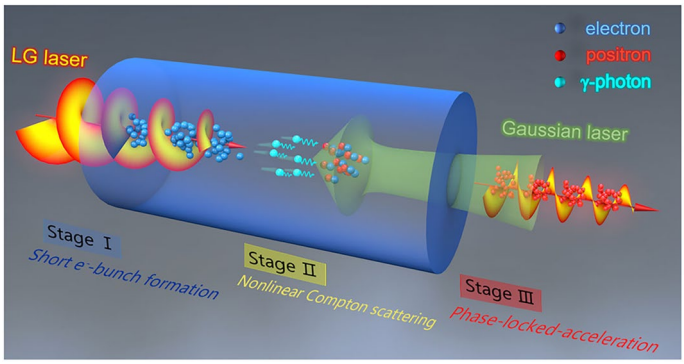

Fig. 13 Schematic diagram of quasi-monoenergetic positron bunches generation by twisted lasers in the NCD plasma. The scheme is divided into three stages: (I) The LG drive laser is incident onto the NCD plasma from the left-side, accelerating electrons to multi-GeV energies. (II) Copious γ-photons are generated via the NCS process when the electron bunches collide head-on with a time-delayed scattering laser pulse. (III) Prolific electron-positron pairs are generated via the non-linear BW process, which are further compressed and accelerated via the phase-locked-accelerations (Zhao et al. 2022)

acceleration. Moreover, it has been proved that the transition radiation field could help in confining the particle beams (Sampath et al. 2021). Recently, Zhao et al. (2023) proposed a possible multi-stage positron acceleration scheme for high energy positron beam acceleration and propagation, as indicated in Fig. 12. In the scheme, strong coherent THz radiation is generated when an injected electron ring beam passes through one or several solid targets. Multi-dimensional PIC simulations demonstrated that each acceleration stage is able to provide nearly 200 MeV energy gain for the positron beams. Meanwhile, the positron beam energy spread can be controlled within 2% with a well-maintained beam emittance. This may promise many potential applications in laboratory physics and high-energy physics.

Since positron constraint is a key issue in the positron acceleration, Zhao et al. (2022) proposed to collide an LG drive laser with a Gaussian scattering laser inside an NCD plasma column, as indicated in Fig. 13. Due to the unique structure of the twisted laser pulse, the positrons are well confined by the radial electric fields and experience phase-locked-acceleration by the longitudinal electric field. Full 3D PIC simulations demonstrated the generation of dense sub-femtosecond quasi-monoenergetic GeV positron bunches with tens of picocoulomb (pC) charge and extremely high brilliance above 10^{14} s^{-1} mm^{-2} $mrad^{-2}$ eV^{-1}. Recently, Sugimoto et al. (2023) discovered a simple regime where NCD plasma irradiated by a laser of experimentally available intensity can self-organize to produce positrons and accelerate them to ultra-relativistic energies. In the regime, the acceleration field is the plasma field generated by the charge separation of the leading electrons and ions, rather than the laser itself. With a 10

PW-class lasers at 10^{22} W/cm^2, the regime predicted the generation of GeV positron beams with a divergence angle of around 10° and a total charge of 0.1 pC.

3.5 Positron polarization in strong laser fields

Positrons have two possible spin values: $\pm\hbar/2$, with different probabilities depending on the state amplitudes. Since spin-polarized positron beams can reveal information about the independent degree of freedom, they have important applications in various fields, such as investigating the internal structure of matter, searching for new physics beyond the standard model and studying spin phenomena at material surfaces. Several physical processes can affect the polarization of particles, such as spin precession described by the Thomas–Bargmann–Michel–Telegdi (T-BMT) equation (Bargmann et al. 1959), the radiative spin-flip (Sokolov-Ternov effect) (Sokolov and Ternov 1964), and the spin-dependent magnetic field gradient force (Stern–Gerlach force) (Wen et al. 2013). Currently, most schemes for generating polarized electrons or positrons are related to the radiative spin-flip, which occurs when an electron or positron emits a high-energy photon and its spin aligns in the opposite/same direction of its magnetic field. The general view is that constructing an asymmetric laser field, such as elliptically polarized or two-color linearly polarized laser pulses, is the key to realize polarized beams.

The generation of spin-polarized positron beams has been extensively investigated. These studies can be classified into three categories. The first category relies on the radiative spin-flip of positrons in storage rings under tesla-level magnetic fields. After emitting photons through synchrotron radiation in a magnetic field, positrons may undergo spin-flip. The probability of positrons transitioning to the state where their spin is oriented in the same direction as the magnetic field is higher. But the saturation is not complete and the degree of polarization can be described by the formula (Sokolov and Ternov 1986):

$$\xi(t) = A(1 - e^{-\frac{t}{\tau}}), \tag{54}$$

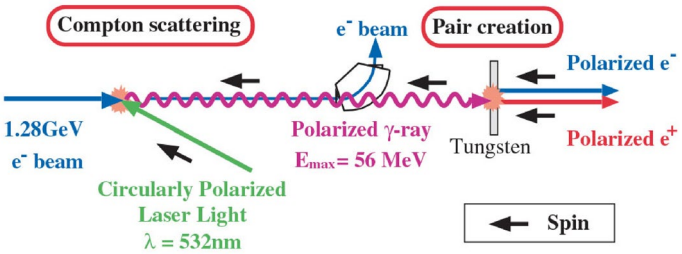

Fig. 14 Scheme of generating polarized positron beams via the BH process by polarized γ-photons (Omori et al. 2006)

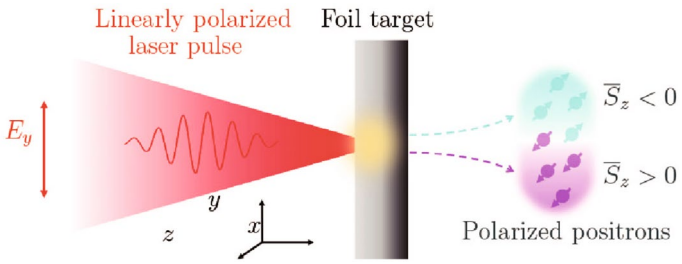

Fig. 15 Schematic for producing polarized positrons by irradiating a foil target with an ultra-strong LP laser beam (Song et al. 2022)

where $A = 8\sqrt{3}/15 \approx 0.924$ is the limiting degree of polarization (92.4%), and τ is the relaxation time

$$\tau = A\frac{4\pi\epsilon_0\hbar^2}{m_e ce^2}\left(\frac{m_e c^2}{E}\right)^2\left(\frac{H_0}{H}\right)^3, \tag{55}$$

where H_0 is the Schwinger magnetic field, and H is the magnetic field. However, this method is quite time-consuming (Liu et al. 2022) due to the weak magnetic field of synchrotron radiation.

The second category utilizes the BH process to produce polarized positrons by irradiating high-Z targets with CP high-energy photons or pre-polarized electrons. For instance, Omori et al. (2006) proposed a two-quantum processes for polarized positron beam generation, i.e., inverse Compton scattering and electron-positron pair creation. As shown in Fig. 14, a right-hand polarized laser pulse scatters off relativistic electrons and generates left-hand polarized γ-photons, which then hit a tungsten plate and create polarized positrons. Finally, they obtained short polarized positron beams with an intensity of 2×10^4 $e^+/bunch$ and a polarization magnitude of $73 \pm 15 \pm 19\%$. However, this method suffers from low conversion efficiency of the BH process [$\sim 10^4$ positrons/shot (Song et al. 2022)] and insufficient brightness of the current available circularly polarized photons.

The third category involves non-linear QED processes when strong laser fields with an intensity exceeding 1×10^{23} W$/cm^2$ interact with plasmas. In this case, electrons can radiate γ photons, which then annihilate into e^-e^+ pairs via the BW process (Reiss 2004). Recently, using QED-PIC simulations, Song et al. (2021) demonstrated that polarized positrons can be generated by two counter-propagating LP laser pulses with peak intensity of 8.9×10^{23} Wcm^{-2} impinging on a thin foil target. Subsequent simulations also indicated that when the laser pulse is sufficiently strong (with intensity exceeding 10^{24} W$/cm^2$), a positron beam with high spin polarization rate can be directly generated when a single laser pulse interacts with plasma, as shown in Fig. 15 (Song et al. 2022). By using a foil target with micrometer-scale-length pre-plasmas, a positron beam with a polarization

rate higher than 30%, a charge larger than 30 nC, and a flux of 10^{12} sr^{-1} can be obtained.

In addition to the two schemes by directly irradiating solid targets with lasers, Liu et al. (2022) also proposed a scheme to trap and accelerate polarized positron beams using plasma wakefields. In this scheme, polarized γ photons are generated by seed electrons colliding with a bichromatic laser, and they split into electron-positron pairs through the non-linear BW process. They obtained a high-quality polarized positron beam with GeV energy, an partial positron polarization above 70% and a divergence angle of around 20 mrad. They also found that the polarization of intermediate γ photons significantly affects the pair yield and polarization degree.

3.6 Generation of muon pairs

The muon, an unstable elementary particle in the standard model of particle physics, was first detected from cosmic radiation in 1936. A muon is similar to an electron with an electric charge of $-e$ and a spin of $\pm\hbar/2$, but with a much larger mass. Since muons are much more deeply penetrating than X/γ-rays, muon image can be used for much thicker materials and objects, e.g., cargo containers, to detect shielded nuclear materials and explosives. Most importantly, precise measurements of muon anomalous magnetic moment (Gorringe and Hertzog 2015) and rare muon decay investigation provide irreplaceable ways of searching the new physics beyond the standard model.

Since muons have a larger mass and greater energy than the decay energy of radioactivity, they are usually not produced by the radioactive decay, but in great amounts in high-energy interactions with matter, in particle accelerator experiments with hadrons, and in cosmic ray interaction with atmosphere. These interactions usually produce π mesons initially and the latter almost always decay into muons. However, the natural muon source, driven by the cosmic ray, just has a flux of 10^4 m^{-2}min^{-1} at sea level. Such a low flux leads to low beam density, undesirable for many potential applications as mentioned above. On the other hand, the RF-based artificial muon factories, e.g., ISIS-RAL (Hillier et al. 2018), PSI (Foroughi et al. 2001), J-PARC (Nagae 2008), TRIUMF (Wright et al. 1992), etc., typically demand a kilometer-scale ion accelerator to achieve a proton beam with energy above 100 MeV and complex beam compression facilities to focus the muon beam. They have become increasingly expensive and huge in size. Thus, new methods of generating dense and short muon sources are in high demand.

Recently, the successful production of GeV electron beams based on laser accelerators has provided an alternative method. For example, Titov et al. (2009) proposed a table-top configuration for muon generation with a PW laser. They divided the processes into two cases. In the first case, the muon pairs are produced in the interaction of bremsstrahlung photons within the electric field of high-Z nuclei via $\gamma + A \rightarrow A + \mu^+\mu^-$. This process is analogous to the well-known BH process and the yield of muon production is defined by

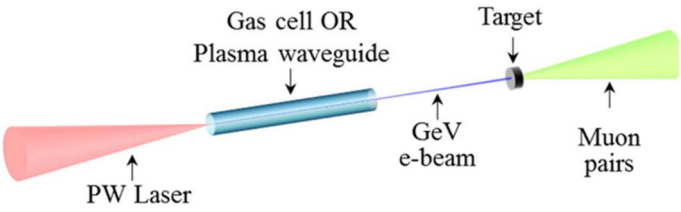

Fig. 16 Schematics for producing highly directional GeV muon pairs using a laser wakefield accelerator (Rao et al. 2018)

$$dN^{\mu^+\mu^-} = \frac{N_A\rho_A}{A}\int_0^L dl \int dE_\gamma \frac{N_A\rho_A}{A}N^e(l)\frac{d\sigma_\gamma\left[E_e(l),E_\gamma\right]}{dE_\gamma} \times (L-l)d\sigma^{\gamma A\to\mu^+\mu^- A}\left(E_\gamma\right), \tag{56}$$

where A is the atomic weight, N_A is Avogadro's number, ρ_A denotes the target density, $d\sigma^{\gamma A\to\mu^+\mu^- A}$ is the elementary cross section of the muon production in the elementary γA interaction, and $d\sigma_\gamma\left[E_e(l),E_\gamma\right]/dE_\gamma$ is the angular-integrated bremsstrahlung cross section. For the gold target with $A = 197$ and $Z_A = 79$, the electron energy versus target length is $E_e(l) \simeq E_e^0 \exp\left(-l/l_0\right)$, where $l_0 \simeq 0.306$ cm. Meanwhile, the electron beam absorption in the target may be accounted for by a linear dependence $N^e(l) \simeq N_0^e\left[1 - l/L_{\max}\left(E_e^0\right)\right]$ with N_0^e is the initial beam intensity and $L_{\max}$ stands for the maximum distance traveled by the energetic electrons.

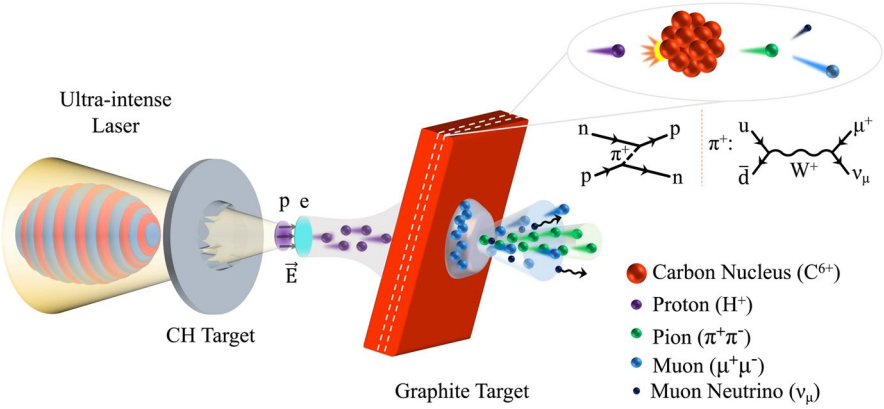

Fig. 17 Sketch of the proposed laser-driven muon source. An ultra-intense laser pulse impinges on the CH target and then accelerates the protons to about 800 MeV with the beam charge up to tens nC. The protons propagate forward and interact with the graphite converter target, while the carbon ions diffuse in space. Pions are thus produced via the proton-nucleus inelastic collision, which can decay immediately into muons and neutrinos due to the weak interaction. Finally, copious surface muons are produced at the rear of the target while the pion beams can continuously radiate muons in flight (Sha et al. 2022)

In the second case, the muon pairs are produced in the direct interaction of energetic electrons with nuclei via $e + A \rightarrow e' + A + \mu^+\mu^-$, which is so-called trident process. The yield of muon production can be expressed as (Titov et al. 2009):

$$dN^{\mu^+\mu^-} = \frac{N_A \rho_A}{A} \int_0^L dl N^e(l) d\sigma^{eA \rightarrow e'\mu^+\mu^- A}\left[E_e(l)\right], \tag{57}$$

where $d\sigma^{eA \rightarrow e'\mu^+\mu^- A}$ is the elementary cross section of the muon production in the elementary eA interaction.

After estimating the muon pairs yield by Eqs. (56) and (57), about 5×10^3 muon pairs can be produced via 20 pC laser-driven electron with energy of 10 GeV impinging 1-cm-thick gold target (Titov et al. 2009). Following this work, Rao et al. (2018) have demonstrated numerically the feasibility of a mm-scale, sub-100ps-duration bright muon source driven by 100 pC laser wakefield electrons with an energy of 10 GeV, as shown in Fig. 16. Such muon source is promising in elemental analysis, muon catalyzed fusion (μCF), proton charge radius measurement, high-order harmonics generation, muon radiography and tomography.

Recently, Wang et al. (2021b) proposed prompt acceleration of an injected low-energy muon beam in a plasma wakefield driven by a laser-accelerated electron beam. Full 3D PIC simulations showed that a muon beam can be accelerated from 275 MeV to more than 10 GeV within 22.5 ps in the wakefield. Sha et al. (2022) also proposed a novel scheme for obtaining an unprecedentedly dense and short muon source by combining the laser-ion accelerator and a conventional beam-converter, as shown in Fig. 17. With full 3D PIC simulations and Geant4 (Agostinelli et al. 2003) simulations, it was shown that when the laser-driven proton beam irradiates the converter target, pions can be first generated, which then decay into a muon and a muon neutrino due to the weak interaction, i.e., $\pi^+ \rightarrow \mu^+ \nu_\mu$ and $\pi^- \rightarrow \mu^- \nu_\mu$. In the process, it is however very difficult to analytically calculate the cross section of proton-nucleus reactions due to the prohibitive number of open channels (Braun-Munzinger and Stachel 1987; Bungau et al. 2013; Bertini 1969). It is finally shown throng linear interpolation of the cross section that a mm-scale, several-nanoseconds-duration surface muon source with a yield of $\sim 10^6$ per shot, and a tens-micron-scale, tens-picoseconds-duration flying pion beam with a yield of $\sim 10^9$ per shot can be achieved by using the 100 PW-class lasers via our scheme. These unique properties make the muon beams promising to improve the spatial resolution of μSR experiments in small samples and the temporal resolution of muon imaging radiography and tomography, together with the sensitivity to rare muon decay investigation.

4 Conclusion

The development of ultra-short high-power lasers has carved out new scientific frontiers, such as relativistic plasma physics, advanced particle accelerators, and strong-field QED physics. Among them, copious high-energy photon emission accompanying the charged particle acceleration in ultra-intense electromagnetic fields has attracted increasing attention due to their unique features such as high flux,

high brightness, and high photon energy. Understanding whether and how strong laser fields and QED effects can generate charged particles and radiation sources that compete with those based upon conventional accelerators is critical, which is not only fundamentally interesting but also essential for their applications. In this review, we introduce recent advances in bright X/γ-rays radiation and lepton generation in the QED regime by the interaction of relativistic laser with various plasma targets. The characteristics of the radiation and secondary particles generated via these schemes are summarized, and the experimental progresses are elaborated.

Though significant progress has been made in the strong-field QED, there are still many predictions to be confirmed, many schemes to be demonstrated in experiments, and many experimental issues to be settled. The quest for experimental demonstration of the conversion from energy to mass by QED has become in full swing worldwide. The upcoming 10–100 PW lasers together with the high energy accelerators around the world would open up new opportunities for strong-field QED physics and related applications.

Acknowledgements This work was supported by the National Natural Science Foundation of China (Grant Nos. 12375244, 12275356, 12205186, 12135009 and 11991074). The authors gratefully acknowledge B. S. Xie and Y. L. Liu for their helpful discussions.

Data availability There is no data associated with this study.

Declarations

Conflict of interest The authors declare that they have no confict of interest.

References

D. Abbott, P. Adderley, A. Adeyemi et al., Production of highly polarized positrons using polarized electrons at MeV energies. Phys. Rev. Lett. **116**(21), 214801 (2016). https://doi.org/10.1103/PhysRevLett.116.214801

N. Abdukerim, B. Xie, Z. Li et al., Enhanced electron-positron pair creation by dynamically assisted combinational fields. Phys. Lett. B **717**(4), 465–469 (2012). https://doi.org/10.1016/j.physletb.2012.09.060

N. Abdukerim, Z. Li, B. Xie, Effects of laser pulse shape and carrier envelope phase on pair production. Phys. Lett. B **726**(4), 820–826 (2013). https://doi.org/10.1016/j.physletb.2013.09.014

M. Abraham, *Theorie der Elektrizität*, vol. 2 (Teubner, Leipzig, 1905)

M. Abraham, Theorie der elektrizität. zweiter band: Elektromagnetische theorie der strahlung. Monatshefte für Mathematik und Physik **17**(1), A39 (1906). https://doi.org/10.1007/bf01697706

J. Adam, L. Adamczyk, J.R. Adams et al., Measurement of e + e - momentum and angular distributions from linearly polarized photon collisions. Phys. Rev. Lett. **127**(5), 052302 (2021). https://doi.org/10.1103/PhysRevLett.127.052302

I.K. Affleck, O. Alvarez, N.S. Manton, Pair production at strong coupling in weak external fields. Nucl. Phys. B **197**(3), 509–519 (1982). https://doi.org/10.1016/0550-3213(82)90455-2

S. Agostinelli, J. Allison, K. Amako et al., Geant4—a simulation toolkit. Nucl. Instrum. Methods Phys. Res., Sect. A **506**(3), 250–303 (2003). https://doi.org/10.1016/S0168-9002(03)01368-8

Z. Akbar, P. Roy, S. Park et al., Measurement of the helicity asymmetry e in $\omega \to \pi^+\pi^-\pi^0$ photoproduction. Phys. Rev. C **96**, 065209 (2017). https://doi.org/10.1103/PhysRevC.96.065209

R. Alkofer, M.B. Hecht, C.D. Roberts et al., Pair creation and an X-ray free electron laser. Phys. Rev. Lett. **87**(19), 193902 (2001). https://doi.org/10.1103/PhysRevLett.87.193902

C.D. Anderson, The positive electron. Phys. Rev. **43**(6), 491–494 (1933). https://doi.org/10.1103/PhysRev.43.491

T. Aoki, T. Kawai, Y. Takei, Algebraic analysis of singular perturbations-on exact WKB analysis. Sugaku Expos **8**(2), 217 (1995)

T. Aoyama, M. Hayakawa, T. Kinoshita et al., Tenth-order QED lepton anomalous magnetic moment: eighth-order vertices containing a second-order vacuum polarization. Phys. Rev. D **85**, 033007 (2012). https://doi.org/10.1103/PhysRevD.85.033007

T.L. Audet, A. Alejo, L. Calvin et al., Ultrashort, MeV-scale laser-plasma positron source for positron annihilation lifetime spectroscopy. Phys. Rev. Accel. Beams **24**(7), 073402 (2021)

B. Badelek, C. Blöchinger, Blümlein. Jea, The photon collider at TESLA. Int. J. Mod. Phys. A **19**(30), 5097–5186 (2004). https://doi.org/10.1142/S0217751X04020737

V.N. Baier, V.M. Katkov, Concept of formation length in radiation theory. Phys. Rep. **409**(5), 261–359 (2005). https://doi.org/10.1016/j.physrep.2004.11.003

C. Bamber, S.J. Boege, T. Koffas et al., Studies of nonlinear QED in collisions of 46.6 GeV electrons with intense laser pulses. Phys. Rev. D **60**(9), 092004 (1999). https://doi.org/10.1103/PhysRevD.60.092004

V. Bargmann, L. Michel, V.L. Telegdi, Precession of the polarization of particles moving in a homogeneous electromagnetic field. Phys. Rev. Lett. **2**, 435–436 (1959). https://doi.org/10.1103/PhysRevLett.2.435

G. Bassompierre, G. Bologna, D. Boget et al., Search for light neutral objects photoproduced in a crystal strong field and decaying into e^+e^- pairs. Phys. Lett. B **355**(3), 584–594 (1995). https://doi.org/10.1016/0370-2693(95)00628-X

H.W. Bertini, Intranuclear-cascade calculation of the secondary nucleon spectra from nucleon-nucleus interactions in the energy range 340 to 2900 mev and comparisons with experiment. Phys. Rev. **188**(4), 1711 (1969)

H.A. Bethe, W. Heitler, On the stopping of fast particles and on the creation of positive electrons. Proc. R. Soc. Lond. A **146**(856), 83–112 (1934)

I. Bialynicki-Birula, P. Górnicki, J. Rafelski, Phase-space structure of the Dirac vacuum. Phys. Rev. D **44**, 1825–1835 (1991). https://doi.org/10.1103/PhysRevD.44.1825

D.H. Bilderback, P. Elleaume, E. Weckert, Review of third and next generation synchrotron light sources. J. Phys. B: At. Mol. Opt. Phys. **38**(9), S773 (2005). https://doi.org/10.1088/0953-4075/38/9/022

T.G. Blackburn, Radiation reaction in electron-beam interactions with high-intensity lasers. Rev. Mod. Plasma Phys. **4**, 5 (2020). https://doi.org/10.1007/s41614-020-0042-0

T.G. Blackburn, C.P. Ridgers, J.G. Kirk et al., Quantum radiation reaction in laser-electron-beam collisions. Phys. Rev. Lett. **112**, 015001 (2014). https://doi.org/10.1103/PhysRevLett.112.015001

D.B. Blaschke, A.V. Prozorkevich, C.D. Roberts et al., Pair production and optical lasers. Phys. Rev. Lett. **96**, 140402 (2006). https://doi.org/10.1103/PhysRevLett.96.140402

A. Blinne, H. Gies, Pair production in rotating electric fields. Phys. Rev. D **89**, 085001 (2014). https://doi.org/10.1103/PhysRevD.89.085001

J.C.R. Bloch, V.A. Mizerny, A.V. Prozorkevich et al., Pair creation: back reactions and damping. Phys. Rev. D **60**, 116011 (1999). https://doi.org/10.1103/PhysRevD.60.116011

M. Boca, V. Florescu, Nonlinear Compton scattering with a laser pulse. Phys. Rev. A **80**, 053403 (2009). https://doi.org/10.1103/PhysRevA.80.053403

J. Bocquet, J. Ajaka, M. Anghinolfi et al., GRAAL: a polarized γ-ray beam at ESRF. Nucl. Phys. A **622**(1), c124–c129 (1997). https://doi.org/10.1016/S0375-9474(97)00337-0

C. Boehm, C. Degrande, O. Mattelaer et al., Circular polarisation: a new probe of dark matter and neutrinos in the sky. J. Cosmol. Astropart. Phys. **05**, 043 (2017). https://doi.org/10.1088/1475-7516/2017/05/043

C. Bostedt, S. Boutet, D.M. Fritz et al., Linac coherent light source: the first five years. Rev. Mod. Phys. **88**, 015007 (2016). https://doi.org/10.1103/RevModPhys.88.015007

S. Bragin, S. Meuren, C.H. Keitel et al., High-energy vacuum birefringence and dichroism in an ultrastrong laser field. Phys. Rev. Lett. **119**, 250403 (2017). https://doi.org/10.1103/PhysRevLett.119.250403

P. Braun-Munzinger, J. Stachel, Pion production in heavy-ion collisions. Annu. Rev. Nucl. Part. Sci. **37**(1), 97–131 (1987)

G. Breit, J.A. Wheeler, Collision of two light quanta. Phys. Rev. **46**(12), 1087–1091 (1934)

L. Brillouin, La mécanique ondulatoire de schrödinger: une méthode générale de resolution par approximations successives'', comptes rendus de l'academie des sciences 183, 24 u26 (1926) ha kramers. Wellenmechanik und halbzählige Quantisierung''. Z. fur Phys. **39**(828), U840 (1926)

A.R. Brown, Schwinger pair production at nonzero temperatures or in compact directions. Phys. Rev. D **98**, 036008 (2018). https://doi.org/10.1103/PhysRevD.98.036008

C. Bula, K.T. McDonald, E.J. Prebys et al., Observation of nonlinear effects in Compton scattering. Phys. Rev. Lett. **76**, 3116–3119 (1996). https://doi.org/10.1103/PhysRevLett.76.3116

A. Bungau, R. Cywinski, C. Bungau et al., Simulations of surface muon production in graphite targets. Phys. Rev. ST Accel. Beams **16**(1), 014701 (2013)

D.L. Burke, R.C. Field, G. Horton-Smith et al., Positron production in multiphoton light-by-light scattering. Phys. Rev. Lett. **79**(9), 1626 (1997)

H.X. Chang, B. Qiao, Z. Xu et al., Generation of overdense and high-energy electron-positron-pair plasmas by irradiation of a thin foil with two ultraintense lasers. Phys. Rev. E **92**, 053107 (2015). https://doi.org/10.1103/PhysRevE.92.053107

Z. Chen, S. Meuren, E. Gerstmayr, et al. Preparation of strong-field qed experiments at facet-ii. Optica High-brightness Sources and Light-driven Interactions Congress 2022 p HF4B.6 (2022). https://doi.org/10.1364/HILAS.2022.HF4B.6

H. Chen, S.C. Wilks, J.D. Bonlie et al., Making relativistic positrons using ultraintense short pulse lasers. Phys. Plasmas **16**, 122702 (2009). https://doi.org/10.1063/1.3271355

L. Chen, W. Yan, Li. Dea, Bright betatron X-ray radiation from a laser-driven-clustering gas target. Sci. Rep. **3**, 1912 (2013). https://doi.org/10.1038/srep01912

S. Chen, N.D. Powers, I. Ghebregziabher et al., MeV-energy X-rays from inverse Compton scattering with laser-Wakefield accelerated electrons. Phys. Rev. Lett. **110**, 155003 (2013). https://doi.org/10.1103/PhysRevLett.110.155003

H. Chen, F. Fiuza, A. Link et al., Scaling the Yield of Laser-Driven Electron-Positron Jets to Laboratory Astrophysical Applications. Phys. Rev. Lett. **114**(21), 215001 (2015)

Y.Y. Chen, J.X. Li, K.Z. Hatsagortsyan et al., γ-ray beams with large orbital angular momentum via nonlinear Compton scattering with radiation reaction. Phys. Rev. Lett. **121**, 074801 (2018). https://doi.org/10.1103/PhysRevLett.121.074801

S. Cipiccia, M. Islam, Ersfeld Bea, Gamma-rays from harmonically resonant betatron oscillations in a plasma wake. Nat. Phys. **7**, 867–871 (2011). https://doi.org/10.1038/nphys2090

J.M. Cole, K.T. Behm, E. Gerstmayr et al., Experimental evidence of radiation reaction in the collision of a high-intensity laser pulse with a laser-Wakefield accelerated electron beam. Phys. Rev. X **8**, 011020 (2018). https://doi.org/10.1103/PhysRevX.8.011020

A.T.L.A.S. Collaboration, Evidence for light-by-light scattering in heavy-ion collisions with the ATLAS detector at the LHC. Nat. Phys. **13**, 852–858 (2017). https://doi.org/10.1038/nphys4208

A.H. Compton, A quantum theory of the scattering of X-rays by light elements. Phys. Rev. **21**, 483–502 (1923). https://doi.org/10.1103/PhysRev.21.483

S. Corde, K. Ta Phuoc, G. Lambert et al., Femtosecond X-rays from laser-plasma accelerators. Rev. Mod. Phys. **85**, 1–48 (2013). https://doi.org/10.1103/RevModPhys.85.1

S. Corde, E. Adli, J.M. Allen et al., Multi-gigaelectronvolt acceleration of positrons in a self-loaded plasma Wakefield. Nature **524**, 442–445 (2015). https://doi.org/10.1038/nature14890

T. Cowan, M. Perry, M. Key et al., High energy electrons, nuclear phenomena and heating in petawatt laser-solid experiments. Laser Part. Beams **17**(4), 773–783 (1999)

C. Danson, P. Brummitt, R. Clarke et al., Vulcan Petawatt-an ultra-high-intensity interaction facility. Nucl. Fusion **44**(12), S239 (2004). https://doi.org/10.1088/0029-5515/44/12/S15

C.N. Danson, C. Haefner, J. Bromage et al., Petawatt and exawatt class lasers worldwide. High Power Laser Sci. Eng. **7**, e54 (2019)
G. Degli Esposti, G. Torgrimsson, Worldline instantons for nonlinear Breit–Wheeler pair production and Compton scattering. Phys. Rev. D **105**, 096036 (2022). https://doi.org/10.1103/PhysRevD.105.096036
E. Delabaere, F. Pham, Resurgent methods in semi-classical asymptotics. Annales de l'IHP Physique théorique **71**(1), 1–94 (1999)
E. Delabaere, H. Dillinger, F. Pham, Exact semiclassical expansions for one-dimensional quantum oscillators. J. Math. Phys. **38**(12), 6126–6184 (1997). https://doi.org/10.1063/1.532206
A. Di Piazza, Ultrarelativistic electron states in a general background electromagnetic field. Phys. Rev. Lett. **113**, 040402 (2014). https://doi.org/10.1103/PhysRevLett.113.040402
A. Di Piazza, K.Z. Hatsagortsyan, C.H. Keitel, Quantum radiation reaction effects in multiphoton Compton scattering. Phys. Rev. Lett. **105**, 220403 (2010). https://doi.org/10.1103/PhysRevLett.105.220403
A. Di Piazza, C. Müller, K.Z. Hatsagortsyan et al., Extremely high-intensity laser interactions with fundamental quantum systems. Rev. Mod. Phys. **84**, 1177–1228 (2012). https://doi.org/10.1103/RevModPhys.84.1177
H. Dillinger, E. Delabaere, F. Pham, Résurgence de Voros et périodes des courbes hyperelliptiques. Ann. Inst. Fourier **43**(1), 163–199 (1993). https://doi.org/10.5802/aif.1326
V. Dinu, T. Heinzl, A. Ilderton, Infrared divergences in plane wave backgrounds. Phys. Rev. D **86**, 085037 (2012). https://doi.org/10.1103/PhysRevD.86.085037
P.A. Dirac, The quantum theory of the electron. Proc. R. Soc. Lond. A **117**(778), 610–624 (1928)
P.A.M. Dirac, A theory of electrons and protons. Proc. R. Soc. Lond. A **126**(801), 360–365 (1930). https://doi.org/10.1098/rspa.1930.0013
P.A.M. Dirac, Classical theory of radiating electrons. Proc. R. Soc. Lond. A **167**, 148 (1938). https://doi.org/10.1098/rspa.1938.0124
P.A.M. Dirac, Classical theory of radiating electrons. Proc. R. Soc. Lond. A **167**(929), 148–169 (1938). https://doi.org/10.1098/rspa.1938.0124
M.J. Duff, R. Capdessus, C.P. Ridgers et al., Multi-stage scheme for nonlinear Breit–Wheeler pair-production utilising ultra-intense laser-solid interactions. Plasma Phys. Control Fusion **61**(9), 094001 (2019)
G.V. Dunne, Heisenberg–Euler effective Lagrangians: basics and extensions (2004). arXiv pp hep–th/0406,216. https://doi.org/10.48550/arXiv.hep-th/0406216
G.V. Dunne, C. Schubert, Worldline instantons and pair production in inhomogenous fields. Phys. Rev. D **72**, 105004 (2005). https://doi.org/10.1103/PhysRevD.72.105004
G.V. Dunne, Qh. Wang, Multidimensional worldline instantons. Phys. Rev. D **74**, 065015 (2006). https://doi.org/10.1103/PhysRevD.74.065015
A. Einstein, Strahlungs-emission und absorption nach der quantentheorie. Verh. Dtsch. Phys. Ges. **18**, 318–323 (1916)
F.R. Elder, A.M. Gurewitsch, R.V. Langmuir et al., Radiation from electrons in a synchrotron. Phys. Rev. **71**, 829–830 (1947). https://doi.org/10.1103/PhysRev.71.829.5
N.V. Elkina, A.M. Fedotov, I.Y. Kostyukov et al., QED cascades induced by circularly polarized laser fields. Phys. Rev. ST Accel. Beams **14**, 054401 (2011). https://doi.org/10.1103/PhysRevSTAB.14.054401
T. Erber, High-energy electromagnetic conversion processes in intense magnetic fields. Rev. Mod. Phys. **38**, 626–659 (1966). https://doi.org/10.1103/RevModPhys.38.626
E. Esarey, B.A. Shadwick, P. Catravas et al., Synchrotron radiation from electron beams in plasma-focusing channels. Phys. Rev. E **65**, 056505 (2002). https://doi.org/10.1103/PhysRevE.65.056505
A.M. Fedotov, N.B. Narozhny, G. Mourou et al., Limitations on the attainable intensity of high power lasers. Phys. Rev. Lett. **105**, 080402 (2010). https://doi.org/10.1103/PhysRevLett.105.080402
A. Fedotov, A. Ilderton, F. Karbstein et al., Advances in qed with intense background fields. Phys. Rep. **1010**, 1–138 (2023). https://doi.org/10.1016/j.physrep.2023.01.003
J. Ferri, S. Corde, A. Doepp et al., High-brilliance betatron γ-ray source powered by laser-accelerated electrons. Phys. Rev. Lett. **120**, 254802 (2018). https://doi.org/10.1103/PhysRevLett.120.254802
R.P. Feynman, Space-time approach to quantum electrodynamics. Phys. Rev. **76**, 769–789 (1949). https://doi.org/10.1103/PhysRev.76.769
R.P. Feynman, *QED: the strange theory of light and matter* (Princeton University Press, Princeton and Oxford, 1985)

K. Fleck, Instrumentation challenges of the strong-field qed experiment luxe at the European xfel. J. Instrum. **17**(08), C08 (2022). https://doi.org/10.1088/1748-0221/17/08/C08022
F. Foroughi, E. Morenzoni, T. Prokscha et al., Upgrading the PSI muon facility. Hyperfine Interact. **138**, 483–488 (2001). https://doi.org/10.1023/A:1020830830050
C. Fu, G. Zhang, Y. Ma, New opportunities for nuclear and atomic physics on the femto- to nanometer scale with ultra-high-intensity lasers. Matter Radiat. Extremes **7**(024), 201 (2022). https://doi.org/10.1063/5.0059405
M. Fukuda, T. Aoki, K. Dobashi et al., Polarimetry of short-pulse gamma rays produced through inverse Compton scattering of circularly polarized laser beams. Phys. Rev. Lett. **91**, 164801 (2003). https://doi.org/10.1103/PhysRevLett.91.164801
W.H. Furry, On bound states and scattering in positron theory. Phys. Rev. **81**, 115–124 (1951). https://doi.org/10.1103/PhysRev.81.115
C. Gahn, G.D. Tsakiris, G. Pretzler et al., Generating positrons with femtosecond-laser pulses. Appl. Phys. Lett. **77**(17), 2662–2664 (2000)
S. Garanin, S. Garnov, A. Sergeev et al., Powerful lasers for high energy density physics. Her. Russ. Acad. Sci. **91**, 250–260 (2021). https://doi.org/10.1134/S1019331621030060
M. Gari, H. Hebach, Photonuclear reactions at intermediate energies (40 MeV $\leq$ e $\gamma \leq$ 400 MeV). Phys. Rep. **72**(1), 1–55 (1981). https://doi.org/10.1016/0370-1573(81)90008-9
S. Gessner, E. Adli, J.M. Allen et al., Demonstration of a positron beam-driven hollow channel plasma Wakefield accelerator. Nat. Commun. **7**(11), 785 (2016). https://doi.org/10.1038/ncomms11785
A. Giulietti, N. Bourgeois, T. Ceccotti et al., Intense γ-ray source in the giant-dipole-resonance range driven by 10-TW laser pulses. Phys. Rev. Lett. **101**, 105002 (2008). https://doi.org/10.1103/PhysRevLett.101.105002
C. Gong, Z.L. Li, B.S. Xie et al., Electron-positron pair production in frequency modulated laser fields. Phys. Rev. D **101**, 016008 (2020). https://doi.org/10.1103/PhysRevD.101.016008
A. Gonoskov, T.G. Blackburn, M. Marklund et al., Charged particle motion and radiation in strong electromagnetic fields. Rev. Mod. Phys. **94**, 045001 (2022). https://doi.org/10.1103/RevModPhys.94.045001
A.J. Gonsalves, K. Nakamura, J. Daniels et al., Petawatt laser guiding and electron beam acceleration to 8 GeV in a laser-heated capillary discharge waveguide. Phys. Rev. Lett. **122**, 084801 (2019). https://doi.org/10.1103/PhysRevLett.122.084801
T.P. Gorringe, D. Hertzog, Precision muon physics. Prog. Part. Nucl. Phys. **84**, 73–123 (2015). https://doi.org/10.1016/j.ppnp.2015.06.001
O. Gould, A. Rajantie, Thermal Schwinger pair production at arbitrary coupling. Phys. Rev. D **96**, 076002 (2017). https://doi.org/10.1103/PhysRevD.96.076002
O. Gould, A. Rajantie, C. Xie, Worldline sphaleron for thermal Schwinger pair production. Phys. Rev. D **98**, 056022 (2018). https://doi.org/10.1103/PhysRevD.98.056022
W. Greiner, J. Reinhardt, *Quantum electrodynamics* (Springer-Verlag, Berlin Heidelberg, 2009). https://doi.org/10.1007/978-3-540-87561-1
W. Greiner, B. Müller, J. Rafelski, *Quantum electrodynamics of strong fields* (Springer-Verlag, Berlin Heidelberg, 1985). https://doi.org/10.1007/978-3-642-82272-8
Y. Gu, O. Klimo, S. Weber et al., High density ultrashort relativistic positron beam generation by laser-plasma interaction. New J. Phys. **18**, 113023 (2016). https://doi.org/10.1088/1367-2630/18/11/113023
Y.J. Gu, O. Klimo, S. Bulanov et al., Brilliant gamma-ray beam and electron-positron pair production by enhanced attosecond pulses. Commun. Phys. **1**, 93 (2018). https://doi.org/10.1038/s42005-018-0095-3
E. Guedj, A. McGonigal, L. Vaugier et al., Metabolic brain PET pattern underlying hyperkinetic seizures. Epilepsy Res. **101**(3), 237–245 (2012)
Z. Guo, L. Ji, Q. Yu et al., Leveraging radiation reaction via laser-driven plasma fields. Plasma Phys. Controlled Fusion **61**(6), 065007 (2019). https://doi.org/10.1088/1361-6587/ab140b
P. Hadjisolomou, T.M. Jeong, D. Kolenaty et al., Gamma-flash generation in multi-petawatt laser-matter interactions. Phys. Plasmas **30**, 093103 (2023). https://doi.org/10.1063/5.0158264
R.T. Hammond, Radiation reaction at ultrahigh intensities. Phys. Rev. A **81**, 062104 (2010). https://doi.org/10.1103/PhysRevA.81.062104
C. He, Y. Shen, A. Forbes, Towards higher-dimensional structured light. Light Sci. Appl. **11**, 205 (2022). https://doi.org/10.1038/s41377-022-00897-3

F. Hebenstreit, Schwinger effect in inhomogeneous electric fields. PhD dissertation (2011). https://doi.org/10.48550/arXiv.1106.5965
F. Hebenstreit, R. Alkofer, G.V. Dunne et al., Momentum signatures for Schwinger pair production in short laser pulses with a subcycle structure. Phys. Rev. Lett. **102**, 150404 (2009). https://doi.org/10.1103/PhysRevLett.102.150404
F. Hebenstreit, R. Alkofer, H. Gies, Schwinger pair production in space- and time-dependent electric fields: Relating the Wigner formalism to quantum kinetic theory. Phys. Rev. D **82**, 105026 (2010). https://doi.org/10.1103/PhysRevD.82.105026
F. Hebenstreit, R. Alkofer, H. Gies, Particle self-bunching in the Schwinger effect in spacetime-dependent electric fields. Phys. Rev. Lett. **107**, 180403 (2011). https://doi.org/10.1103/PhysRevLett.107.180403
T. Heinzl, A. Ilderton, M. Marklund, Finite size effects in stimulated laser pair production. Phys. Lett. B **692**(4), 250–256 (2010)
W. Heisenberg, H. Euler, Consequences of the dirac theory of positrons. Z. Phys. **98**, 714–732 (1936)
M.T. Hibberd, A.L. Healy, D.S. Lake et al., Acceleration of relativistic beams using laser-generated terahertz pulses. Nat. Photonics **14**, 755–759 (2020). https://doi.org/10.1038/s41566-020-0674-1
A.D. Hillier, J.S. Lord, K. Ishida et al., Muons at ISIS. Philos. Trans. A Math. Phys. Eng. Sci. **377**, 20180064 (2018). https://doi.org/10.1098/rsta.2018.0064
J. Holloway, P. Norreys, Thomas Aea, Brilliant X-rays using a two-stage plasma insertion device. Sci. Rep. **7**, 3985 (2017). https://doi.org/10.1038/s41598-017-04124-7
W. Hong, S. He, J. Teng et al., Commissioning experiment of the high-contrast SILEX-I multi-petawatt laser facility. Matter. Radiat. Extremes **6**, 064401 (2021). https://doi.org/10.1063/5.0016019
C.R. Howell, M.W. Ahmed, A. Afanasev et al., International workshop on next generation gamma-ray source. J. Phys. G: Nucl. Part. Phys. **49**(1), 010502 (2021). https://doi.org/10.1088/1361-6471/ac2827
H. Hu, Seed and vacuum pair production in strong laser field. Contemp. Phys. **61**(1), 12–25 (2020). https://doi.org/10.1080/00107514.2020.1775415
H. Hu, C. Müller, C.H. Keitel, Complete QED theory of multiphoton trident pair production in strong laser fields. Phys. Rev. Lett. **105**(8), 080401 (2010)
Y.T. Hu, J. Zhao, H. Zhang et al., Attosecond γ-ray vortex generation in near-critical-density plasma driven by twisted laser pulses. Appl. Phys. Lett. **118**(5), 054101 (2021). https://doi.org/10.1063/5.0028203
T.W. Huang, C.M. Kim, C.T. Zhou et al., Tabletop laser-driven gamma-ray source with nanostructured double-layer target. Plasma Phys. Controlled Fusion **60**(11), 115006 (2018). https://doi.org/10.1088/1361-6587/aadbeb
A. Ilderton, G. Torgrimsson, Scattering in plane-wave backgrounds: infrared effects and pole structure. Phys. Rev. D **87**, 085040 (2013). https://doi.org/10.1103/PhysRevD.87.085040
I.P. Ivanov, Colliding particles carrying nonzero orbital angular momentum. Phys. Rev. D **83**, 093001 (2011). https://doi.org/10.1103/PhysRevD.83.093001
I.P. Ivanov, Promises and challenges of high-energy vortex states collisions. Prog. Part. Nucl. Phys. **127**, 103987 (2022). https://doi.org/10.1016/j.ppnp.2022.103987
J.D. Jackson, *Classical electrodynamics* (Wiley, New York, 1998)
N. Jain, T.M. Antonsen, J.P. Palastro, Positron acceleration by plasma wakefields driven by a hollow electron beam. Phys. Rev. Lett. **115**, 195001 (2015). https://doi.org/10.1103/PhysRevLett.115.195001
O. Jansen, T. Tückmantel, A. Pukhov, Scaling electron acceleration in the bubble regime for upcoming lasers. Eur. Phys. J. Spec. Top. **223**, 1017–1030 (2014)
H. Jeffreys, On certain approximate solutions of linear differential equations of the second order. Proc. Lond. Math. Soc. **23**, 428–436 (1925). https://doi.org/10.1112/plms/s2-23.1.428
L.L. Ji, A. Pukhov, I.Y. Kostyukov et al., Radiation-reaction trapping of electrons in extreme laser fields. Phys. Rev. Lett. **112**, 145003 (2014). https://doi.org/10.1103/PhysRevLett.112.145003
L.L. Ji, A. Pukhov, E.N. Nerush et al., Energy partition, γ-ray emission, and radiation reaction in the near-quantum electrodynamical regime of laser-plasma interaction. Phys. Plasmas **21**, 023109 (2014). https://doi.org/10.1063/1.4866014
S. Jiang, A. Link, D. Canning et al., Enhancing positron production using front surface target structures. Appl. Phys. Lett. **118**(9), 094101 (2021)
P. Jójárt, I. Seres, Z. Bengery et al., Status of the eli-alps high repetition rate (hr) laser systems. In: 2023 Conference on Lasers and Electro-Optics Europe & European Quantum Electronics Conference

(CLEO/Europe-EQEC), p. 1 (2023) https://doi.org/10.1109/CLEO/Europe-EQEC57999.2023.10231605
S.P. Kim, D.N. Page, Schwinger pair production via instantons in strong electric fields. Phys. Rev. D. **65**, 105002 (2002). https://doi.org/10.1103/PhysRevD.65.105002
J. Kim, A. Link, D. Canning et al., Dynamic focusing of laser driven positron jets by self-generated fields. New J. Phys. **22**(12), 123020 (2020)
B. King, S. Tang, Nonlinear Compton scattering of polarized photons in plane-wave backgrounds. Phys. Rev. A **102**, 022809 (2020). https://doi.org/10.1103/PhysRevA.102.022809
S. Kiselev, A. Pukhov, I. Kostyukov, X-ray generation in strongly nonlinear plasma waves. Phys. Rev. Lett. **93**, 135004 (2004). https://doi.org/10.1103/PhysRevLett.93.135004
O. Klein, Y. Nishina, Über die streuung von strahlung durch freie elektronen nach der neuen relativistischen quantendynamik von Dirac. Z Physik **52**, 853–868 (1929). https://doi.org/10.1007/BF01366453
Y. Kluger, E. Mottola, J.M. Eisenberg, Quantum Vlasov equation and its Markov limit. Phys. Rev. D **58**, 125015 (1998). https://doi.org/10.1103/PhysRevD.58.125015
S. Kneip, S.R. Nagel, C. Bellei et al., Observation of synchrotron radiation from electrons accelerated in a petawatt-laser-generated plasma cavity. Phys. Rev. Lett. **100**, 105006 (2008). https://doi.org/10.1103/PhysRevLett.100.105006
C. Kohlfürst, Electron-positron pair production in inhomogeneous electromagnetic fields. PhD dissertation (2015). https://doi.org/10.48550/arXiv.1512.06082
C. Kohlfürst, R. Alkofer, On the effect of time-dependent inhomogeneous magnetic fields in electron-positron pair production. Phys. Lett. B **756**, 371–375 (2016). https://doi.org/10.1016/j.physletb.2016.03.027
C. Kohlfürst, H. Gies, R. Alkofer, Effective mass signatures in multiphoton pair production. Phys. Rev. Lett. **112**, 050402 (2014). https://doi.org/10.1103/PhysRevLett.112.050402
C. Kohlfürst, N. Ahmadiniaz, J. Oertel et al., Sauter–Schwinger effect for colliding laser pulses. Phys. Rev. Lett. **129**, 241801 (2022). https://doi.org/10.1103/PhysRevLett.129.241801
D. Kolenatý, P. Hadjisolomou, R. Versaci et al., Electron-positron pairs and radioactive nuclei production by irradiation of high-z target with γ-photon flash generated by an ultra-intense laser in the λ^3 regime. Phys. Rev. Res. **4**, 023124 (2022). https://doi.org/10.1103/PhysRevResearch.4.023124
M. Korwar, A.M. Thalapillil, Finite temperature Schwinger pair production in coexistent electric and magnetic fields. Phys. Rev. D **98**, 076016 (2018). https://doi.org/10.1103/PhysRevD.98.076016
H. Kramers, Wellenmechanik und halbzahlige quantisierung. Z. Phys. **39**, 828–840 (1926). https://doi.org/10.1007/BF01451751
L.D. Landau, E.M. Lifshitz (eds.), *The classical theory of fields* (Butterworth-Heinemann, Oxford, 1980)
M. L'Annunziata, *Handbook of radioactivity analysis* (Academic Press, San Diego, 2003)
S. Lee, T. Katsouleas, R.G. Hemker et al., Plasma-Wakefield acceleration of a positron beam. Phys. Rev. E **64**, 045501 (2001). https://doi.org/10.1103/PhysRevE.64.045501
B. Lei, J. Wang, V. Kharin et al., γ-ray generation from plasma Wakefield resonant wiggler. Phys. Rev. Lett. **120**, 134801 (2018). https://doi.org/10.1103/PhysRevLett.120.134801
K.V. Lezhnin, P.V. Sasorov, G. Korn et al., High power gamma flare generation in multi-petawatt laser interaction with tailored targets. Phys. Plasmas **25**, 123105 (2018). https://doi.org/10.1063/1.5062849
Z.L. Li, D. Lu, B.S. Xie, Multiple-slit interference effect in the time domain for boson pair production. Phys. Rev. D **89**, 067701 (2014). https://doi.org/10.1103/PhysRevD.89.067701
Z.L. Li, D. Lu, B.S. Xie et al., Enhanced pair production in strong fields by multiple-slit interference effect with dynamically assisted Schwinger mechanism. Phys. Rev. D **89**, 093011 (2014). https://doi.org/10.1103/PhysRevD.89.093011
Z.L. Li, D. Lu, B.S. Xie, Effects of electric field polarizations on pair production. Phys. Rev. D **92**, 085001 (2015). https://doi.org/10.1103/PhysRevD.92.085001
H.Z. Li, Y. Tong-Pu, J.J. Liu et al., Ultra-bright γ-ray emission and dense positron production from two laser-driven colliding foils. Sci. Rep. **7**, 17312 (2017). https://doi.org/10.1038/s41598-017-17605-6
H.Z. Li, T.P. Yu, L.X. Hu et al., Ultra-bright γ-ray flashes and dense attosecond positron bunches from two counter-propagating laser pulses irradiating a micro-wire target. Opt. Express **25**(18), 21583-21593 (2017). https://doi.org/10.1364/OE.25.021583
W. Li, Z. Gan, L. Yu et al., 339 J high-energy Ti:sapphire chirped-pulse amplifier for 10 PW laser facility. Opt. Lett. **43**, 5681 (2018). https://doi.org/10.1364/OL.43.005681

Y.F. Li, R. Shaisultanov, Y.Y. Chen et al., Polarized ultrashort brilliant multi-GeV γ rays via single-shot laser-electron interaction. Phys. Rev. Lett. **124**, 014801 (2020). https://doi.org/10.1103/PhysRevLett.124.014801

E. Liang, T. Clarke, A. Henderson et al., High e+/e− Ratio Dense Pair Creation with 10^{21}W.cm^{-2} Laser Irradiating Solid Targets. Sci. Rep. **5**(1), 13968 (2015)

A. Liénard, Champ électrique et magnétique produit par une charge concentrée en un point et animée d'un mouvement quelconque. L'Éclairage Électrique **16**, 5 (1898)

J.J. Liu, T.P. Yu, Y. Yin et al., All-optical bright γ-ray and dense positron source by laser driven plasmas-filled cone. Opt. Express **24**(14), 15978-15986 (2016). https://doi.org/10.1364/OE.24.015978

J.X. Liu, Y.Y. Ma, T.P. Yu et al., Enhanced electron- positron pair production by ultra intense laser irradiating a compound target. Plasma Phys. Control Fusion **58**(12), 125007 (2016)

J.X. Liu, L.F. Gan, Y.Y. Ma et al., Positron generation via two sequent laser pulses irradiating a solid aluminum target. Phys. Plasmas **24**(8), 083113 (2017)

K. Liu, T.P. Yu, D.B. Zou et al., Twisted radiation from nonlinear Thomson scattering with arbitrary incident angle. Eur. Phys. J. D **74**, 7 (2020). https://doi.org/10.1140/epjd/e2019-100437-4

W.Y. Liu, K. Xue, F. Wan et al., Trapping and acceleration of spin-polarized positrons from γ photon splitting in Wakefields. Phys. Rev. Res. **4**, L022028 (2022). https://doi.org/10.1103/PhysRevResearch.4.L022028

M. Lobet, X. Davoine, E. D'Humières et al., Generation of high-energy electron-positron beams in the collision of a laser-accelerated electron beam and a multi-petawatt laser. Phys. Rev. Accel. Beams **20**, 043401 (2015). https://doi.org/10.1103/PhysRevAccelBeams.20.043401

M. Lobet, X. Davoine, E. d'Humières et al., Generation of high-energy electron-positron pairs in the collision of a laser-accelerated electron beam with a multipetawatt laser. Phys. Rev. Accel. Beams **20**(4), 043401 (2017)

H.A. Lorentz, Weiterbildung der maxwellschen theorie. elektronentheorie. Encykl Mathe Wiss. **14**, 145–280 (1904)

H.A. Lorentz, *La Théorie Électromagnétique de Maxwell et Son Application Aux Corps Mouvants, Collected Papers* (Springer, 1936). https://doi.org/10.1007/978-94-015-3447-5_4

W. Lu, M. Tzoufras, C. Joshi et al., Generating multi-GeV electron bunches using single stage laser Wakefield acceleration in a 3d nonlinear regime. Phys. Rev. ST Accel. Beams **10**, 061301 (2007). https://doi.org/10.1103/PhysRevSTAB.10.061301

Y. Lu, T.P. Yu, L.X. Hu et al., Enhanced copious electron- positron pair production via electron injection from a mass-limited foil. Plasma Phys. Control Fusion **60**(12), 125008 (2018)

Y. Lu, G.B. Zhang, J. Zhao et al., Ultra-brilliant GeV betatronlike radiation from energetic electrons oscillating in frequency-downshifted laser pulses. Opt. Express **29**, 8926–8940 (2021)

W. Luo, S.D. Wu, W.Y. Liu et al., Enhanced electron-positron pair production by two obliquely incident lasers interacting with a solid target. Plasma Phys. Control Fusion **60**(9), 095006 (2018)

F. Lureau, G. Matras, O. Chalus et al., High-energy hybrid femtosecond laser system demonstrating 2 × 10 PW capability. High Power Laser Sci. Eng. **8**, e43 (2020). https://doi.org/10.1017/hpl.2020.41

Q.Z. Lv, E. Raicher, C.H. Keitel et al., High-brilliance ultranarrow-band X rays via electron radiation in colliding laser pulses. Phys. Rev. Lett. **128**, 024801 (2022). https://doi.org/10.1103/PhysRevLett.128.024801

Y. Ma, J. Hua, D. Liu et al., Compact polarized X-ray source based on all-optical inverse Compton scattering. Phys. Rev. Appl. **19**, 014073 (2023). https://doi.org/10.1103/PhysRevApplied.19.014073

F. Mackenroth, A. Di Piazza, Nonlinear Compton scattering in ultrashort laser pulses. Phys. Rev. A **83**, 032106 (2011). https://doi.org/10.1103/PhysRevA.83.032106

F. Mackenroth, A. Di Piazza, C.H. Keitel, Determining the carrier-envelope phase of intense few-cycle laser pulses. Phys. Rev. Lett. **105**, 063903 (2010). https://doi.org/10.1103/PhysRevLett.105.063903

A.J. MacLeod, P. Hadjisolomou, T.M. Jeong et al., All-optical nonlinear Breit-wheeler pair production with γ-flash photons. Phys. Rev. A **107**, 012215 (2023). https://doi.org/10.1103/PhysRevA.107.012215

MAGIC Collaboration, P. Veres, P. Bhat, Observation of inverse Compton emission from a long γ-ray burst. Nature **575**, 459–463 (2019). https://doi.org/10.1038/s41586-019-1754-6

J. Magnusson, A. Gonoskov, M. Marklund et al., Laser-particle collider for multi-GeV photon production. Phys. Rev. Lett. **122**, 254801 (2019). https://doi.org/10.1103/PhysRevLett.122.254801

S.S. Masood, QED plasma in the early universe. Arab. J. Math. **8**, 183–192 (2019). https://doi.org/10.1007/s40065-018-0232-6

W.H. McMaster, Matrix representation of polarization. Rev. Mod. Phys. **33**, 8–28 (1961). https://doi.org/10.1103/RevModPhys.33.8
P.W. Milonni, W.A. Smith, Radiation reaction and vacuum fluctuations in spontaneous emission. Phys. Rev. A **11**, 814–824 (1975). https://doi.org/10.1103/PhysRevA.11.814
M. Mohamedsedik, L.J. Li, B.S. Xie, Schwinger pair production in inhomogeneous electric fields with symmetrical frequency chirp. Phys. Rev. D **104**, 016009 (2021). https://doi.org/10.1103/PhysRevD.104.016009
G.A. Mourou, T. Tajima, S.V. Bulanov, Optics in the relativistic regime. Rev. Mod. Phys. **78**, 309–371 (2006). https://doi.org/10.1103/RevModPhys.78.309
P. Musumeci, C. Boffo, S.S. Bulanov et al., Positron sources for future high energy physics colliders (2022). arXiv:2204.13245
T. Nagae, The J-PARC project. Nuclear Phys. A **805**(1), 486c–493c (2008). https://doi.org/10.1016/j.nuclphysa.2008.02.287
T. Nakamura, T. Hayakawa, Quasi-monoenergetic positron beam generation from ultra-intense laser-matter interactions. Phys. Plasmas **23**(10), 103109 (2016)
T. Nakamura, J.K. Koga, T.Z. Esirkepov et al., High-power γ-ray flash generation in ultraintense laser-plasma interactions. Phys. Rev. Lett. **108**, 195001 (2012). https://doi.org/10.1103/PhysRevLett.108.195001
K. Nakashima, H. Takabe, Numerical study of pair creation by ultraintense lasers. Phys. Plasmas **9**(5), 1505–1512 (2002)
N. Narozhnyi, M. Fofanov, Photon emission by an electron in a collision with a short focused laser pulse. Sov. J. Exp. Theor. Phys. **83**, 14–23 (1996). https://doi.org/10.1134/1.557958
J. Nejdl, U. Chaulagain, D. Mai et al., Optica high-brightness sources and light-driven interactions congress 2022 (2022)
J. Oertel, R. Schützhold, WKB approach to pair creation in spacetime-dependent fields: the case of a spacetime-dependent mass. Phys. Rev. D **99**, 125014 (2019). https://doi.org/10.1103/PhysRevD.99.125014
B. Ohayon, G. Janka, I. Cortinovis et al., Precision measurement of the lamb shift in muonium. Phys. Rev. Lett. **128**, 011802 (2022). https://doi.org/10.1103/PhysRevLett.128.011802
H. Olsen, L.C. Maximon, Photon and electron polarization in high-energy bremsstrahlung and pair production with screening. Phys. Rev. **114**, 887–904 (1959). https://doi.org/10.1103/PhysRev.114.887
T. Omori, M. Fukuda, T. Hirose et al., Efficient propagation of polarization from laser photons to positrons through Compton scattering and electron-positron pair creation. Phys. Rev. Lett. **96**, 114801 (2006). https://doi.org/10.1103/PhysRevLett.96.114801
H. Peng, C. Riconda, S. Weber et al., Frequency conversion of lasers in a dynamic plasma grating. Phys. Rev. Appl. **15**, 054053 (2021). https://doi.org/10.1103/PhysRevApplied.15.054053
M.E. Peskin, D.V. Schroeder, *An introduction to quantum field theory* (Westview Press, Boulder, 1995). https://doi.org/10.1201/9780429503559
V. Petrillo, I. Drebot, M. Ruijter et al., State of the art of high-flux Compton/Thomson X-rays sources. Appl. Sci. **13**, 752 (2023). https://doi.org/10.3390/app13020752
K. Phuoc, S. Corde, C. Thaury et al., All-optical Compton gamma-ray source. Nat. Photonics **6**, 308–311 (2012). https://doi.org/10.1038/nphoton.2012.82
N. Pietralla, Z. Berant, V.N. Litvinenko et al., Parity measurements of nuclear levels using a free-electron-laser generated γ-ray beam. Phys. Rev. Lett. **88**, 012502 (2001). https://doi.org/10.1103/PhysRevLett.88.012502
K. Poder, M. Tamburini, G. Sarri et al., Experimental signatures of the quantum nature of radiation reaction in the field of an ultraintense laser. Phys. Rev. X **8**, 031004 (2018). https://doi.org/10.1103/PhysRevX.8.031004
T. Popmintchev, M. Chen, P. Arpin et al., The attosecond nonlinear optics of bright coherent X-ray generation. Nat. Photon **4**, 822–832 (2010). https://doi.org/10.1038/nphoton.2010.256
V.S. Popov, Pair production in a variable and homogeneous electric field as an oscillator problem. Sov. Phys. JETP **35**, 659 (1972)
V.S. Popov, Pair production in a variable external field (quasiclassical approximation). Sov. Phys. JETP **34**, 709 (1972)
A. Pukhov, J. Meyer-ter Vehn, Laser wake field acceleration: the highly non-linear broken-wave regime. Appl. Phys. B **74**, 355–361 (2002)
B.S. Rao, J.H. Jeon, H.T. Kim et al., Bright muon source driven by GeV electron beams from a compact laser Wakefield accelerator. Plasma Phys. Control Fusion **60**(9), 095002 (2018)

J. Reinhardt, W. Greiner, Quantum electrodynamics of strong fields. Rep. Prog. Phys. **40**, 219 (1977). https://doi.org/10.1088/0034-4885/40/3/001
H.R. Reiss, Absorption of Light by Light. J. Math. Phys. **3**(1), 59–67 (2004). https://doi.org/10.1063/1.1703787
B.A. Remington, High energy density laboratory astrophysics. Plasma Phys. Control Fusion **47**, A191 (2005). https://doi.org/10.1088/0741-3335/47/5A/014
C.P. Ridgers, C.S. Brady, R. Duclous et al., Dense electron-positron plasmas and ultraintense γ rays from laser-irradiated solids. Phys. Rev. Lett. **108**, 165006 (2012). https://doi.org/10.1103/PhysRevLett.108.165006
C.P. Ridgers, J.G. Kirk, R. Duclous et al., Modelling gamma-ray photone mission and pair production in high-intensity laser-matter interactions. J. Comput. Phys. **260**, 273–285 (2014). https://doi.org/10.1016/j.jcp.2013.12.007
C.P. Ridgers, T.G. Blackburn, D. Del Sorbo et al., Signatures of quantum effects on radiation reaction in laser-electron-beam collisions. J. Plasma Phys. **83**(5), 715830502 (2017). https://doi.org/10.1017/S0022377817000642
V.I. Ritus, Quantum effects of the interaction of elementary particles with an intense electromagnetic field. J. Russ. Laser Res. **6**, 497–617 (1985). https://doi.org/10.1007/BF01120220
A. Rousse, K.T. Phuoc, R. Shah et al., Production of a kev X-ray beam from synchrotron radiation in relativistic laser-plasma interaction. Phys. Rev. Lett. **93**, 135005 (2004). https://doi.org/10.1103/PhysRevLett.93.135005
A. Sampath, X. Davoine, S. Corde et al., Extremely dense gamma-ray pulses in electron beam-multifoil collisions. Phys. Rev. Lett. **126**, 064801 (2021). https://doi.org/10.1103/PhysRevLett.126.064801
G. Sarri, D.J. Corvan, W. Schumaker et al., Ultrahigh brilliance multi-MeV γ-ray beams from nonlinear relativistic Thomson scattering. Phys. Rev. Lett. **113**, 224801 (2014). https://doi.org/10.1103/PhysRevLett.113.224801
G. Sarri, K. Poder, J.M. Cole et al., Generation of neutral and high-density electron-positron pair plasmas in the laboratory. Nat. Commun. **6**, 6747 (2015). https://doi.org/10.1038/ncomms7747
S. Schmidt, D. Blaschke, G. Röpke et al., A quantum kinetic equation for particle production in the Schwinger mechanism. Int. J. Mod. Phys. E **07**, 709–722 (1998). https://doi.org/10.1142/S0218301398000403
S. Schmidt, D. Blaschke, G. Röpke et al., Non-Markovian effects in strong-field pair creation. Phys. Rev. D **59**, 094005 (1999). https://doi.org/10.1103/PhysRevD.59.094005
C. Schubert, Perturbative quantum field theory in the string-inspired formalism. Phys. Rep. **355**, 73–234 (2001). https://doi.org/10.1016/S0370-1573(01)00013-8
W. Schumaker, G. Sarri, M. Vargas et al., Measurements of high-energy radiation generation from laser-Wakefield accelerated electron beams. Phys. Plasmas **21**, 056704 (2014). https://doi.org/10.1063/1.4875336
J. Schwinger, On the classical radiation of accelerated electrons. Phys. Rev. **75**, 1912–1925 (1949). https://doi.org/10.1103/PhysRev.75.1912
J. Schwinger, On gauge invariance and vacuum polarization. Phys. Rev. **82**(5), 664–679 (1951)
D. Seipt, B. Kämpfer, Nonlinear Compton scattering of ultrashort intense laser pulses. Phys. Rev. A **83**, 022101 (2011). https://doi.org/10.1103/PhysRevA.83.022101
D. Seipt, B. Kämpfer, Asymmetries of azimuthal photon distributions in nonlinear Compton scattering in ultrashort intense laser pulses. Phys. Rev. A **88**, 012127 (2013). https://doi.org/10.1103/PhysRevA.88.012127
D. Seipt, S.G. Rykovanov, A. Surzhykov et al., Narrowband inverse Compton scattering x-ray sources at high laser intensities. Phys. Rev. A **91**, 033402 (2015). https://doi.org/10.1103/PhysRevA.91.033402
D. Seipt, V. Kharin, S. Rykovanov et al., Analytical results for nonlinear Compton scattering in short intense laser pulses. J. Plasma Phys. **82**, 655820203 (2016). https://doi.org/10.1017/S002237781600026X
R. Sha, J.H. Cheng, D.A. Li et al., Dense short muon source based on laser-ion accelerators. Eur. Phys. J. A **58**, 249 (2022). https://doi.org/10.1140/epja/s10050-022-00900-w
J.W. Shearer, J. Garrison, J. Wong et al., Pair production by relativistic electrons from an intense laser focus. Phys. Rev. A **8**(3), 1582–1588 (1973)
X.L. Sheng, R.H. Fang, Q. Wang et al., Wigner function and pair production in parallel electric and magnetic fields. Phys. Rev. D **99**, 056004 (2019). https://doi.org/10.1103/PhysRevD.99.056004

A. Sokolov, M. Ternov, On polarization and spin effects in the theory of synchrotron radiation. In: Sov. Phys.-Dokl., pp. 1203–1205 (1964)
A. Sokolov, I. Ternov, Radiation from Relativistic Electrons. American Institute of Physics Translation Series, New York (1986)
I.V. Sokolov, N.M. Naumova, J.A. Nees et al., Dynamics of emitting electrons in strong laser fields. Phys. Plasmas **16**, 093115 (2009). https://doi.org/10.1063/1.3236748
H.H. Song, W.M. Wang, Y.F. Li et al., Spin and polarization effects on the nonlinear Breit-wheeler pair production in laser-plasma interaction. New J. Phys. **23**(7), 075005 (2021). https://doi.org/10.1088/1367-2630/ac0dec
H.H. Song, W.M. Wang, Y.T. Li, Dense polarized positrons from laser-irradiated foil targets in the QED regime. Phys. Rev. Lett. **129**, 035001 (2022). https://doi.org/10.1103/PhysRevLett.129.035001
D.J. Stark, T. Toncian, A.V. Arefiev, Enhanced multi-MeV photon emission by a laser-driven electron beam in a self-generated magnetic field. Phys. Rev. Lett. **116**, 185003 (2016). https://doi.org/10.1103/PhysRevLett.116.185003
M. Stone, Lifetime and decay of "excited vacuum'' states of a field theory associated with nonabsolute minima of its effective potential. Phys. Rev. D **14**, 3568–3573 (1976). https://doi.org/10.1103/PhysRevD.14.3568
D. Strickland, G. Mourou, Compression of amplified chirped optical pulses. Opt. Commum. **56**(3), 219–221 (1985). https://doi.org/10.1016/0030-4018(85)90120-8
E. Strobel, S.S. Xue, Semiclassical pair production rate for time-dependent electrical fields with more than one component: WKB-approach and world-line instantons. Nucl. Phys. B **886**, 1153–1176 (2014). https://doi.org/10.1016/j.nuclphysb.2014.07.017
E. Strobel, S.S. Xue, Semiclassical pair production rate for rotating electric fields. Phys. Rev. D **91**, 045016 (2015). https://doi.org/10.1103/PhysRevD.91.045016
K. Sugimoto, Y. He, N. Iwata et al., Positron generation and acceleration in a self-organized photon collider enabled by an ultraintense laser pulse. Phys. Rev. Lett. **131**, 065102 (2023). https://doi.org/10.1103/PhysRevLett.131.065102
J.H. Sung, S.K. Lee, H.W. Lee et al., High-contrast 0.1-Hz 4-PW laser at CoReLS. 2016 IEEE Photonics Conference (IPC) pp. 456–457 (2016)
J.H. Sung, H.W. Lee, J.Y. Yoo et al., 4.2 PW, 20 fs Ti:sapphire laser at 0.1 Hz. Opt. Lett. **42**(11), 2058–2061 (2017). https://doi.org/10.1364/OL.42.002058
P. Ta, E. Esarey, V. Leurent et al., Betatron radiation from density tailored plasmas. Phys. Plasmas **15**, 6 (2008). https://doi.org/10.1063/1.2918657
Y. Taira, T. Hayakawa, M. Katoh, Multi-gigaelectronvolt acceleration of positrons in a self-loaded plasma Wakefield. Sci. Rep. **7**, 5018 (2017). https://doi.org/10.1038/s41598-017-05187-2
T. Tajima, J.M. Dawson, Laser electron accelerator. Phys. Rev. Lett. **43**, 267–270 (1979). https://doi.org/10.1103/PhysRevLett.43.267
M. Tamburini, F. Pegoraro, A. Di Piazza et al., Radiation reaction effects on radiation pressure acceleration. New J. Phys. **12**, 123005 (2010). https://doi.org/10.1088/1367-2630/12/12/123005
J. Tan, Y. Li, D. Li et al., Observation of high efficiency betatron radiation from femtosecond petawatt laser irradiated near critical plasmas. ArXiv preprint, (2021) arXiv:2109.12467
S. Tang, B. King, H. Hu, Highly polarised gamma photons from electron-laser collisions. Phys. Lett. B **809**, 135701 (2020). https://doi.org/10.1016/j.physletb.2020.135701
H. Taya, T. Fujimori, T. Misumi et al., Exact WKB analysis of the vacuum pair production by time-dependent electric fields. J. High Energy Phys. **2021**, 82 (2021). https://doi.org/10.1007/JHEP03(2021)082
M. Tecimer, High power coupled midinfrared free-electron-laser oscillator scheme as a driver for up-frequency conversion processes in the x-ray region. Phys. Rev. ST Accel. Beams **15**, 020703 (2012). https://doi.org/10.1103/PhysRevSTAB.15.020703
A.G.R. Thomas, C.P. Ridgers, S.S. Bulanov et al., Strong radiation-damping effects in a gamma-ray source generated by the interaction of a high-intensity laser with a wakefield-accelerated electron beam. Phys. Rev. X **2**, 041004 (2012). https://doi.org/10.1103/PhysRevX.2.041004
J.J. Thomson, On electrical oscillations and the effects produced by the motion of an electrified sphere. Proc. Lond. Math. Soc. **1**, 197–219 (1883). https://doi.org/10.1112/plms/s1-15.1.197
U. Timm, Coherent bremsstrahlung of electrons in crystals. Fortschr. Phys. **17**(12), 765–808 (1969). https://doi.org/10.1002/prop.19690171202
A.I. Titov, B. Kampfer, H. Takabe, Dimuon production by laser-Wakefield accelerated electrons. Phys. Rev. ST Accel. Beams **12**, 111301 (2009)

A.I. Titov, H. Takabe, B. Kämpfer et al., Enhanced subthreshold e + e - production in short laser pulses. Phys. Rev. Lett. **108**(24), 240406 (2012)
M. Turner, S. Bulanov, C. Benedetti et al., Strong-field qed experiments using the bella pw laser dual beamlines. Eur. Phys. J. D **76**, 205 (2022). https://doi.org/10.1140/epjd/s10053-022-00535-y
U.I. Uggerhøj, The interaction of relativistic particles with strong crystalline fields. Rev. Mod. Phys. **77**, 1131–1171 (2005). https://doi.org/10.1103/RevModPhys.77.1131
G. Venkataraman, *Quantum revolution II—QED: the jewel of physics* (Universities Press, Hyderabad, 1994)
J. Vieira, J.T. Mendonça, Nonlinear laser driven donut wakefields for positron and electron acceleration. Phys. Rev. Lett. **112**, 215001 (2014). https://doi.org/10.1103/PhysRevLett.112.215001
A. Voros, The return of the quartic oscillator. The complex WKB method. Annales de l'IHP Physique théorique **39**(3), 211–338 (1983)
K. Wang, X.H. H, B.S. DSX Effect of symmetrical frequency chirp on pair production. Chinese Phys B 30(6):060204 (2021a). https://doi.org/10.1088/1674-1056/abeee8
S. Wang, C.E. Clayton, B.E. Blue et al., X-ray emission from betatron motion in a plasma wiggler. Phys. Rev. Lett. **88**, 135004 (2002). https://doi.org/10.1103/PhysRevLett.88.135004
W.M. Wang, Z.M. Sheng, P. Gibbon et al., Collimated ultrabright gamma rays from electron wiggling along a petawatt laser-irradiated wire in the QED regime. Proc. Natl. Acad. Sci. **115**(201809), 649 (2018). https://doi.org/10.1073/pnas.1809649115
J. Wang, B. Zhu, T.P. Yu et al., High-flux x-ray photon emission by a superluminal hybrid electromagnetic mode of intense laser in a plasma waveguide. Plasma Phys. Controlled Fusion **61**(8), 085026 (2019). https://doi.org/10.1088/1361-6587/ab27d4
X.N. Wang, X.F. Lan, Y.S. Huang et al., Prompt acceleration of a short-lifetime low-energy muon beam. Phys. Plasmas **28**(9), 093101 (2021). https://doi.org/10.1063/5.0051850
L. Wang, L.J. Li, M. Mohamedsedik et al., Enhancement of electron-positron pairs in combined potential wells with linear chirp frequency. Chin. Phys. B **32**(1), 010301 (2023). https://doi.org/10.1088/1674-1056/ac744b
J.F.C. Wardle, D.C. Homan, R. Ojha et al., Electron- positron jets associated with the quasar 3C279. Nature **395**(6701), 457–461 (1998)
S. Weinberg, *The quantum theory of fields*, vol. 1 (Cambridge University Press, 1995)
M. Wen, H. Bauke, C.H. Keitel, Identifying the Stern-Gerlach force of classical electron dynamics. Phys. Rev. Lett. **111**, 141803 (2013). https://doi.org/10.1103/PhysRevLett.111.141803
G. Wentzel, Eine verallgemeinerung der quantenbedingungen für die zwecke der wellenmechanik. Z Physik **38**, 518–529 (1926). https://doi.org/10.1007/BF01397171
E. Wiechert, Elektrodynamische elementargesetze. Ann. Phys. **309**, 667–689 (1901). https://doi.org/10.1002/andp.19013090403
T.N. Wistisen, A. Di Piazza, H. Knudsen et al., Experimental evidence of quantum radiation reaction in aligned crystals. Nat. Commun. **9**, 795 (2018). https://doi.org/10.1038/s41467-018-03165-4
D.M. Wolkow, Über eine klasse von lösungen der Diracschen gleichung. Z. Phys. **94**, 250–260 (1935). https://doi.org/10.1007/BF01331022
J.C. Wood, D.J. Chapman, K. Poder et al., Ultrafast imaging of laser driven shock waves using betatron X-rays from a laser wakefield accelerator. Sci. Rep. **8**, 11010 (2018). https://doi.org/10.1038/s41598-018-29347-0
D. Wright, S. Ahmad, D. Armstrong et al., The triumf radiative muon capture facility. Nucl. Instrum. Methods Phys. Res., Sect. A **320**(1), 249–262 (1992). https://doi.org/10.1016/0168-9002(92)90783-Z
B. Xie, Z. Li, S. Tang, Electron-positron pair production in ultrastrong laser fields. Matter Radiat. Extremes **2**, 225–242 (2017). https://doi.org/10.1016/j.mre.2017.07.002
Z. Xu, L. Yi, B. Shen et al., Driving positron beam acceleration with coherent transition radiation. Commun. Phys. **3**(1), 191 (2020)
K. Xue, Z.K. Dou, F. Wan et al., Generation of highly-polarized high-energy brilliant γ-rays via laser-plasma interaction. Matter Radiat. Extremes **5**, 054402 (2020). https://doi.org/10.1063/5.0007734
V. Yakimenko, L. Alsberg, E. Bong et al., FACET-II facility for advanced accelerator experimental tests. Phys. Rev. Accel. Beams **22**(10), 101301 (2019)
W.C. Yan, C. Fruhling, G. Golovin et al., High-order multiphoton Thomson scattering. Nat. Photonics **11**, 514–520 (2017). https://doi.org/10.1038/nphoton.2017.100
Y. Yan, Y. Wu, J. Chen et al., Positron acceleration by sheath field in ultra-intense laser-solid interactions. Plasma Phys. Controlled Fusion **59**(4), 045015 (2017). https://doi.org/10.1088/1361-6587/aa5f77

N. Yasen, B. Xie, W. Liu, Dense positrons and γ -rays generation by lasers interacting with convex target. Plasma Sci. Technol. **23**(1), 015003 (2021)
P. Yi, Toward one-loop tunneling rates of near-extremal magnetic black hole pair production. Phys. Rev. D **51**, 2813–2826 (1995). https://doi.org/10.1103/PhysRevD.51.2813
L. Yi, A. Pukhov, B. Shen, Radiation from laser-microplasma-waveguide interactions in the ultra-intense regime. Phys. Plasmas **23**, 073110 (2016). https://doi.org/10.1063/1.4958314
T.P. Yu, A. Pukhov, Z.M. Sheng et al., Bright betatronlike X rays from radiation pressure acceleration of a mass-limited foil target. Phys. Rev. Lett. **110**, 045001 (2013). https://doi.org/10.1103/PhysRevLett.110.045001
C. Yu, R. Qi, Wang Wea, Ultrahigh brilliance quasi-monochromatic MeV γ-rays based on self-synchronized all-optical Compton scattering. Sci. Rep. **6**, 29518 (2016). https://doi.org/10.1038/srep29518
J.Q. Yu, H.Y. Lu, T. Takahashi et al., Creation of electron-positron pairs in photon-photon collisions driven by 10-PW laser pulses. Phys. Rev. Lett. **122**(1), 014802 (2019)
T. Yu, F. Pegoraro, G. Sarri et al., Introduction to the topical issue high field QED physics. Eur. Phys. J. D **77**, 55 (2023). https://doi.org/10.1140/epjd/s10053-023-00617-5
J. Zhang, Y.T. Li, L.M. Chen et al., Studies of high energy density physics and laboratory astrophysics driven by intense lasers. J. Phys: Conf. Ser. **717**(1), 012004 (2016). https://doi.org/10.1088/1742-6596/717/1/012004
H. Zhang, J. Zhao, Y.T. Hu et al., Efficient bright γ-ray vortex emission from a laser-illuminated light-fan-in-channel target. High Power Laser Sci. Eng. **9**, 1–24 (2021). https://doi.org/10.1017/hpl.2021.29
L.Q. Zhang, K. Liu, S. Tang et al., Generation of isolated and polarized γ-ray pulse by few-cycle laser irradiating a nanofoil. Plasma Phys. Control Fusion **64**, 105011 (2022). https://doi.org/10.1088/1361-6587/ac85a7
J. Zhao, Y.T. Hu, Y. Lu et al., All-optical quasi-monoenergetic GeV positron bunch generation by twisted laser fields. Commun. Phys. **5**(1), 1–10 (2022). https://doi.org/10.1038/s42005-021-00797-9
J. Zhao, Y.T. Hu, H. Zhang et al., Multistage positron acceleration by an electron beam-driven strong terahertz radiation. Photonics **10**, 364 (2023). https://doi.org/10.3390/photonics10040364
S. Zhou, J. Hua, W. An et al., High efficiency uniform Wakefield acceleration of a positron beam using stable asymmetric mode in a hollow channel plasma. Phys. Rev. Lett. **127**, 174801 (2021). https://doi.org/10.1103/PhysRevLett.127.174801
X.L. Zhu, Y. Yin, T.P. Yu et al., Enhanced electron trapping and γ ray emission by ultra-intense laser irradiating a near-critical-density plasma filled gold cone. New J. Phys. **17**(5), 053039 (2015). https://doi.org/10.1088/1367-2630/17/5/053039
X.L. Zhu, T.P. Yu, Z.M. Sheng et al., Dense GeV electron-positron pairs generated by lasers in near-critical-density plasmas. Nat. Commun. **7**(1), 13686 (2016)
X.L. Zhu, M. Chen, T.P. Yu et al., Bright attosecond γ-ray pulses from nonlinear Compton scattering with laser-illuminated compound targets. Appl. Phys. Lett. **112**(17), 174102 (2018). https://doi.org/10.1063/1.5028555
X.L. Zhu, M. Chen, T.P. Yu et al., Collimated GeV attosecond electron- positron bunches from a plasma channel driven by 10 PW lasers. Matter Radiat. Extremes **4**(1), 014401 (2019)
X.L. Zhu, M. Chen, S.M. Weng et al., Extremely brilliant GeV γ-rays from a two-stage laser-plasma accelerator. Sci. Adv. **6**(22), eaaz7240 (2020). https://doi.org/10.1126/sciadv.aaz7240
X.L. Zhu, W.M. Wang, T.P. Yu et al., Research progress of ultrabright γ-ray radiation and electron-positron pair production driven by extremely intense laser fields. Acta Phys. Sin. **70**, 085202 (2021). https://doi.org/10.7498/aps.70.20202224